

3. SITE 408

Shipboard Scientific Party¹

SITE DATA

Date Occupied: 1910Z 29 July 1976

Date Departed: 2148Z 31 July 1976

Time on Hole: 50.6

Position: Latitude: 63°22.63'N; Longitude 28°54.71'W

Water Depth (sea level): 1624 corrected meters, echo sounding

Water Depth (rig floor): 1634 corrected meters, echo sounding

Bottom Felt at: 1634 meters, drill pipe

Penetration: 361.0 meters

Number of Holes: 1

Number of Cores: 38

Total Length of Cored Section: 361.0 meters

Total Core Recovered: 219.6 meters

Percentage Core Recovery: 61 per cent

Oldest Sediment Cored:

Depth sub-bottom: 344.3 meters

Nature: Glauconitic marly ooze

Chronostratigraphic unit: Lower Miocene

Basement:

Depth sub-bottom: 321.6 meters²

Nature: vesicular basalt and hyaloclastite

Principal Results: Site 408 is on the west flank of the Reykjanes Ridge on anomaly 6 (about 20 m.y.). The hole was continuously cored to 361 meters; 220 meters (61%) was recovered. Upper Miocene nannofossil ooze interlayered with basalt occurs at 344 meters.

The sediment section consists of: 9.5 meters of Pleistocene calcareous sandy mud turbidites, 9.5 meters of Pliocene marly ooze, 164.5 meters of Pliocene and upper Miocene nannofossil ooze, 78.5 meters of middle to upper Miocene calcareous mud, overlying basement. Sediments above 48 meters are ash-rich; those below 238 meters contain occasional turbidites.

Basement is 37.4 meters of vesicular aphyric basalt, extensively altered, with some interlayered sediment and breccia. The hole was abandoned early because of illness onboard.

BACKGROUND AND OBJECTIVES

This site was drilled for many of the same reasons as Site 407, since it forms part of the same three-site latitudinal transect of the Mid-Atlantic Ridge. The primary aim was to investigate the activity of the Iceland eruptive anomaly through time, and this led to the first of the problems with this site: where it should be drilled. Advice we received from the Ocean Crust Panel, via J.C. Sclater and W.J. Morgan, was that if we found a petrographic anomaly at Site 407, we should place Site 408 farther southwest, away from Iceland, along anomaly 13. If we found no petrographic anomaly at Site 407, however, we should place Site 408 on anomaly 6 along a mantle flow line from Site 407 toward Site 409 and the crest of the Reykjanes Ridge. Without the XRF onboard, it was difficult to be reasonably sure whether there was a chemical anomaly at Site 407. We decided that before placing two sites on anomaly 13 we should be positive that there was some eruptive anomaly at Site 407. In fact, as the site report for Site 407 (this volume) shows, although we did notice some differences in petrography between the rocks at Site 407 and typical ocean floor lavas, these might have been related to off-axis volcanism. Because of our unsure conclusions, we selected a site on anomaly 6 along the mantle flow line from Site 407 toward the ridge, thereby obtaining a historical view of the geochemical anomaly.

The reason for choosing anomaly 6 (about 20 m.y.) rather than anomaly 5 (about 10 m.y.) for this site (several other holes in the Atlantic are on anomaly 5) is that 20 m.y. is just older than the oldest visible crust above sea level in Iceland, and so would give additional information on that part of Icelandic history which is no longer visibly represented, if indeed there was any Icelandic history at that time.

On the way to Site 407, we obtained a seismic reflection and a magnetic anomaly profile over Site 408, and this was the basis for our choice of the site's precise position. In order to drill into uniformly magnetized crust, we needed a position on the northwest side of the peak of an anomaly, because of the asymmetry of magnetic anomalies with respect to causative bodies of this strike at this latitude, as explained in the corresponding section for Site 407. The most prominent anomaly in this region was anomaly 6, and this constrained the choice of the precise site.

The sedimentary section obtained at Site 407 acted as a constraint on placing Site 408. A similar-looking, draped sedimentary sequence could be seen over the region of anomaly 6 along the traverse we had made in going on to

¹Bruce P. Luyendyk (Co-Chief Scientist), University of California, Santa Barbara, Santa Barbara, California; Joe. R. Cann (Co-Chief Scientist), University of East Anglia, Norwich, England; George Sharman, Scripps Institution of Oceanography, La Jolla, California; William P. Roberts, Madison College, Harrisonburg, Virginia; Alexander N. Shor, Woods Hole Oceanographic Institution, Woods Hole, Massachusetts; Wendell A. Duffield, U.S. Geological Survey, Menlo Park, California; Jacques Varet, Dt. Géothermie, B.R.G.M., Orleans, France; Boris P. Zolotarev, Geological Institute of the USSR Academy of Sciences, Moscow, USSR; Richard Z. Poore, U.S. Geological Survey, Menlo Park, California; John C. Steinmetz, University of Miami, Miami, Florida; Angela M. Faller, Leeds University, Leeds, England; Kazuo Kobayashi, University of Tokyo, Nakano, Tokyo, Japan; Walter Vennum, California State College, Sonoma, Rohnert Park, California; David A. Wood, Bedford College, London, England; and Maureen Steiner, University of Wyoming, Laramie, Wyoming.

²From drilling log.

Site 407, and it seemed useful to position Site 408 on a bathymetric high where sediment accumulation would be unaffected by local slumping and turbidity currents. Reflection profiles immediately north of the site show turbidites which evidently originated from Iceland (Figure 1).

OPERATIONS

At Site 408 we drilled one hole to 361 meters and recovered 219.55 meters with continuous coring (Table 1).

The site is within OCP Site 11A on anomaly 6 (about 20 m.y.). Site survey data consisted of two *Vema* seismic profiles, trending southwest to northeast, and two *Meteor* 42B magnetic lines trending northwest to southeast (Figure 2). On the way to Site 407, *Glomar Challenger* made a magnetic and CSP profile through the region. We selected a drill site on anomaly 6 because it was easily identified, and is wide and reasonably continuous along the Reykjanes Ridge.

We approached the site at half-speed from the southeast, on course 313°T (310° made good), profiling with 5- and 10-in.³ airguns and the magnetometer (Figure 3). We selected our site atop a small abyssal hill which seemed to have an unusual sediment blanket about 370 ms (DT) thick (Figure 4). This was also just slightly down the northwest flank of anomaly 6. This small hill appears to be a sediment drift about 100 meters high. Anomaly 6 has a central low here, and evidently farther north too, according to other data. We dropped the beacon at 1910Z 29 July. Spud-in was at 0245Z 30 July, 7½ hours after beacon drop. Two hours of this time were spent on repair to bow thruster systems. While running in the hole, the drillpipe pinger was run. The bottom was felt at a pipe length of 1634 meters from the rig floor, which agreed with the EDO depth.

Coring was continuous down to 361 meters sub-bottom (Core 38). We terminated the hole when a medical emergency developed which required us to steam for Reykjavik. We began pulling pipe at 1800Z 31 July, and got underway at 2148Z, about four hours later.

The plot of coring time (time per 9.5 m of core, not including wire time) versus depth sub-bottom (Figure 5) shows about five minutes per core above 100 meters and 10 minutes per core below this level. Coring time increases greatly below Core 33 (313.5 m), correlating with basement rocks recovered in Core 34 and below. No correlations are obvious between sedimentary units and coring time. The upper basement drilled faster than the lower, indicating a contrast in flow vesicularity, thickness, or integrity.

SEDIMENT LITHOSTRATIGRAPHY

Introduction

Drilling at Hole 408 yielded 6 per cent recovery of sediment overlying basalt, which was penetrated at 323.6 meters below the sea floor. One thin unit of sediment interlayered within the basalt occurs between 343.43 and 345.0 meters (core recovery depth).

Three major units and six sub-units have been distinguished by lithologic characteristics (Figure 6) (depths quoted are core recovery depths, not correlated with drilling logs):

Unit 1 (0 to 38.0 m): Pleistocene calcareous sandy mud with some graded turbidite units.

Unit 2 (38.0 to 294.5 m): Pliocene to middle Miocene, predominantly nannofossil ooze, with three sub-units:

Sub-unit 2A (38.0 to 47.5 m): Pliocene siliceous marly nannofossil ooze.

Sub-unit 2B (47.5 to 212.0 m): Pliocene to upper Miocene nannofossil ooze.

Sub-unit 2C (212.0 to 294.5 m): middle to upper Miocene siliceous nannofossil ooze.

Unit 3 (294.5 to 323.6 m): lower Miocene calcareous mud grading to basalt gravel above the sediment/basalt contact, with two sub-units.:

Sub-unit 3A (294.5 to 313.5 m): lower Miocene calcareous mud.

Sub-unit 3B (313.5 to 323.6 m): lower Miocene glauconitic marly nannofossil ooze grading downward into basaltic sand and gravel.

Interlayered sediments (343.4 to 345.0 m): lower Miocene glauconitic ash-rich nannofossil ooze.

Description of Lithologic Units

Unit 1 (Hole 408, Cores 1 to 4, 0 to 38.0 m)

The sediments of Unit 1 are Pleistocene calcareous sandy mud with erratic basalt (probably ice-rafted), sand to gravel size, dispersed throughout the unit. Cores 2 and 3 (9.5 to 28.5 m) contain several graded turbidite sequences. In these beds, firm medium sandy mud grades upward into marly ooze. Parts of Cores 1 (0 to 9.5 m) and 4 (28.5 to 38.0 m) also may contain turbidite sequences, although distinct grading is not evident. Similarities in mineral components, benthic shell fragments, and poorly preserved laminations suggest a possible turbidity current origin in these moderately to intensely deformed cores.

The calcareous sandy mud consists of 70 to 80 per cent detrital minerals, of which 40 to 70 per cent is terrigenous clay in most samples. Coarse (>63 µm) detrital minerals (quartz, feldspar, and opaque minerals) generally total about 10 per cent, but vary from 2 to 35 per cent. Large (up to 1 cm in diameter) benthic foraminifers and pelecypod fragments are scattered throughout the unit. Carbonate analyses indicate a range of 4 to 70 per cent CaCO₃, with the average about 25 per cent. The carbonate is principally nannofossils and foraminifers. Volcanic ash is present as both fresh glass shards and lumps of clay-size material interpreted to be palagonite (altered ash). Ash content varies from 5 to 35 per cent.

The sediment color alternates between yellowish brown, grayish brown, and gray, with fluctuations caused by graded bedding; the lighter color usually occurs in the coarser basal sequences.

Mottling caused by bioturbation occurs throughout the unit, except in the firmer sandy basal units of turbidite sequences and in sections strongly deformed by the drilling process.

Unit 2 (Hole 408, Cores 5 to 31, 38.0 to 294.5 m)

Unit 2 consists predominantly of Pliocene to middle Miocene nannofossil ooze. Three sub-units are distinguished, owing to variable admixtures of biogenic silica.

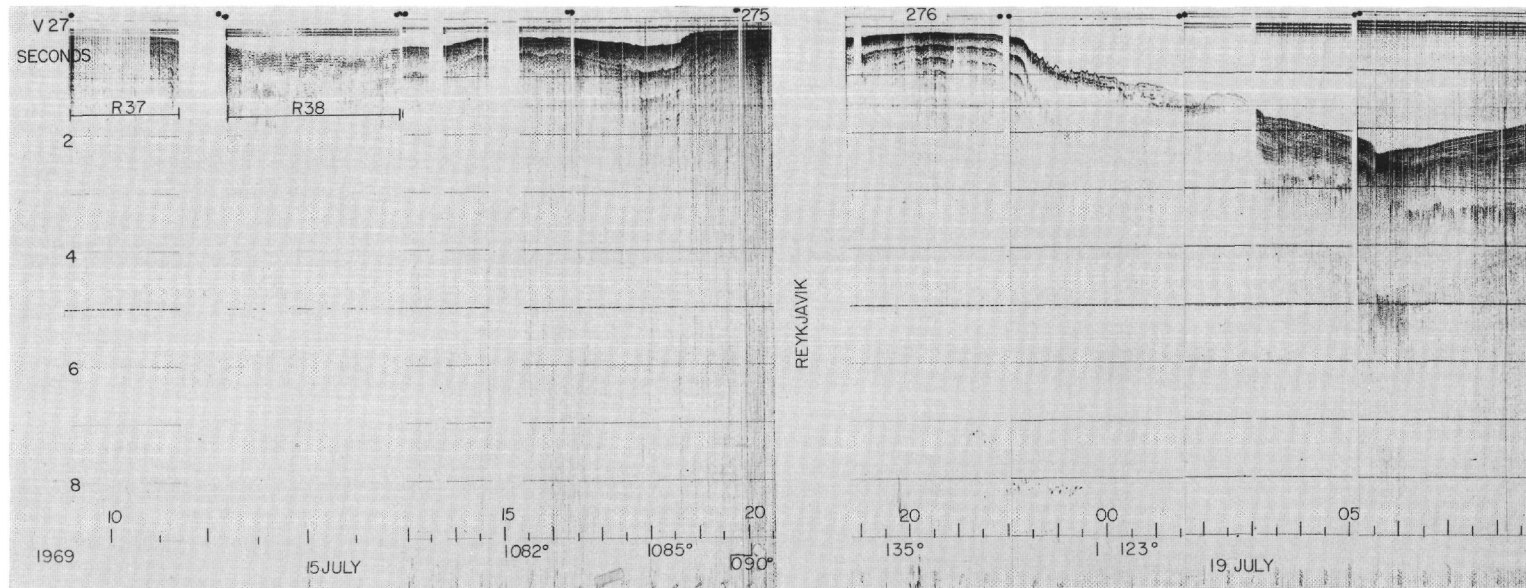
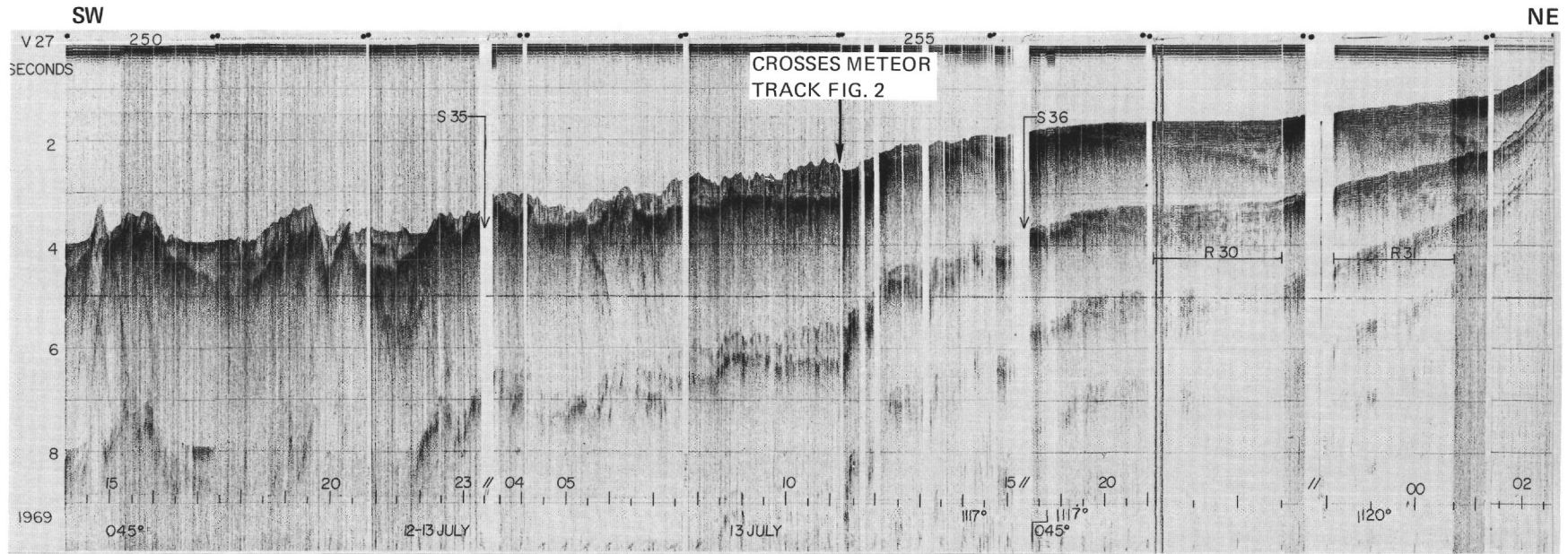


Figure 1. Reflection profiles near Site 408, taken by R/V Vema. Location in Figure 2.

TABLE 1
Coring Summary, Site 408

Core	Date (July 1976)	Time	Depth From Drill Floor (m)	Depth Below Sea Floor (m)	Length Cored (m)	Length Recovered (m)	Recovery (%)
1	30	0410	1634.0-1643.5	0.0- 9.5	9.5	8.64	91
2	30	0500	1643.5-1653.0	9.5- 19.0	9.5	7.30	77
3	30	0538	1653.0-1662.5	19.0- 28.5	9.5	6.57	69
4	30	0611	1662.5-1672.0	28.5- 38.0	9.5	7.70	81
5	30	0655	1672.0-1681.5	38.0- 47.5	9.5	6.42	68
6	30	0720	1681.5-1691.0	47.5- 57.0	9.5	4.23	45
7	30	0759	1691.0-1700.5	57.0- 66.5	9.5	2.15	23
8	30	0846	1700.5-1710.0	66.5- 76.0	9.5	2.80	29
9	30	0926	1710.0-1719.5	76.0- 85.5	9.5	3.20	34
10	30	1015	1719.5-1729.0	85.5- 95.0	9.5	6.60	69
11	30	1155	1729.0-1738.5	95.0-104.5	9.5	8.21	86
12	30	1240	1738.5-1748.0	104.5-114.0	9.5	3.29	35
13	30	1335	1748.0-1757.5	114.0-123.5	9.5	4.89	51
14	30	1430	1757.5-1767.0	123.5-133.0	9.5	0.20	42
15	30	1555	1767.0-1776.5	133.0-142.5	9.5	7.10	75
16	30	1645	1776.5-1786.0	142.5-152.0	9.5	3.85	41
17	30	1740	1786.0-1795.5	152.0-161.5	9.5	6.85	72
18	30	1820	1795.5-1805.0	161.5-171.0	9.5	5.10	54
19	30	2005	1805.0-1814.5	171.0-180.5	9.5	9.63	101
20	30	2100	1814.5-1824.0	180.5-190.0	9.5	3.42	36
21	30	2200	1824.0-1833.5	190.0-199.5	9.5	5.76	61
22	31	0007	1833.5-1843.0	199.5-209.0	9.5	4.15	44
23	31	0058	1843.0-1852.5	209.0-218.5	9.5	4.21	44
24	31	0146	1852.5-1862.0	218.5-228.0	9.5	8.30	87
25	31	0237	1862.0-1871.5	228.0-237.5	9.5	9.16	96
26	31	0322	1871.5-1881.0	237.5-247.0	9.5	7.92	83
27	31	0455	1881.0-1890.5	247.0-256.5	9.5	9.64	101
28	31	0550	1890.5-1900.0	256.5-266.0	9.5	5.05	53
29	31	0635	1900.0-1909.5	266.0-275.5	9.5	3.20	34
30	31	0720	1909.5-1919.0	275.5-285.0	9.5	6.84	72
31	31	0804	1919.0-1928.5	285.0-294.5	9.5	8.38	88
32	31	0850	1928.5-1938.0	294.5-304.0	9.5	8.63	91
33	31	0939	1938.0-1947.5	304.0-313.5	9.5	9.25	97
34	31	1049	1947.5-1957.0	313.5-323.0	9.5	8.10	85
35	31	1210	1957.0-1966.5	323.0-332.5	9.5	1.00	11
36	31	1405	1966.5-1976.0	332.5-342.0	9.5	5.11	54
37	31	1640	1976.0-1985.5	342.0-351.5	9.5	3.00	32
38	31	1853	1985.5-1995.0	351.5-361.0	9.5	3.70	39
Total					361.0	219.55	61

Sub-unit 2A (Core 5, 38.0 to 47.5 m)

This unit, the top of which coincides with the Pleistocene/Pliocene boundary (hiatus), shows a marked decrease in coarse detrital components from Unit 1, to less than 10 per cent. Biogenic silica (sponge spicules and radiolarians) increases to 10 to 30 per cent and volcanic ash to 70 to 80 per cent in palagonitic ash zones. Calcareous microfossils range up to 75 per cent.

Color varies between olive-gray to gray in the siliceous nannofossil ooze and dark gray or black in the ash layers.

The core is moderately to strongly deformed, and although some laminations and sedimentary clasts occur, there is no mottling caused by bioturbation.

Sub-unit 2B (Cores 6 to 23, 47.5 to 212.0 m)

This sub-unit is a homogeneous sequence of nannofossil ooze with some intervals of foraminiferal nannofossil ooze. Carbonate analyses indicate 70 to 100 per cent CaCO₃ in this sub-unit. Coarse detrital grains generally make up less than 10 per cent, and consist mostly of opaque grains with rare feldspars. Biogenic silica, composed mainly of sponge spicules but also including radiolarian fragments and rare diatoms, averages about 10 per cent in most samples. Volcanic ash is uniformly below 10 per cent, except in rare ash layers.

Most cores in the upper half of the sub-unit are intensely deformed. Even in the firmer lower portion of Sub-unit 2B, sedimentary structures are not prominent, except for rare grayish green glauconite-rich (2 to 3% glauconite) laminations. Bioturbation is almost completely absent from the unit, except near the base, which is slightly mottled.

Sub-unit 2C (Cores 23 to 31, 212.0 to 294.5 m)

Near the bottom of Core 23, the biogenic silica content increases to 10 to 15 per cent in most samples, and up to 20 to 30 per cent in Cores 28 to 30 (265.5 to 285 m). The most common siliceous component is sponge spicules, but large numbers of silt-size siliceous needles lacking central tubes are interpreted as radiolarian spines. Volcanic ash content is about the same as in Sub-unit 2B above (Figure 6). Black basaltic sand grains are scattered uniformly throughout the sub-unit. Coarse detrital components are rare (less than 3% in most samples).

Beginning near the bottom of Core 26 (Section 5, 243.5 m) and continuing through Core 28 (to 261 m), and in Core 31 (285 to 294.5 m), are several graded units interpreted as turbidites. The basal unit of the turbidites is firm, dark gray muddy sand, generally about 5 cm thick, which grades upward into lighter gray calcareous mud. The basal contacts of turbidite units are sharp and erosional where they have not been obscured by bioturbation, which is common in all but the firmest of the basal turbidite units. Cores 29 and 30 are too highly disturbed to show sedimentary structures, but have a lithology similar to cores above and below.

This sub-unit is generally greenish gray or olive-gray, except in the darker gray basal units of turbidites.

Unit 3 (Hole 408, Cores 32 to 35, 294.5 to 323.6 m)

Unit 3 is lower Miocene calcareous mud with increasing glauconite content toward the sediment/basalt contact.

Sub-unit 3A (Cores 32 to 33, 294.5 to 313.5 m)

This sub-unit is lower Miocene calcareous mud with glauconite content increasing downward from 2 to 3 per cent at the top to as much as 15 per cent at the bottom of the sub-unit. Black basaltic sand is dispersed uniformly throughout.

Carbonate content ranges between 23 to 35 per cent, and terrigenous clay makes up to 30 to 60 per cent of the sub-unit. Coarse detrital grains (mostly opaques) total less than 5 per cent. Biogenic silica, mostly sponge spicules, make up less than 5 per cent of most samples, and ash contents range from 5 to 10 per cent.

Bioturbation mottling occurs at the base of Cores 32 and 33. The remainder of both cores is disturbed. Colors are grayish olive to olive-green.

Sub-unit 3B (Cores 34 to 35, 313.5 to 323.6 m)

This sub-unit is lower Miocene glauconitic marly nannofossil ooze, very similar in its upper part to Sub-unit 3A, except for high glauconite (25%) and CaCO₃ (35 to 55%) contents.

Black basaltic sand is uniformly dispersed through the two cores, and biogenic silica and ash contents range from 5 to 10 per cent.

Except for one possible turbidite unit in Core 34, Section 5, most of the sub-unit is intensely deformed. Colors range from grayish olive-green with some mottles to dusky yellow-green.

The lower 31 cm of the sub-unit grades from nannofossil-rich basaltic sand to basalt gravel just above the basalt in Core 35. The sand is composed of basalt fragments

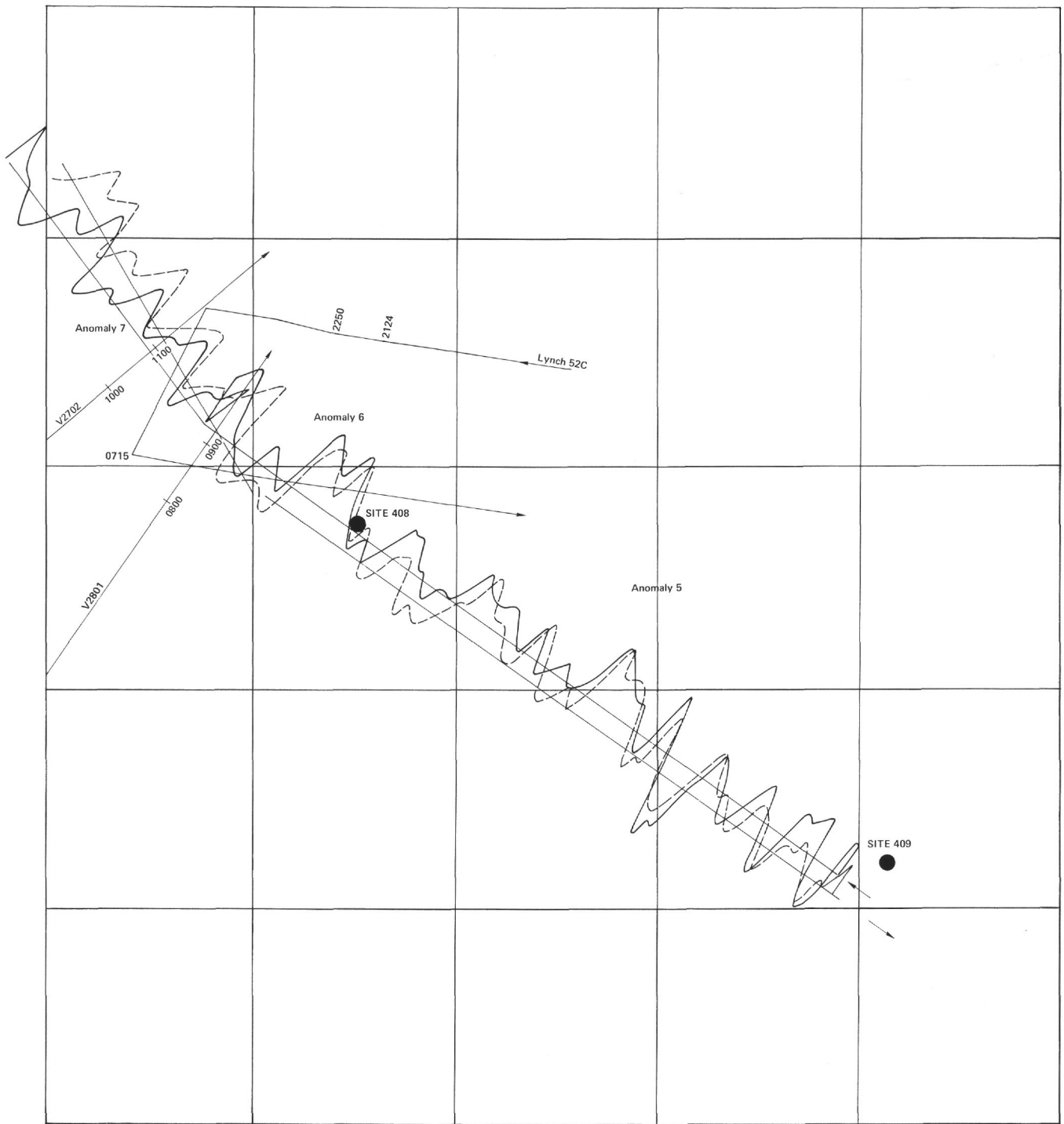


Figure 2. Meteor Cruise 42B magnetic lines, taken near Site 408.

(50%), volcanic glass (20%), nannofossils (20%), and clay (10%).

Interlayered Sediments (Hole 408, Cores 36 to 37, 343.3 to 345 m)

In the bottom of Core 36 and all of Core 37 are 21 pieces of what appear to be baked glauconitic ash-rich nannofossil chalk interlayered with basalt. In addition to nannofossils

dated as lower Miocene, the sediments consists of 5 to 10 per cent glauconite and 10 to 15 per cent volcanic ash.

BIOSTRATIGRAPHY

Sediments ranging from Quaternary to Miocene were recovered at Site 408. The oldest sediments recovered, which were interlayered with basalt in Cores 35 and 37 (323 to 345 m sub-bottom), are lower Miocene.

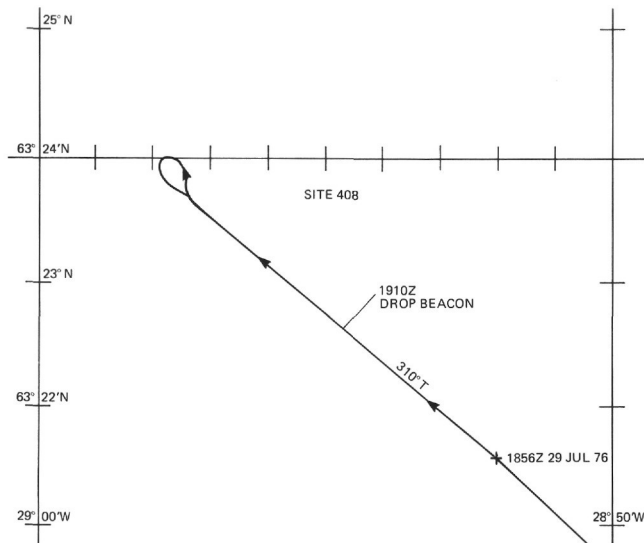


Figure 3. Track chart of D/V Glomar Challenger in vicinity of Site 408.

A Pleistocene turbidite sequence was recovered in Cores 1 to 4 (0 to 36.5 m sub-bottom). Ice-rafted mineral grains are common to abundant throughout the sequence, and

occasional larger basalt erratics are present in all cores. Here as at Site 407, the base of the glacial section is Pleistocene, again suggesting that a portion of the upper Pliocene to lower Pleistocene is absent or highly condensed. The occurrence of this feature at both Sites 407 and 408 suggests that it may be present over a large area of the western Reykjanes Ridge.

The Pliocene section, in general, grades downward from siliceous marly nannofossil ooze to light gray to white nannofossil ooze; the Miocene/Pliocene boundary occurs between Samples 13, CC (119 m sub-bottom) and 14, CC (123.5 m sub-bottom). For the present, Core 14 is considered to represent the top of the Miocene.

The upper Miocene section consists of relatively uniform nannofossil ooze. In contrast to Site 407, the upper Miocene/middle Miocene boundary at Site 408 could not be clearly delineated, but our preliminary data indicate that it occurs between Samples 23, CC and (213 m sub-bottom) and 26, CC (245.5 m sub-bottom). The transitional nature of the microfossil assemblages in this interval indicates only a minor middle Miocene/upper Miocene unconformity in Hole 408.

The middle Miocene section consists of light gray to gray siliceous nannofossil ooze and siliceous marly calcareous ooze. These sediments are similar to those of equivalent age at Site 407, except that they lack the greenish yellow color

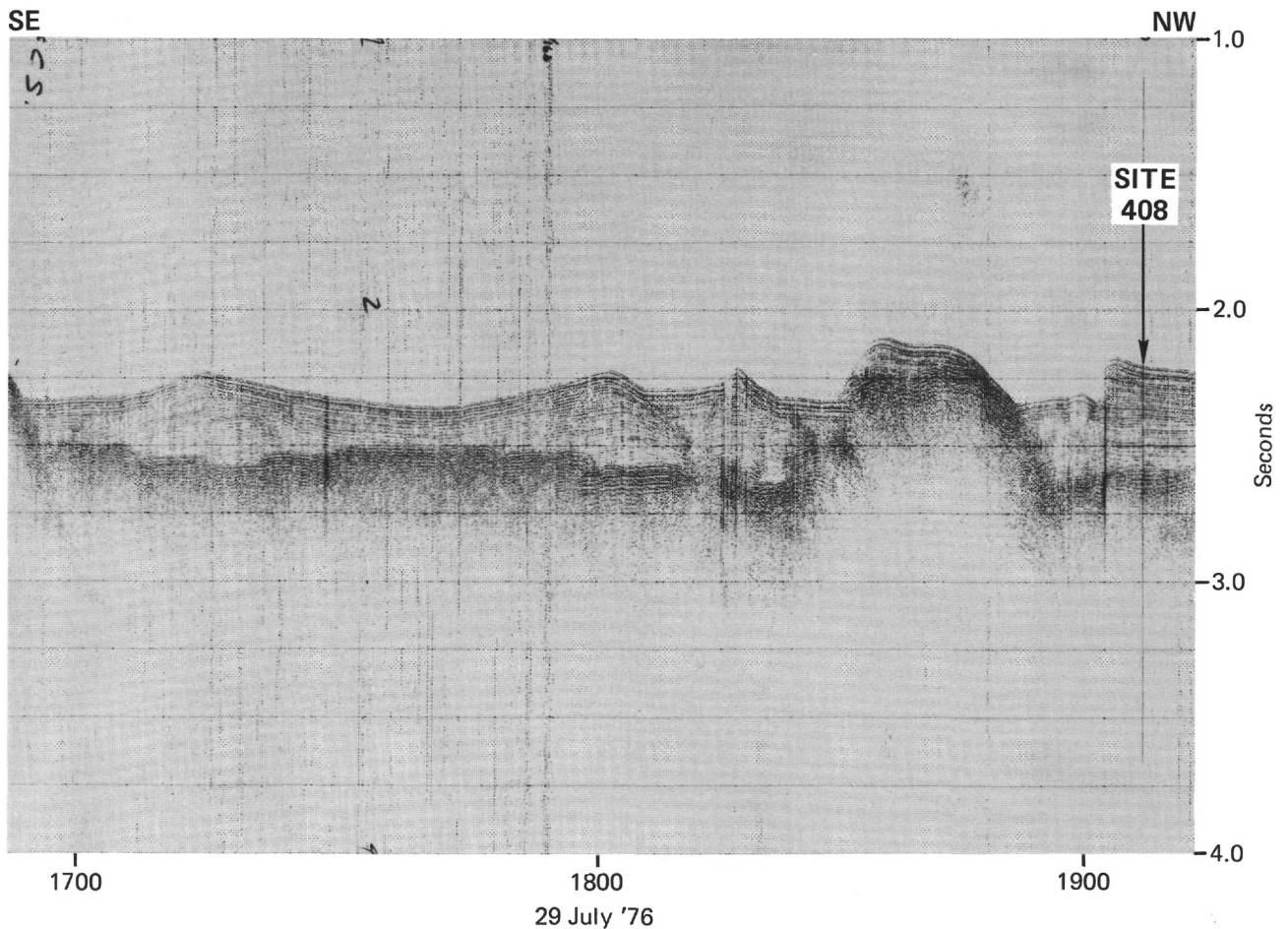


Figure 4. Seismic profile from Glomar Challenger in the vicinity of Site 408.

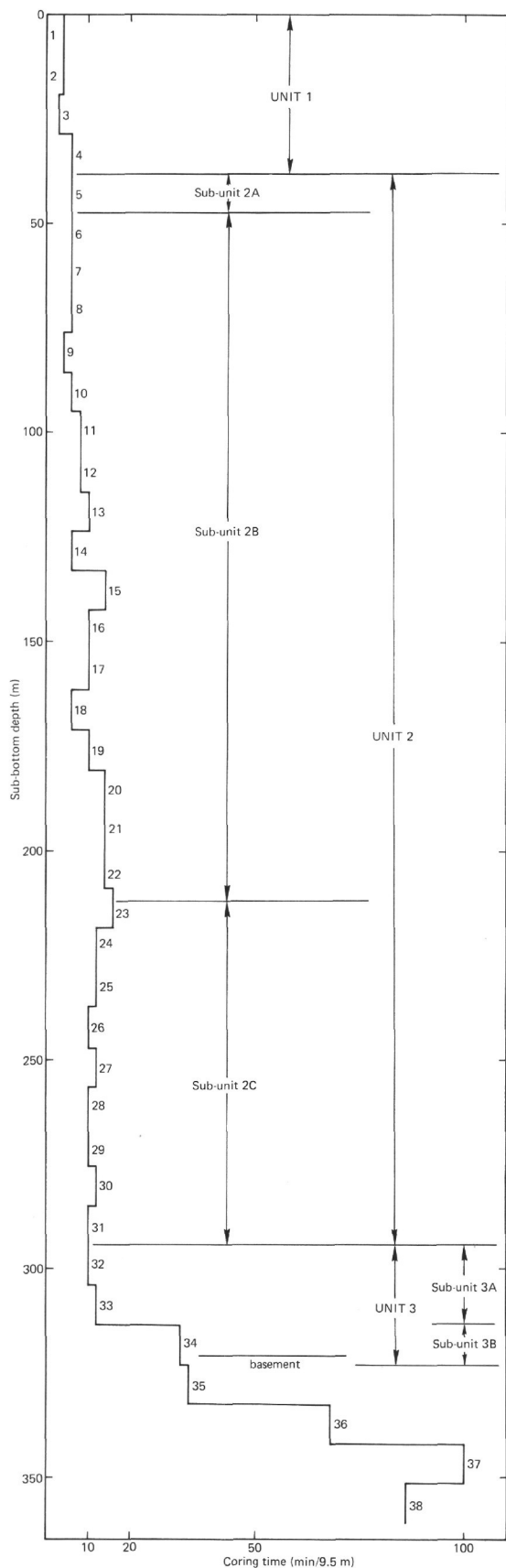


Figure 5. Coring time versus depth for Hole 408.

and are less indurated. The lower Miocene/middle Miocene boundary is placed between Samples 32, CC (303 m sub-bottom) and 31, CC (293 m sub-bottom). A discontinuity in the nannofossil assemblages between Samples 30, CC (282 m sub-bottom) and 31, CC (293.5 m sub-bottom) suggests a possible hiatus within the middle Miocene.

Lower Miocene glauconitic calcareous mud and glauconitic marly nannofossil ooze occur above basalt (Cores 33 and 34). Nannofossil assemblages recovered from glauconitic chalk interlayered with basalt in Cores 35 (~323 m sub-bottom) and 37 (~345 m sub-bottom) are lower Miocene, probably Zones NN1 to NN3.

Planktonic Foraminifers

What follows is based on shipboard examination of core-catcher samples. (See also Table 2.) Depths for core-catcher samples are rounded to the nearest one-half meter.

Samples 1, CC to 4, CC contain assemblages dominated by *Neogloboquadrina pachyderma* (sinistral). Other taxa include *Globorotalia inflata*, *G. scitula*, *Globigerina bulloides*, and *Turborotalita quinqueloba*. The occurrence of *Neogloboquadrina atlantica* (sinistral) in Sample 5, CC suggests that the Pliocene/Pleistocene boundary lies between Samples 4, CC (36 m sub-bottom) and 5, CC (44.5 m sub-bottom).

Pliocene assemblages at Site 408 are characterized by common to abundant occurrences of left-coiling *Neogloboquadrina atlantica*. Accessory taxa include *Orbulina universa*, *Globorotalia scitula*, *Neogloboquadrina acostaensis*, and *N. humerosa*.

The occurrence of *Globorotalia puncticulata* in Samples 6, CC to 9, CC suggests that this interval is lower Pliocene, but the nannofossil assemblages from Samples 6, CC and 7, CC suggest the upper Pliocene. The first occurrence (downward) of abundant right-coiling *Neogloboquadrina atlantica* is in Sample 14, CC (~124 m sub-bottom). This level is considered to be upper Miocene, and the Miocene/Pliocene boundary is placed between this level and Sample 13, CC (199 m sub-bottom).

Upper Miocene assemblages from Samples 14, CC to 23, CC (213 m sub-bottom) are characterized by common to abundant *Neogloboquadrina acostaensis* and *Globigerina bulloides*; *N. atlantica* (dextral) is an important faunal component in the upper part of this interval. Sample 24, CC (227 m sub-bottom) contains a few specimens of *N. acostaensis*, and is also upper Miocene. Sample 26, CC (245.5 m sub-bottom) contains *Globigerina druryi*, *G. aff. G. nepenthes*, and *Globorotalia mayeri*, which suggests assignment to middle Miocene Zone N 14. The assemblage from Sample 25, CC is not particularly diagnostic as to age; so the middle Miocene/upper Miocene boundary falls somewhere between Samples 26, CC and 24, CC.

The occurrence of *Globigerinoides siccanus* in Sample 32, CC suggests a level close to the lower Miocene/middle Miocene boundary, so we place this boundary somewhat arbitrarily between Samples 32, CC (303 m sub-bottom) and 31, CC (293 m sub-bottom).

Preservation of foraminifers in Samples 33, CC and 34, CC varies from poor to moderate, and glauconite casts of

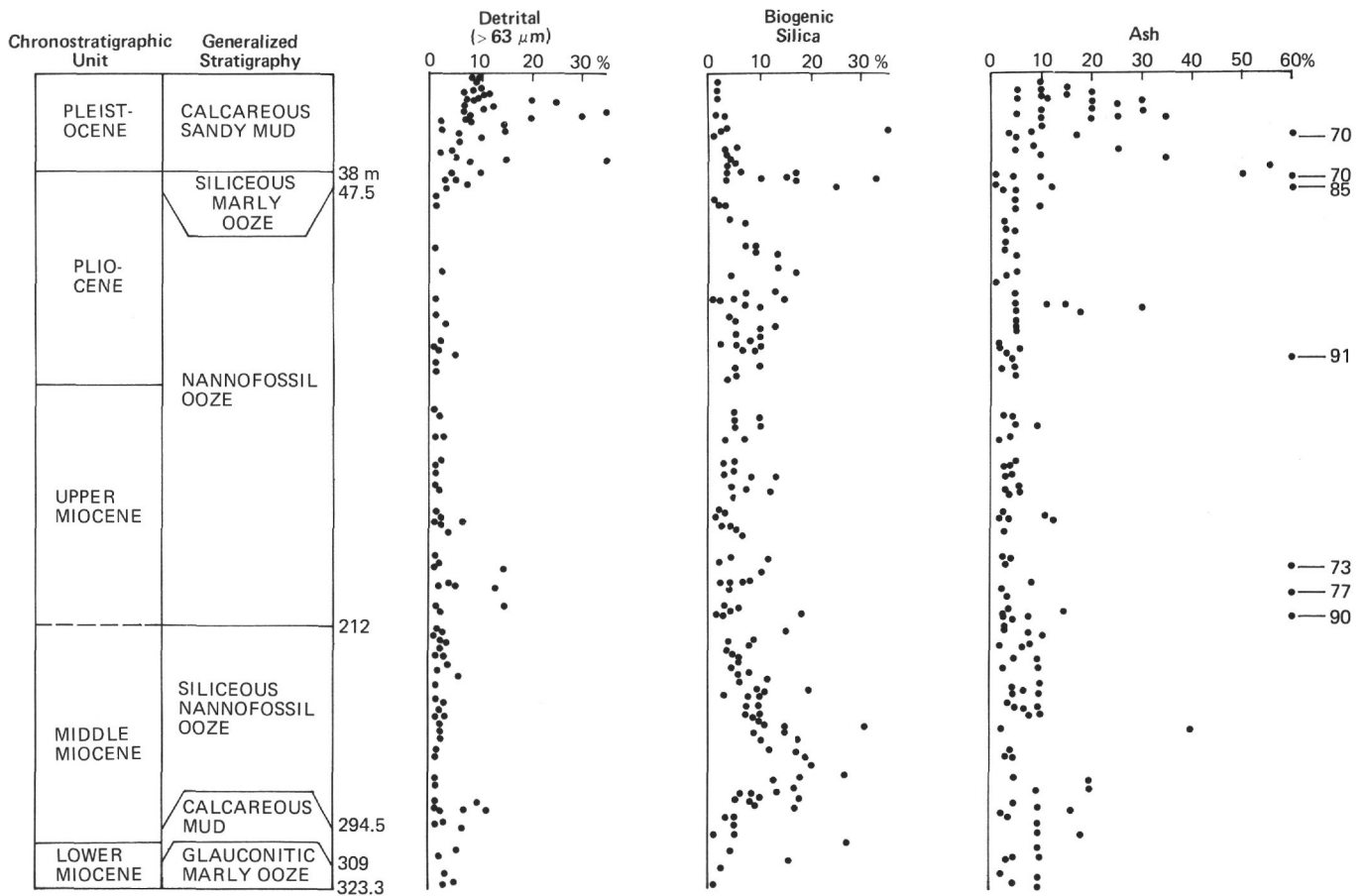


Figure 6. Lithologic units and smear-slide analyses, Hole 408.

foraminifers and fairly large broken specimens are common, perhaps indicating transport by bottom currents. All taxa identified are compatible with the lower Miocene assignment indicated for these samples by the associated nannofossil assemblage.

Nannofossils

Site 408 sediments can be generally characterized here as nannofossil ooze in which the taxa present are well preserved. The abundance of biogenic silica (i.e., sponge spicules, diatoms, and radiolarians) (Samples 23, CC to 29, CC) and of volcanic ash (Samples 1, CC to 4, CC and 32, CC to 35, CC) causes some dilution of the nannofossils, but enough are usually present to establish the characteristics of the assemblage. Age determinations here are not considered rigorous, owing to the low assemblage diversity and lack of reliable indicators (in most cases discoasters, ceratoliths, and sphenoliths) at this high latitude. All observations reported here were made only on core-catcher (CC) samples, unless otherwise noted. (See also Table 2.)

Samples 1,CC through 3,CC (8.6 to 25.6 m sub-bottom) are Pleistocene (Zones NN 19/20), and are characterized by *Coccolithus pelagicus*, *Cyclococcolithina leptopora*, *Gephyrocapsa* spp., and *Syracosphaera histrica*. *Gephyrocapsa oceanica* is present in these samples, and first occurs in Sample 3,CC, establishing the lower boundary of Zone NN 19. *Emiliania annula* last occurs in

Sample 2,CC, establishing the lower/upper Pleistocene boundary (between NN 19 and NN 20) between Samples 1,CC and 2,CC. Sample 4,CC (36.2 m) is essentially barren, and yields only rare *C. pelagicus* among the volcanic ash.

Samples 5,CC through 7,CC (44.4 to 59.2 m) are designated upper Pliocene (Zones NN 16/18), on the basis of the following assemblage: *C. pelagicus*, *C. leptopora*, *E. annula*, *S. histrica*, and *Helicopontosphaera sellii*. *Discoaster brouweri* occurs in rare abundance in Sample 5,CC, and together with the last occurrence of *H. sellii*, defines the upper limit of the uppermost Pliocene Zone (NN 18). The first occurrence of *E. annula*, in Sample 7,CC, defines the lower limit of the upper Pliocene (Zone NN 16).

Samples 8,CC through 26,CC (69.3 to 245.4 m) are characterized by assemblages transitional from the lower Pliocene to the upper Miocene. No good markers are present which would allow subdivision of this long interval. The taxa present consist of *C. pelagicus*, *C. leptopora*, *R. pseudumbilica*, *Helicopontosphaera kamptneri*, *H. sellii*, and *Sphenolithus abies*. *Discoaster bollii*, *D. challengerii*, *D. exilis*, and *D. variabilis* occur sporadically and as a rule sparsely throughout the interval. The lower limit of the upper Miocene at Sample 26,CC is determined by the occurrence of middle Miocene species, namely *Coronocylus* sp. and *Cyclicargolithus floridanus*, in Sample 27,CC (256.6 m). Middle Miocene species may

TABLE 2
Paleo/Biostratigraphic Summary of Core-Catcher Samples (CC)

Core	Depth (m)	Chronostratigraphic Unit	Planktonic Foraminifers	Calcareous Nannofossils	
1	8.5	Pleistocene	<i>Neogloboquadrina pachyderma</i> (S) <i>Globigerina bulloides</i> <i>Globorotalia inflata</i> <i>G. scitula</i> <i>Turborotalia quinqueloba</i>	<i>Coccolithus pelagicus</i> <i>Cyclococcolithina leptopora</i> <i>Gephyrocapsa oceanica</i> <i>G. caribbeanica</i> <i>Syracosphaera histrica</i>	
2	17.0	Pleistocene	<i>N. pachyderma</i> (S) <i>Turborotalita quinqueloba</i> <i>G. bulloides</i> <i>G. inflata</i>	<i>C. pelagicus</i> <i>C. leptopora</i> <i>G. oceanica</i> <i>Emiliania annula</i>	
3	25.5	Pleistocene	As above	<i>C. pelagicus</i> <i>C. leptopora</i> <i>G. oceanica</i> <i>Helicopontosphaera kamptneri</i>	
4	36.0	Pleistocene	<i>N. pachyderma</i> (S) <i>G. scitula</i> <i>T. quinqueloba</i>	Essentially barren <i>C. pelagicus</i>	
5	44.5	Pliocene	<i>Neogloboquadrina atlantica</i> (S) <i>G. bulloides</i> <i>Orbulina universa</i> <i>T. quinqueloba</i> <i>G. aff. G. inflata</i>	<i>C. pelagicus</i> <i>E. annula</i> <i>Reticulofenestra pseudumbilica</i> <i>Discoaster brouweri</i> <i>Helicopontosphaera sellii</i>	
6	51.5	Pliocene	<i>Neogloboquadrina atlantica</i> (S) <i>Globigerina bulloides</i> <i>Globorotalia puncticulata</i> <i>Orbulina universa</i> <i>Turborotalita quinqueloba</i>	<i>C. pelagicus</i> <i>H. kamptneri</i> <i>E. annula</i> <i>R. pseudumbilica</i> <i>H. sellii</i>	
7	59.0	Pliocene	As above	<i>C. pelagicus</i> <i>C. leptopora</i> <i>H. sellii</i> <i>R. pseudumbilica</i>	<i>E. annula</i>
8	69.5	Pliocene	As above	<i>C. pelagicus</i> <i>H. sellii</i> <i>H. kamptneri</i> <i>C. leptopora</i>	<i>R. pseudumbilica</i>
9	79.0	Pliocene	As above	<i>C. pelagicus</i> <i>R. pseudumbilica</i> <i>C. leptopora</i> <i>H. kamptneri</i>	<i>H. sellii</i> <i>Discoaster brouweri</i>
10	92.0	Pliocene	<i>Neogloboquadrina acostaensis</i> <i>N. atlantica</i> (S) <i>Globigerina bulloides</i> <i>Orbulina universa</i> <i>Globorotalia scitula</i>	As above	
11	103.0	Lower Pliocene	<i>Neogloboquadrina atlantica</i> (S) <i>N. pachyderma sensulato</i>	<i>C. pelagicus</i> <i>R. pseudumbilica</i>	
			<i>Globigerina bulloides</i> <i>Turborotalita quinqueloba</i>	<i>H. kamptneri</i> <i>C. leptopora</i>	
12	108.0	Lower Pliocene	As above, plus <i>N. acostaensis</i> <i>N. humerosa</i>	<i>C. pelagicus</i> <i>C. leptopora</i> <i>R. pseudumbilica</i> <i>Discoaster exilis</i>	<i>Discoaster bollii</i> <i>D. brouweri</i>
13	119.0	Lower Pliocene	As above	<i>C. pelagicus</i> <i>C. leptopora</i> <i>H. kamptneri</i> <i>R. pseudumbilica</i>	<i>D. exilis</i> <i>D. brouweri</i>
14	123.5	Upper Miocene	<i>N. atlantica</i> (D) <i>N. acostaensis</i> <i>N. humerosa</i> <i>Globigerina bulloides</i>	<i>D. exilis</i> <i>D. brouweri</i> <i>D. variabilis</i> <i>C. pelagicus</i>	<i>R. pseudumbilica</i> <i>H. kamptneri</i>
15	140	Upper Miocene	As above	<i>C. pelagicus</i> <i>Helicopontosphaera intermedia</i> <i>C. leptopora</i> <i>R. pseudumbilica</i> <i>Sphenolithus abies</i>	<i>H. kamptneri</i>
16	146.5	Upper Miocene	<i>Neogloboquadrina atlantica</i> (D) <i>N. acostaensis</i> <i>N. humerosa</i> <i>Globorotalia scitula</i> <i>Turborotalita quinqueloba</i>	<i>C. pelagicus</i> <i>H. kamptneri</i> <i>S. abies</i> <i>R. pseudumbilica</i>	<i>D. bollii</i>

TABLE 2 – Continued

Core	Depth (m)	Chronostratigraphic Unit	Planktonic Foraminifers	Calcareous Nannofossils
17	159.0	Upper Miocene	<i>N. acostaensis</i> <i>N. aff. N. atlantica</i> (D) <i>N. aff. N. pachyderma</i> <i>G. bulloides</i> <i>G. scitula</i>	<i>D. exilis</i> <i>D. brouweri</i> <i>D. challengeri</i> <i>D. quinquaramus</i> <i>H. sellii</i> <i>R. pseudoumbilica</i> <i>C. pelagicus</i> <i>S. abies</i> <i>H. kamptneri</i>
18	166.5	Upper Miocene	As above	<i>S. abies</i> <i>C. leptopora</i> <i>C. pelagicus</i> <i>R. pseudoumbilica</i> <i>H. kamptneri</i> <i>D. brouweri</i>
19	180.5	Upper Miocene	As above	<i>R. pseudoumbilica</i> <i>C. pelagicus</i> <i>S. abies</i> <i>C. leptopora</i>
20	184.0	Upper Miocene	As above	<i>S. abies</i> <i>S. moriformis</i> <i>C. pelagicus</i> <i>R. pseudoumbilica</i> <i>Coccolithus eopelagicus</i>
21	196.0	Upper Miocene	<i>Neogloboquadrina acostaensis</i> <i>Globorotalia continuosa</i> <i>Turborotalita quinqueloba</i> <i>Globoquadrina dehiscens</i>	<i>C. pelagicus</i> <i>R. pseudoumbilica</i> <i>H. kamptneri</i> <i>S. abies</i> <i>S. moriformis</i>
22	203.5	Upper Miocene	<i>N. acostaensis</i> <i>N. aff. N. atlantica</i> (D) <i>G. continuosa</i> <i>G. bulloides</i>	<i>C. pelagicus</i> <i>R. pseudoumbilica</i> <i>H. kamptneri</i> <i>S. abies</i> <i>S. moriformis</i>
23	213.0	Upper Miocene	<i>N. acostaensis</i> <i>G. continuosa</i> <i>T. quinqueloba</i> <i>G. bulloides</i> <i>G. scitula</i>	as above, plus <i>Discoaster brouweri</i>
24	227.0	Upper Miocene	<i>N. acostaensis</i> <i>G. continuosa</i> <i>Globigerina woodi</i> <i>T. quinqueloba</i>	<i>C. pelagicus</i> <i>R. pseudoumbilica</i> <i>S. abies</i> <i>H. kamptneri</i>
25	237.0	Middle/Upper Miocene	<i>Globigerina praebulloides</i> <i>G. bulloides</i> <i>Globorotalia mayeri</i> <i>G. continuosa</i> <i>T. quinqueloba</i>	As above, plus <i>C. eopelagicus</i>
26	245.5	Middle Miocene	<i>Globigerina praebulloides</i> <i>G. aff. G. bulloides</i> <i>G. druryi</i> <i>G. aff. G. nepenthes</i> <i>Globorotalia mayeri</i>	<i>C. pelagicus</i> <i>R. pseudoumbilica</i> <i>H. kamptneri</i> <i>S. abies</i> <i>S. moriformis</i> <i>C. eopelagicus</i> <i>C. leptopora</i>
27	256.5	Middle Miocene	<i>C. praebulloides</i> <i>Globorotalia miozea</i> <i>Globoquadrina altispira</i>	As above, plus <i>Coronocycclus</i> sp.
28	261.5	Middle Miocene	<i>G. praebulloides</i> <i>Orbulina suturalis</i> <i>Globorotalia miozea</i> <i>G. praemenardii</i>	<i>C. pelagicus</i> <i>R. pseudoumbilica</i> <i>H. kamptneri</i> <i>S. abies</i> <i>S. moriformis</i>
29	269.0	Middle Miocene	<i>Globigerina praebulloides</i> <i>G. druryi</i> <i>G. miozea</i> <i>G. praemenardii</i> <i>Sphaeroidinellopsis seminulina</i>	<i>C. pelagicus</i> <i>C. leptopora</i> <i>R. pseudoumbilica</i> <i>H. sellii</i> <i>S. abies</i> <i>H. kamptneri</i>
30	282.5	Middle Miocene	<i>Globigerina praebulloides</i> <i>Globigerinoides triloba</i> <i>Globoquadrina altispira</i> <i>G. spp.</i>	<i>C. pelagicus</i> <i>R. pseudoumbilica</i> <i>C. leptopora</i> <i>H. kamptneri</i> <i>Cyclicargolithus floridanus</i>
31	293.5	Middle Miocene	<i>G. praebulloides</i> <i>Globorotalia praescitula</i> <i>Globigerinoides trilobus</i> <i>Sphaeroidinellopsis seminulina</i> <i>Globoquadrina</i> spp.	<i>C. pelagicus</i> <i>R. pseudoumbilica</i> <i>S. heteromorphus</i> <i>H. kamptneri</i> <i>D. kugleri</i> <i>S. moriformis</i> <i>D. deflandrei</i> <i>D. exilis</i> <i>D. challengeri</i>
32	303.5	Lower Miocene	<i>G. praebulloides</i> <i>G. trilobus</i> <i>G. sicanus</i> <i>G. praescitula</i> <i>Globigerina woodi</i>	<i>R. pseudoumbilica</i> <i>S. moriformis</i> <i>H. kamptneri</i> <i>S. heteromorphus</i> <i>C. pelagicus</i> <i>H. intermedia</i> <i>C. floridanus</i> <i>D. deflandrei</i>

TABLE 2 – Continued

Core	Depth (m)	Chronostratigraphic Unit	Planktonic Foraminifers	Calcareous Nannofossils
33	313.0	Lower Miocene	<i>G. praebulloides</i> <i>G. woodi</i> <i>G. trilobus</i> <i>Globoquadrina</i> spp.	<i>C. pelagicus</i> <i>R. pseudoumbilica</i> <i>S. moriformis</i> <i>H. kamptneri</i> <i>D. deflandrei</i> <i>C. floridanus</i>
34	321.5	Lower Miocene	<i>G. praebulloides</i> <i>G. woodi</i> s. l. <i>G. praescitula</i> <i>Globoquadrina</i> spp.	<i>R. pseudoumbilica</i> <i>C. pelagicus</i> <i>S. heteromorphus</i> <i>D. deflandrei</i> <i>H. kamptneri</i> <i>C. floridanus</i>
35	324.0	Lower Miocene	Not examined for foraminifers	<i>R. pseudoumbilica</i> <i>R. bisecta</i> <i>S. moriformis</i> <i>H. kamptneri</i> <i>C. pelagicus</i> <i>D. deflandrei</i>
36	–	Lower Miocene	Not examined for foraminifers	Sample 35-1, piece 4a <i>R. pseudoumbilica</i> <i>S. moriformis</i> <i>H. kamptneri</i> <i>R. bisecta</i> <i>C. pelagicus</i> <i>C. floridanus</i> <i>D. deflandrei</i>
37	–	Lower Miocene	Not examined for foraminifers	Sample 37-2, piece 12 <i>C. pelagicus</i> <i>S. moriformis</i> <i>R. pseudoumbilica</i> <i>D. deflandrei</i> <i>H. kamptneri</i> <i>R. bisecta</i> <i>C. floridanus</i>

range farther up in the core, but because of their rarity were not noted.

Samples 28,CC through 30,CC (261.6 to 282.3 m) contain unremarkable middle Miocene taxa: *C. pelagicus*, *C. leptopora*, *H. intermedia*, *H. kamptneri*, *R. pseudoumbilica*, *S. abies*, and *S. moriformis*. Samples 31,CC and 32,CC (293.4 to 303.1 m) are in the middle Miocene *Sphenolithus heteromorphus* Zone (NN 5), according to the same above assemblage, but they also contain a particularly notable abundance of *S. heteromorphus*. Sample 33,CC (313.2 m) is middle Miocene. *Reticulofenestra bisecta* occurs in Sample 34,CC (321.6 m) and establishes it as being no older than the *Helicopontosphaera ampliapertura* Zone (NN 4).

Samples from Core 35, Section 1, Piece 4a, (323 m) and Core 37, Section 2, Piece 12 (345 m), were obtained from chalks on basalt substrates. Neither chalk sample shows evidence of baking, and nannofossils present are fairly abundant and in good condition among the ash matrix. Both contain assemblages characteristic of the lower Miocene: *C. floridanus*, *C. pelagicus*, *D. deflandrei*, *H. kamptneri*, *R. bisecta*, *R. pseudoumbilica*, and *S. moriformis*.

PHYSICAL PROPERTIES OF SEDIMENTS

Sonic velocity, wet bulk density, and water content measurements of samples of the sedimentary column at Site 408 are shown in Figures 7, 8, and 9.

The sonic velocity profile shows an increased velocity for two samples at about 160 meters sub-bottom, a pattern that apparently yielded a seismic reflection at Site 407, yet none was observed here. The very deepest sediments show a rise in seismic velocity just above basement.

The wet bulk density and water-content data show the characteristic inverse relationship, and show two distinct groups in the sedimentary column, separated at approximately 50 meters sub-bottom. Above this level lie less dense sediments with a higher water content than those below. This division corresponds roughly to the base of

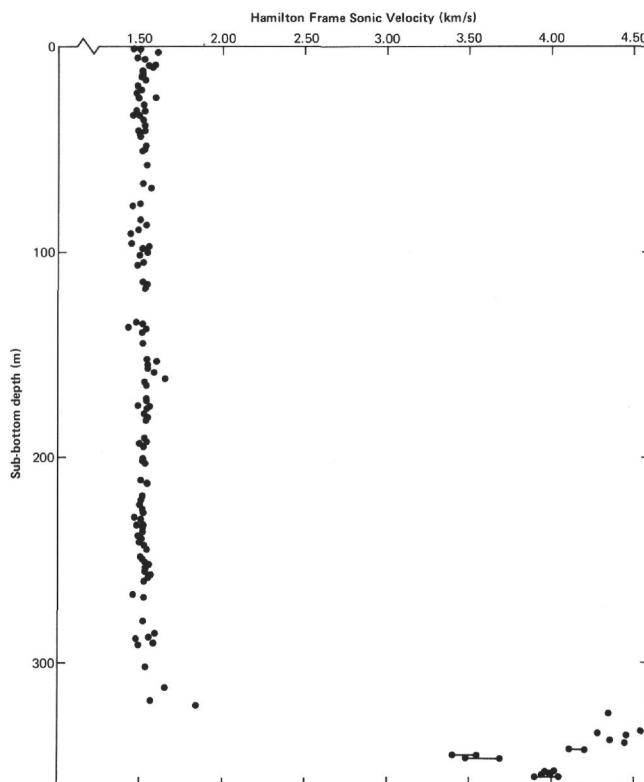


Figure 7. Sonic velocity versus depth, Hole 408.

sedimentary Sub-unit 2A (see section on lithostratigraphy). No indication of the sonic velocity peak at 160 meters occurs in the other two measurements.

GEOCHEMISTRY

In contrast to the interstitial solutions sampled from the sediments of Site 407, small but significant compositional changes are found in the interstitial solutions sampled from Site 408.

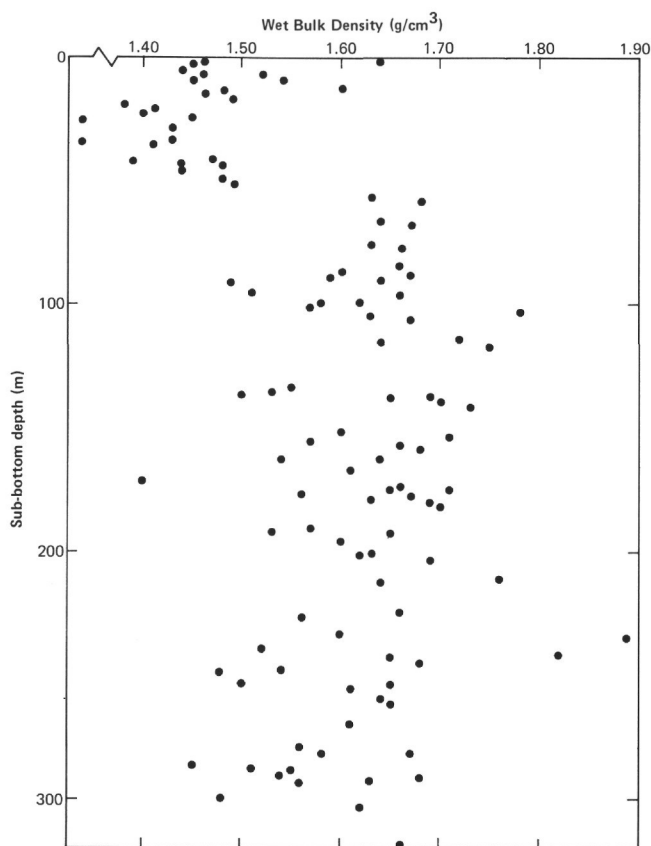


Figure 8. Wet-bulk density versus depth, Hole 408.

The sediment accumulation rate for Hole 408 has been calculated at approximately 2 cm/1000 years, with continued deposition since the middle Miocene (approximately 15 m.y.). The sediments, mainly calcareous nanofossil ooze which becomes more siliceous toward the base of the 320-meter succession, can be broadly considered as biogenic sediments for the purpose of the interstitial water studies (Sayles and Manheim, 1975). The compositional changes in the interstitial solution chemistry include a general increase in Ca^{++} and a concomitant decrease in Mg^{++} from the top to the bottom of the sedimentary succession (Figure 10). Alkalinity shows an overall decrease, pH a slight increase; chlorinity and salinity apparently remain constant throughout the sequence (Figure 10). These changes are consistent with those found by Sayles and Manheim (1975, cf. Table 3) for similar biogenic sediments.

Figure 11 shows a correlation between Ca^{++} and Mg^{++} suggesting that these ions are controlled by a related reaction(s). Two samples which lie off the dashed line, at 40 and 220 meters sub-bottom depth, both show corresponding decreases in alkalinity and small increases in pH , which suggests that these reflect calcium carbonate deposition at these depths. The sample taken at 220 meters is from a siliceous nanofossil ooze, whereas the sediments above this are predominantly calcareous nanofossil ooze. This may account for the relative depletion of Ca^{++} and HCO_3^- in the interstitial waters at this depth.

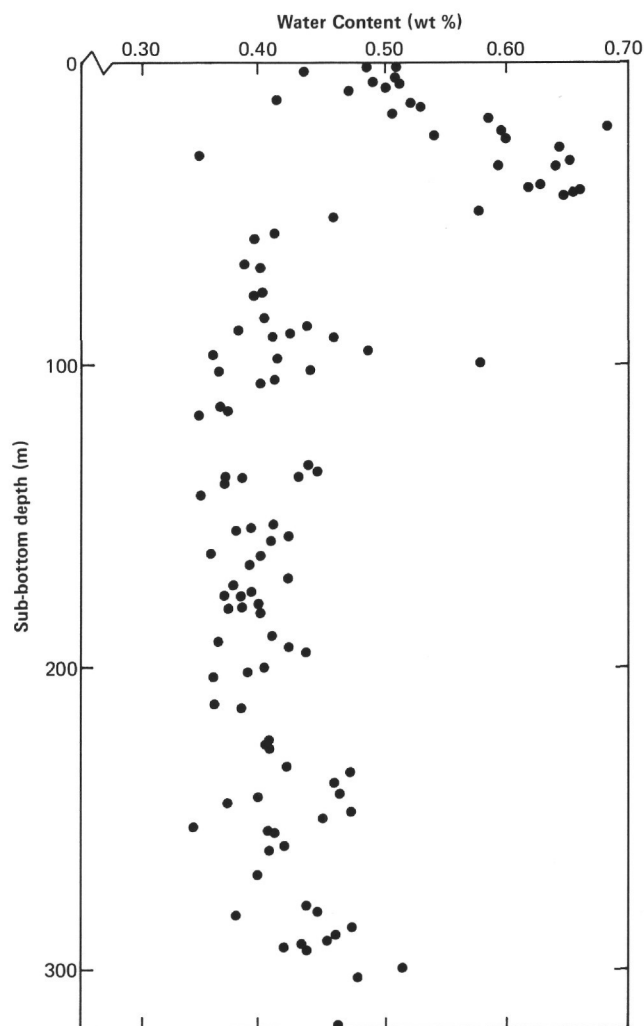


Figure 9. Water content versus depth, Hole 408.

Two explanations have been proposed for the Ca^{++} and Mg^{++} changes described above and commonly found in biogenic ocean-floor sediments: recrystallization of biogenic calcite and substitution of Mg^{++} for Ca^{++} during this reaction (Sayles and Manheim, 1975); silicate reconstitution reactions involving volcanic ash, glass, and basalt material within the sediment and interstitial solutions, to produce smectite-type clay minerals, zeolites, and high-magnesium aluminosilicates (Gieskes, 1975). It is not possible to distinguish between these reactions with the available shipboard data. However, the latter reactions should involve a decrease in Na^+ content in the interstitial solutions; this might be measurable with the necessary accuracy during shore-based studies.

Site 408 provides interesting data on the interstitial-solution chemistry of the sediment, and indicates that further shore-based studies of the solutions and the solid phases of the sediments may be worthwhile. The sedimentary successions recovered at Sites 407 and 408 are broadly similar, and if the differences in the chemical gradients within the interstitial solutions are found to be

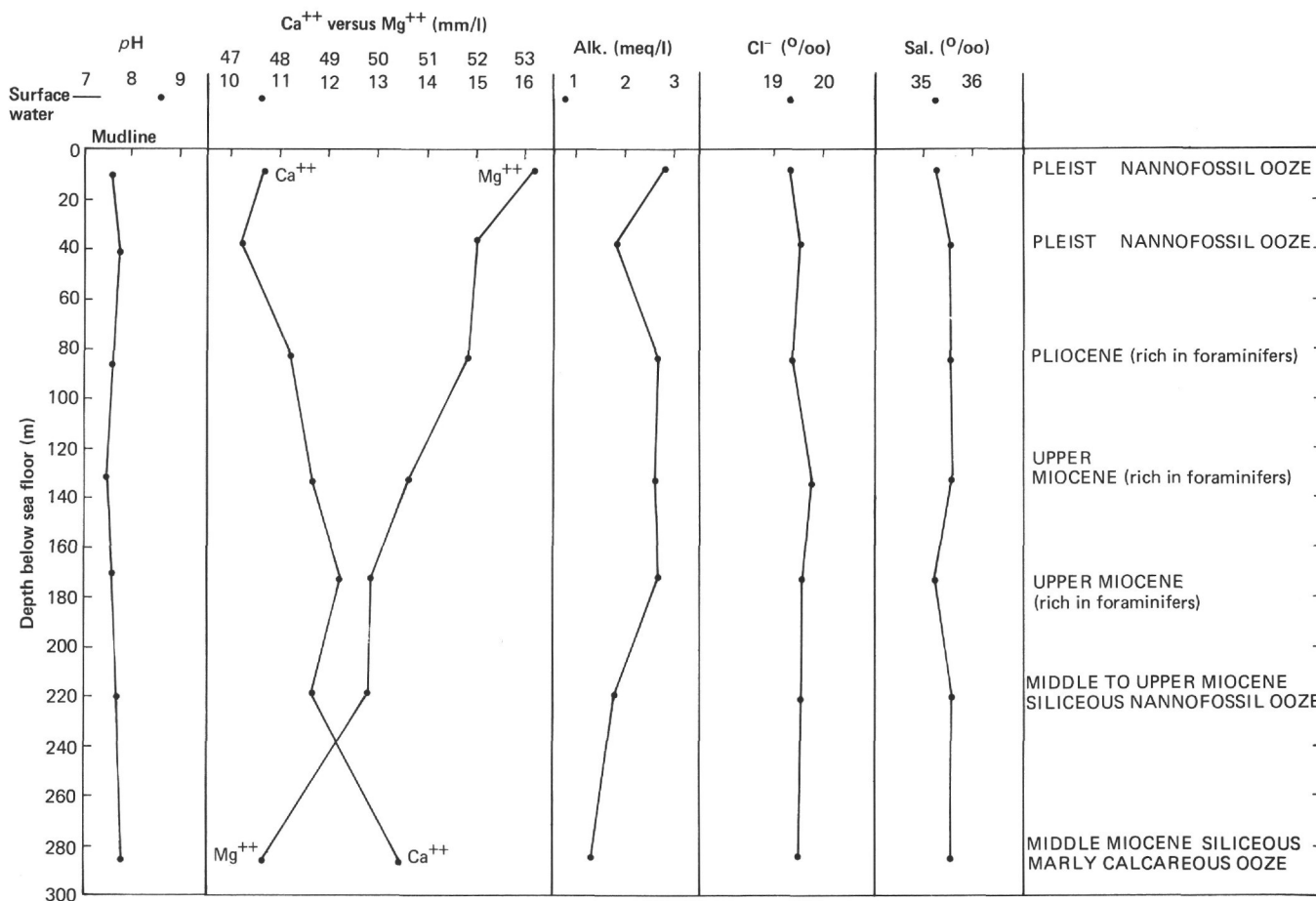


Figure 10. Interstitial water chemistry, Hole 408.

primary and not induced during drilling, as discussed for Site 407, then further studies to elucidate the causes of those differences may be worth undertaking.

PALEOENVIRONMENTAL INTERPRETATION

Site 408 was positioned on a steep-sided bathymetric high, to try to avoid encountering turbidites in the section. This attempt was unsuccessful, because graded units occur both at the top (Cores 1 to 4) and near the base of the hole (Cores 26 to 28, and 31). The basalt turbidite sequence can be readily explained as resulting from deposition near the ridge axis in a different tectonic setting from the present; but, the uppermost 38 meters cannot be explained so easily. It is tempting to hypothesize late Pleistocene faulting of the hill to its present elevation, allowing Pleistocene turbidite accumulation prior to uplift. Such a hypothesis has some support, in that a basement offset appears in the airgun profile made on the way to Site 407 (Figure 12). However, the offset in basement is considerably less than that of the sediment surface, and in fact *no* offset in basement appears in the airgun profile made while approaching the actual drill site (Figure 4). The conclusion we tentatively put forward is that either (1) the block is not an isolated hill, but rather a narrow north-south ridge with a shallow northward slope, or (2) the block was tilted rather than vertically faulted, and the sediment morphology is the result of slumping toward the

lower end of the block. Neither of these explanations is entirely satisfactory; neither helps us to understand the regional relationship between the regional faulted basement and the irregular sediment accumulations.

The Pleistocene section at Site 408 is lithologically similar to that at Site 407, and that leads us to suspect that the coarse surface sediments at both sites were transported from Iceland by turbidity currents. Coarse (gravel-size) glacial erratics occur from the top of the core down through Sample 4-4, 110 cm (34.1 m). Sand-size detrital grains (> 10%) continue through Sample 4-5, 85 cm (35.35 m), although this probably represents turbidity-current transport rather than ice-rafting.

The contact between the turbidites in Cores 1 to 4 and the underlying marly siliceous nannofossil ooze may occur between Cores 4 and 5 (36.2 to 38.0 m) or possibly at a color change at Sample 4-5, 110 cm (35.6 m). The Pliocene, ash- and biogenic silica-rich ooze in Core 5 lacks coarse ice-rafted detritus; the coarse fraction consists primarily of broken foraminifers, sponge spicules, clear ash, and altered ash clumps ("palagonite") (some as beds, some scattered throughout). The large number of thin units of different colors (average thickness 25 to 30 cm) suggests changes in supply of ash and biogenic silica, possibly controlled by bottom-current winnowing. The absence of glacial erratics in upper Pliocene sediments this far north is

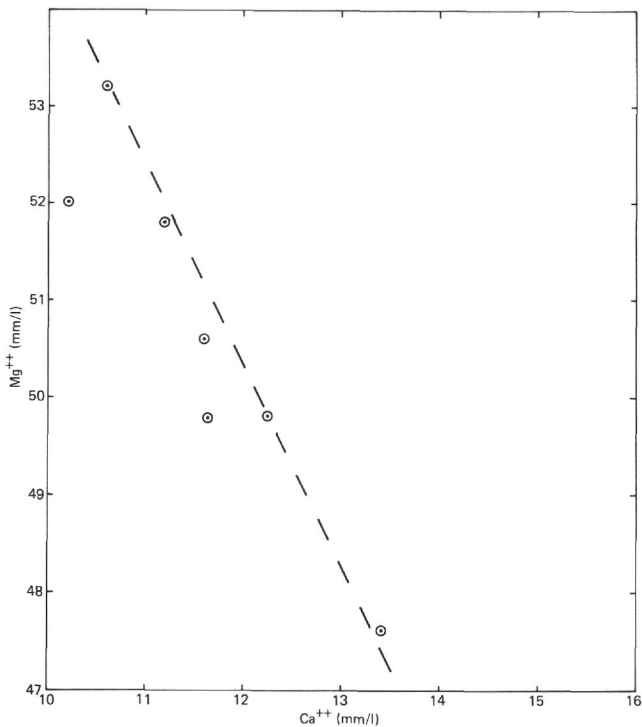


Figure 11. Correlation of Ca⁺⁺ and Mg⁺⁺ for Hole 408 interstitial water.

puzzling, and suggests that a portion of the upper Pliocene section is missing.

Below Core 5 is a 154.5-meter sequence of nannofossil ooze (47.5 to 212.0 m) dated as lower Pliocene (Cores 6 to 13) and upper Miocene (Cores 14 to 24). Volcanic glass (both clear and brown) and glauconite are scattered through; other detrital coarse material is rare or absent. Beginning in Core 16 (Sample 16-3, 50 cm; 146.0 m) and continuing downward to at least Sample 30-5, 70 cm (282.2 m), glauconite laminations, generally a few millimeters thick, commonly occur in bands up to 10 cm thick. Although laminations are not evident above Core 16, occasional streaks and chips of greenish gray clay occur as high up as Core 8, and some of these may represent fine laminations disturbed by coring and splitting, although others may be attributable to bioturbation. The coarse fraction in these units is composed predominantly of foraminifers, but with several per cent glauconite and brown ash. It seems likely that these represent current-winnowed sand/silt laminations of brown volcanic ash which has later been altered to glauconite in the nannofossil ooze matrix and within foraminifers and sponge spicules. Some individual ash grains have spherical green rims developed around them in the nannofossil ooze, suggesting ion migration and subsequent glauconitization at depth, rather than in-situ alteration of brown ash at the sediment surface.

Cores 23 to 31 (212.0 to 291.0 m) are generally similar to the unit above, except that they contain more than 10 per

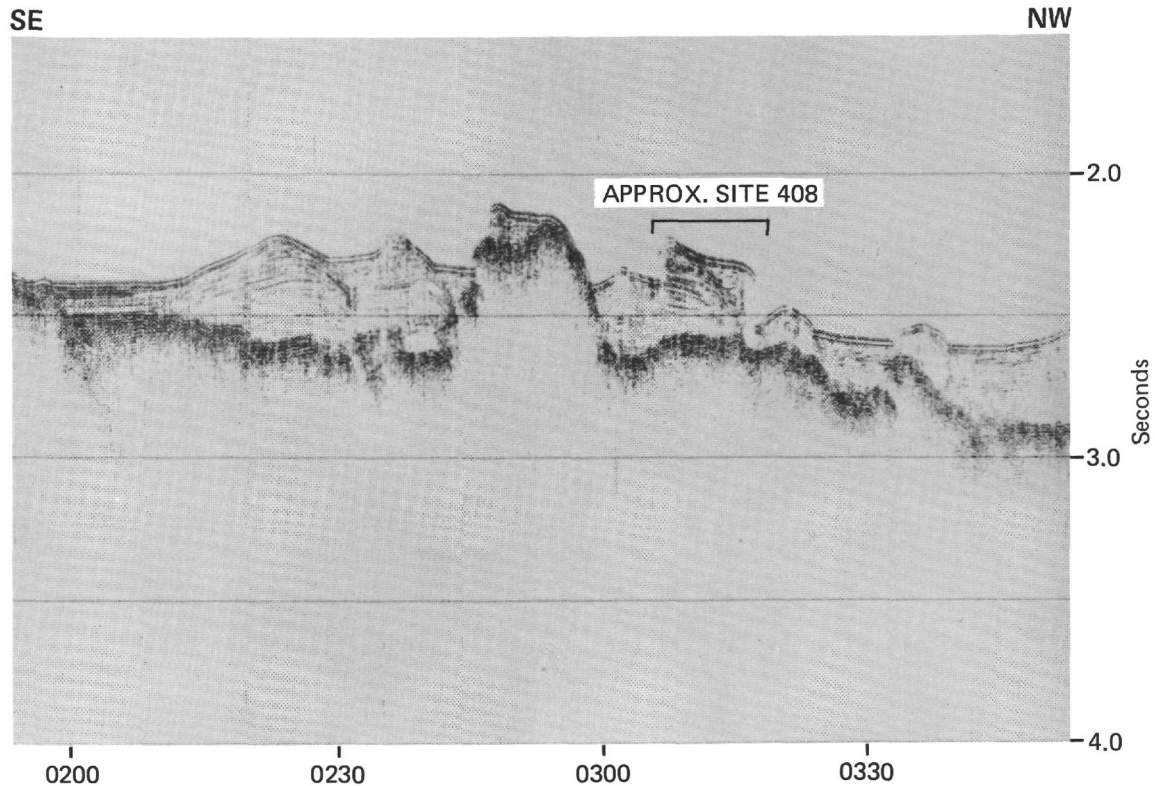


Figure 12. Reflection profile over Site 408 taken from Glomar Challenger on the approach to Site 407.

cent biogenic silica. A similar middle Miocene silica peak occurs at Site 407, although interpretation was complicated there by a hiatus. There is no evidence of a hiatus as shallow as Core 21 at Site 408, but the biogenic silica increases sharply between Samples 21-3, 117 cm, and 21-4, 50 cm, and remains high (going downcore) until a sharp decrease between Samples 30-4, 36 cm, and 30, CC. (The silica does not exceed 10% within Cores 21 and 22, however). The glauconite laminations continue as before; the increase in biogenic silica is principally diatoms and fine (radiolarian?) spines; large sponge spicules remain near 5 per cent. This is similar to the middle Miocene silica-rich unit at Site 407.

Turbidites occur in Cores 26, 27, 28, and 31, and may also be present in some other disturbed cores between 26 and 33. The graded units are of variable thickness, ranging from about 5 cm to as much as 3 or 4 meters (the interval from Sample 27-2, 140 cm, to Sample 27-5, 50 cm, appears to be a single unit). No shallow-water indicators were noted in the shipboard visual analysis. Basalt sand (locally derived?) is scattered throughout.

Unit 3 (see Sediment Lithostratigraphy) is basal calcareous mud and basaltic sand containing increasing amounts of glauconite downward from Core 32 to basalt at Sample 35-1, 32 cm. The large amounts of glauconite in the basal section (10 to 25%) suggest slow accumulation in the presence of volcanic ash and/or exposed basalt, and possibly bottom-current activity which would have enhanced alteration by exposure to seawater.

SEDIMENT ACCUMULATION RATES

Sediment accumulation rates have been calculated for the upper Miocene/lower Pliocene and middle/lower Miocene portions of Site 408 (Figure 13). As at Site 407 there is good agreement between nannofossil and foraminifer age assignments. The accumulation rates on either side of the upper/middle Miocene hiatus show a pattern similar to the rates at Site 407, with younger sediments accumulating 2 to 3 times as fast as those below (Figure 13). We infer that the hiatus at Site 408 resulted from erosion by a northward-flowing bottom current originating at the Iceland Faeroes Ridge, and that the higher accumulation rates above were caused by the influx of sediment carried by the same current. The hiatus is younger than at Site 407, presumably because the site was shallower than the current before the upper/middle Miocene (Shor and Poore, this volume).

An accumulation rate of 20 m/m.y. is calculated for the Quaternary section. As discussed for Site 407, a portion of the Quaternary turbidite section may be absent.

BASEMENT LITHOSTRATIGRAPHY

Lithostratigraphy of Igneous Rocks

The first pieces of drill core believed to represent parts of a lava flow were recovered in Core 35 (323.6 m³). Except for three samples of indurated fossiliferous sediment attached to fragments of basalt in Core 37, all the recovered material from 323.6 meters to the bottom of the hole at 361 meters (Core 38) is basalt. Of the 37.4 meters of igneous section drilled, 34 per cent was recovered.

³Depths refer to drilled intervals determined from drilling logs.

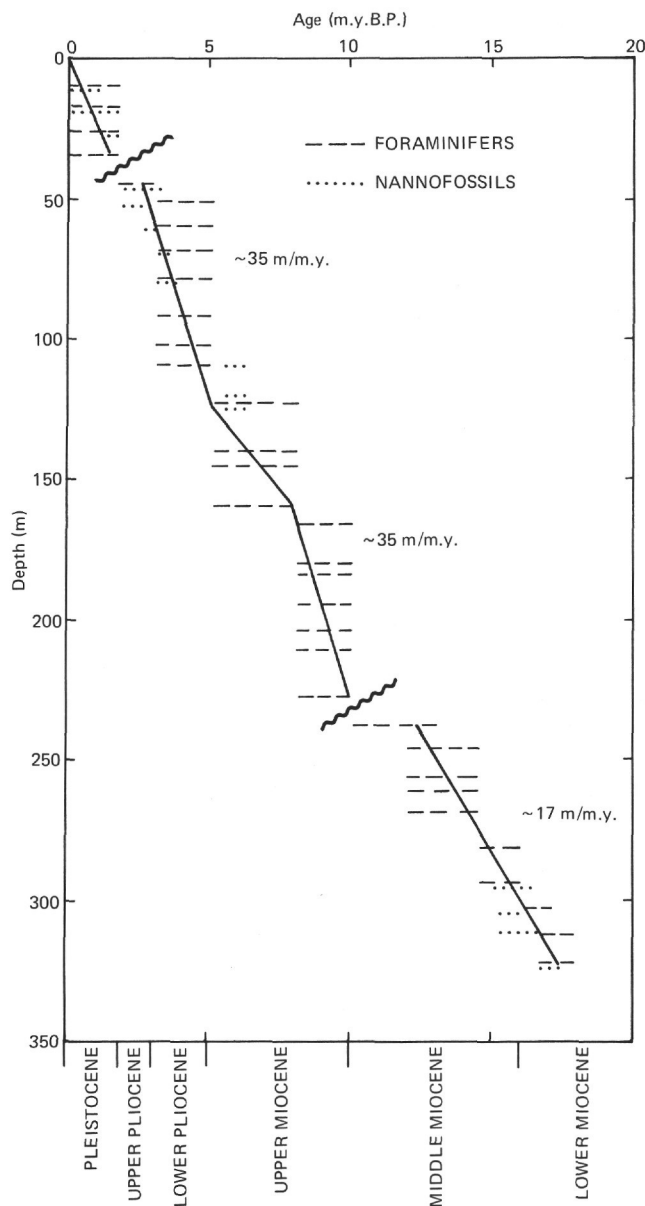


Figure 13. Sediment accumulation rates for Hole 408. Age estimates for foraminifer and nannofossil zone boundaries from Berggren (1972).

The igneous section consists principally of aphyric basalt that varies somewhat in degree of vesicularity and secondary alteration, but otherwise is homogeneous in appearance. Nonetheless, the section can be subdivided into at least nine flows or groups of flows, on the basis of petrography, the presence of interlayered sediments, and chilled margins; and changes in drilling rate and geochemical and magnetic measurements all show that the section is divided into two major lithostratigraphic units, with the boundary between Sections 1 and 2 of Core 37.

Interlayered sediments were recovered in Core 37, Section 2 (343.5 m). Three fragments of basalt in Section 37-2 (numbers 7, 10, and 11) are chilled against indurated fossiliferous sediment. It is not clear whether these are pieces from the chilled margins of separate flows or from a

single flow. This level corresponds to the top of the lower geochemical unit. High drilling rates scattered throughout the igneous section (see Figure 14) suggest the presence of other interlayered sediments, but none was recovered as core.

Chilled margins are present in Core 37, Section 1, piece 2 (342.1 m), and Core 37, Section 2, piece 16 (344.5 m). An abrupt decrease in grain size between pieces 3 and 4 in Core 36, Section 1 (332.7 m) and a similar abrupt change from a rather massive altered fragment to a very vesicular rather unaltered fragment with a chilled margin in Core 37, Section 1, pieces 14 and 15 (343.4 m) suggest two more flow contacts.

Correlation of changes in drilling rate with core recovery is illustrated by a graph of drilling rate versus depth (Figure 14). "Soft" sandy to silty material of the sedimentary section was typically drilled at less than 1/2 minute per meter (see Core 33 on Figure 14). Coarser volcaniclastic sediment (Core 34) was penetrated at as little as a tenth of this rate, and the more resistant lavas required about ten or even more minutes per meter. As pointed out in a similar analysis for Site 407, interpretation of the drilling rate in terms of lithologies drilled is often speculative; still, with that *caveat* in mind, we have constructed a complete hypothetical stratigraphic section (Figure 15) by assigning recovered core to periods of appropriate drilling rate and taking into account the evidence for flow boundaries described earlier. This section indicates that at least nine flows or groups of flows were penetrated by the drill, and that basement was penetrated at 321.6 meters. The reconstructed thickness of these units ranges from 5 meters to 1 meter, and averages about 3 meters.

Magnetic inclination defines a twofold sequence in the lava flows. All samples studied show normal magnetic polarity, but those in and above Core 37, Section 1 (343.4 m) yield inclinations from about 50° to 65°, whereas those below Core 37, Section 1 (343.4m) yield inclinations from about 80° to 85° (Figure 15). This latter group consists of aphyric lavas with common glassy selvages and interlayered fossiliferous sediments; the former group is largely sparsely phytic lavas. More details of these petrographic contrasts are described in the following section.

Two geochemical units were defined, mainly on the basis of Zr, TiO₂, and Fe₂O₃* (Figure 16), with generally higher values in the lower part. The upper part of Unit 1 is relatively variable, and tends to iron enrichment and magnesium depletion toward its top.

IGNEOUS PETROGRAPHY

Petrography of the Volcanic Rocks

Hole 408 penetrated 37.4 meters of basaltic lava flows, which underlie a sedimentary section rich in pyroclastic material. A single fragment of alkali granite may be of shallow sub-volcanic origin.

Volcanic Fragments in the Sediments

Some volcanic fragments are present in almost all smear slides of the sediments. The abundance of this material varies from a few per cent in the nannofossil ooze to 10 to 30 per cent in the lowermost (218 to 321 m) and uppermost (0 to 47.5 m) parts of the section. If the material was erupted on Iceland, an assumed average abundance of 10 per cent in 150 meters of sediments covering an area of

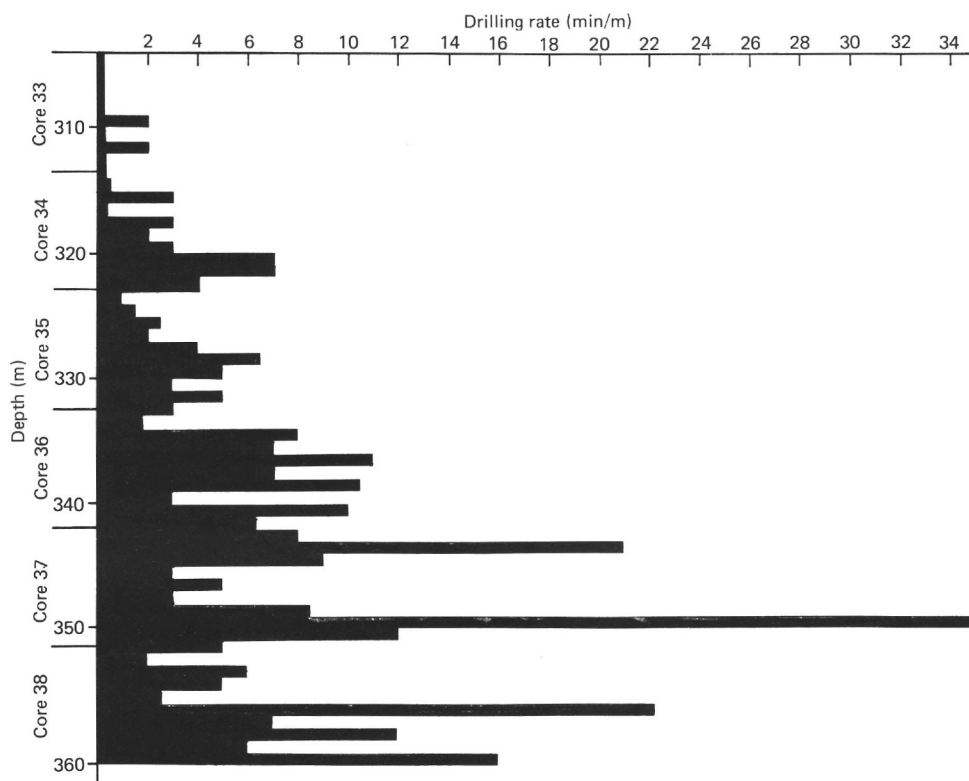


Figure 14. Drilling rate versus depth, Cores 33 to 38, Hole 408.

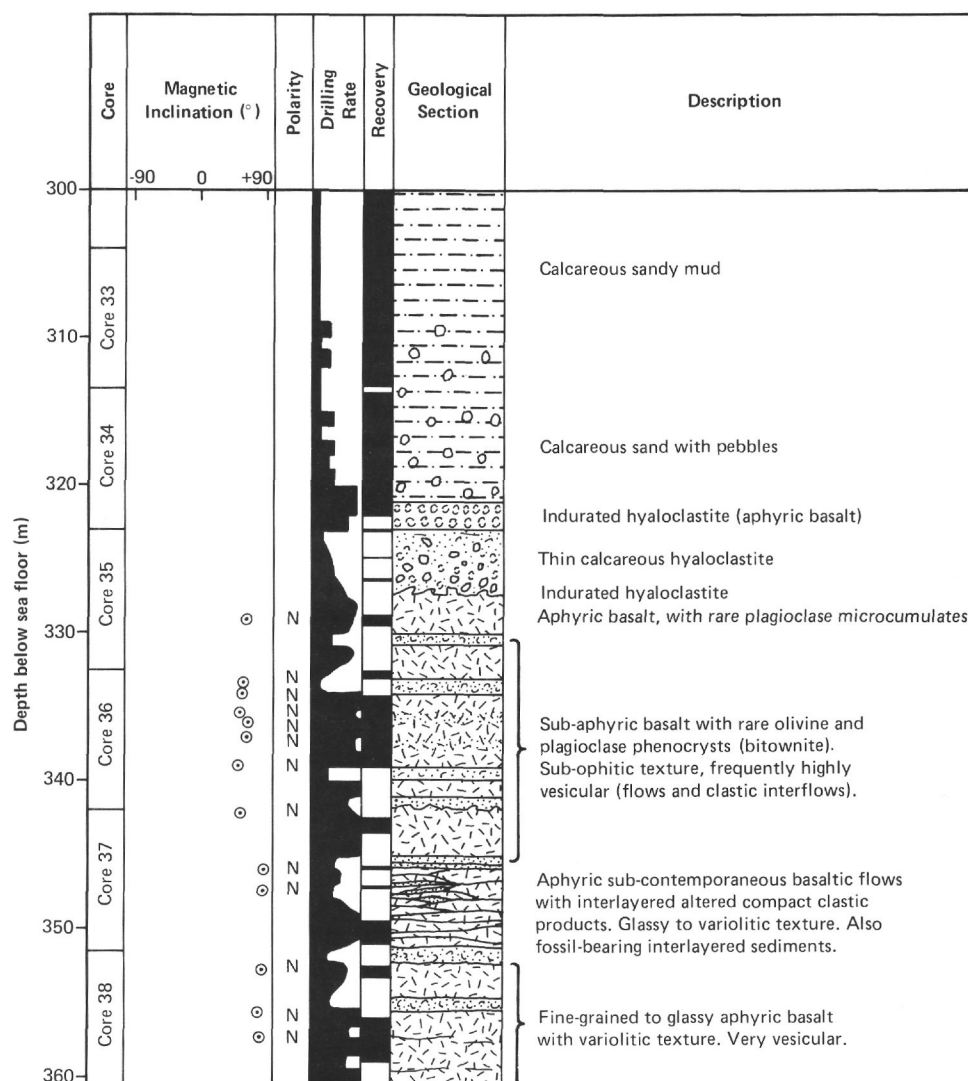


Figure 15. Proposed stratigraphic section for Site 408.

10^6 km^2 around Iceland corresponds to a volume of $0.15 \times 10^5 \text{ km}^3$. For comparison, the volume of the subaerial part of Iceland is about $4 \times 10^5 \text{ km}^3$.

Several virtually pure ash layers were penetrated. The uppermost sediment at the site is predominantly colorless glass of low refractive index (rhyolite?), associated with grains of quartz, alkali feldspar, and a green clinopyroxene. Basalt glass fractions are also present.

Other nearly pure ash layers occur at 36.5 meters, 37 meters, 40 meters, 114 meters, 115 meters, 116 meters, and 118.9 meters, and there are five more between 199.5 and 212.5 meters. These layers are generally 0.1 to 2 cm thick, and consist mostly of basaltic glass, sometimes plagioclase phyrlic (Figure 17). A 1.5-meter-thick ash layer contains both basaltic and rhyolitic glassy fragments (Figure 18).

Alkali Granite Fragment in the Nannofossil Ooze

An angular fragment of granite, measuring roughly $10 \text{ cm} \times 6 \text{ cm} \times 3 \text{ cm}$, was recovered in Core 23 (Sample 23-1, 5-7 cm) at 209 meters (lower/upper Miocene section). Though embedded in nannofossil ooze, this fragment comes

from a 13-meter thick zone containing several ash layers. A dark brown patina covers part of the rock. In thin section, the rock is fine-grained alkali granite consisting of nearly 15 per cent oligoclase (An_{12}), 45 per cent sanidine rich in fluid and glassy inclusions, 30 per cent interstitial quartz, and 10 per cent aegirine-augite, sodic amphibole, and a red-brown alteration product of an undetermined mineral. Euhedral crystals occur in druses. The mineralogy suggests an alkaline, or slightly peralkaline composition, but alteration is such that this would probably not show in chemical analysis.

The fragment is tentatively considered to be of shallow subvolcanic origin, possibly erupted by a silicic volcano on Iceland or a submarine rhyolitic volcano near the drill site.

Compacted Hyaloclastites

Two layers of indurated hyaloclastite, separated by a thin layer of calcareous hyaloclastite, immediately overlie the sequence of basalt flows. The hyaloclastite consists of pale brown, transparent glass that may be hydrated. The glass contains rare phenocrysts of plagioclase and clinopyroxene.

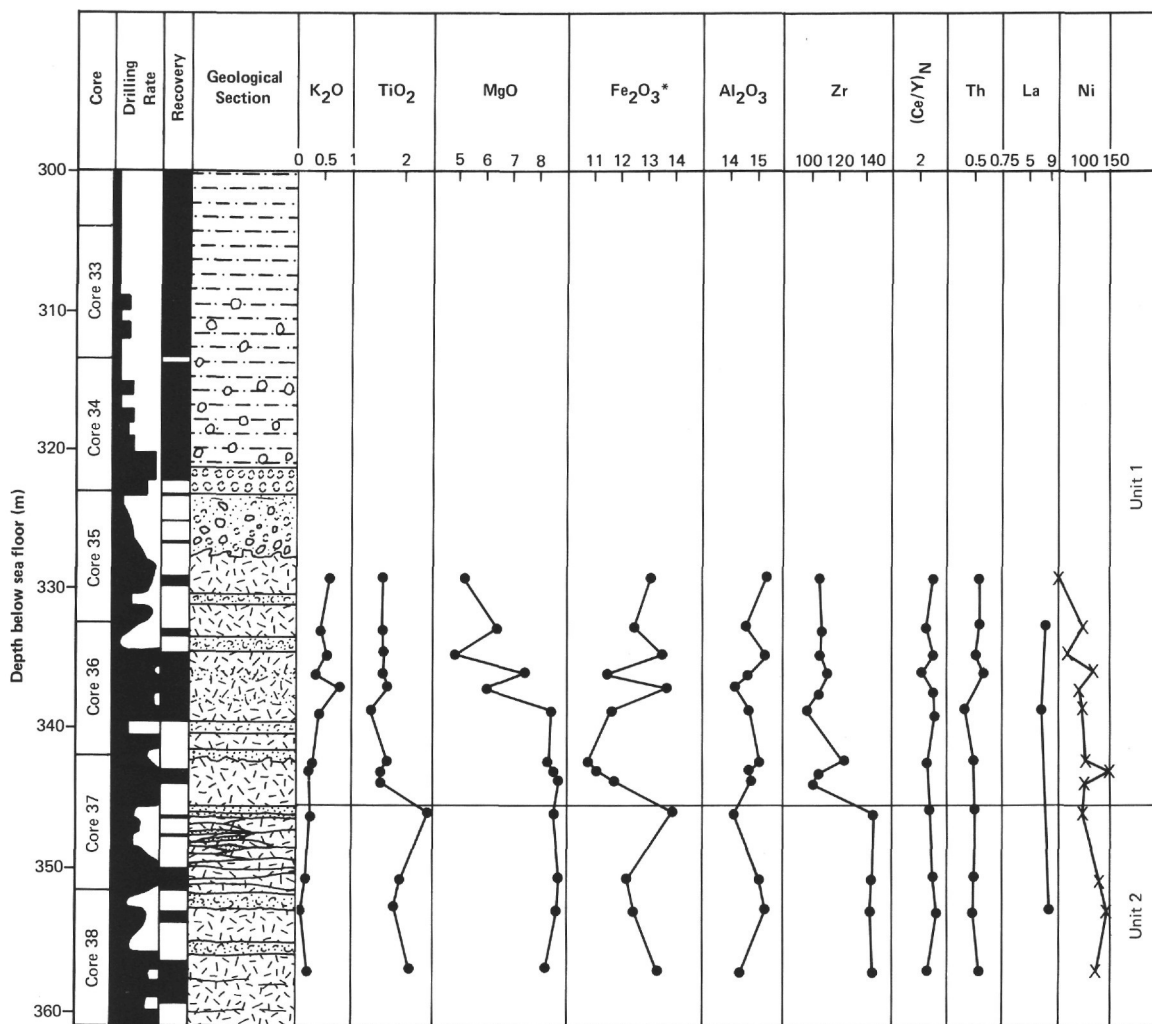


Figure 16. Geochemical units derived for stratigraphic section of Cores 33 to 38, Hole 408.

Aphyric Basalt, with Rare Plagioclase Microcumulate

Sparsely phyric basalt immediately underlies the hyaloclastite. It contains 1 per cent altered olivine microphenocrysts and rare plagioclase (An₆₆) microcumulates, up to 1 cm in diameter. The groundmass has a variolitic texture formed by elongated (up to 1 mm) laths of plagioclase, and also contains clinopyroxene and glass-rich titanomagnetite crystallites.

Some vesiculation occurred after the crystallization of the feldspars, yielding diktytaxitic texture.

Sparsely Phyric Basalt with Rare Olivine and Plagioclase Phenocrysts

Four flows with similar petrographic characteristics were penetrated between 330 and 345 meters depth. The best recovery was in Core 36, and in Core 37, Section 1. The rocks are sparsely phyric basalt with rare olivine (< 1%) and plagioclase (1 to 3%) phenocrysts in a sub-ophitic groundmass. The lower part of this sequence is relatively rich in plagioclase (An₈₀₋₆₀) phenocrysts, whereas the upper part contains fewer and more sodic plagioclase (An₆₀₋₅₄) phenocrysts in a variolitic groundmass. Late pyroxene in the

upper part (327 to 330 m) shows strong brown to violet pleochroism, indicating Fe-Ti enrichment. The uppermost flow of this unit is apparently somewhat fractionated. The base of this group of flows corresponds to the boundary between geochemical Units 1 and 2.

Aphyric to Sparsely Phyric Basaltic Flows

A series of thin basaltic flows, with a variolitic texture in the inner part and glassy partly recrystallized chilled margins, was recovered in Core 37 (Sections 2 and 3) between 345 and 352 meters depth. Several fragments with interlayered sediments containing lower Miocene fossils were also recovered. Rare crystals of olivine and plagioclase are present in some glassy margins. In the most crystalline parts of the flows, olivine is absent, plagioclase is in the range An₆₂₋₄₅, and pyroxene is pleochroic.

Fine-Grained to Glassy Aphyric Basalts

The deepest sequence of basalt flows penetrated consists of aphyric lavas very similar to the overlying sequence (6). The lower lavas, however, are more compact and coarse grained, and have variolitic to sub-ophitic textures. Olivine

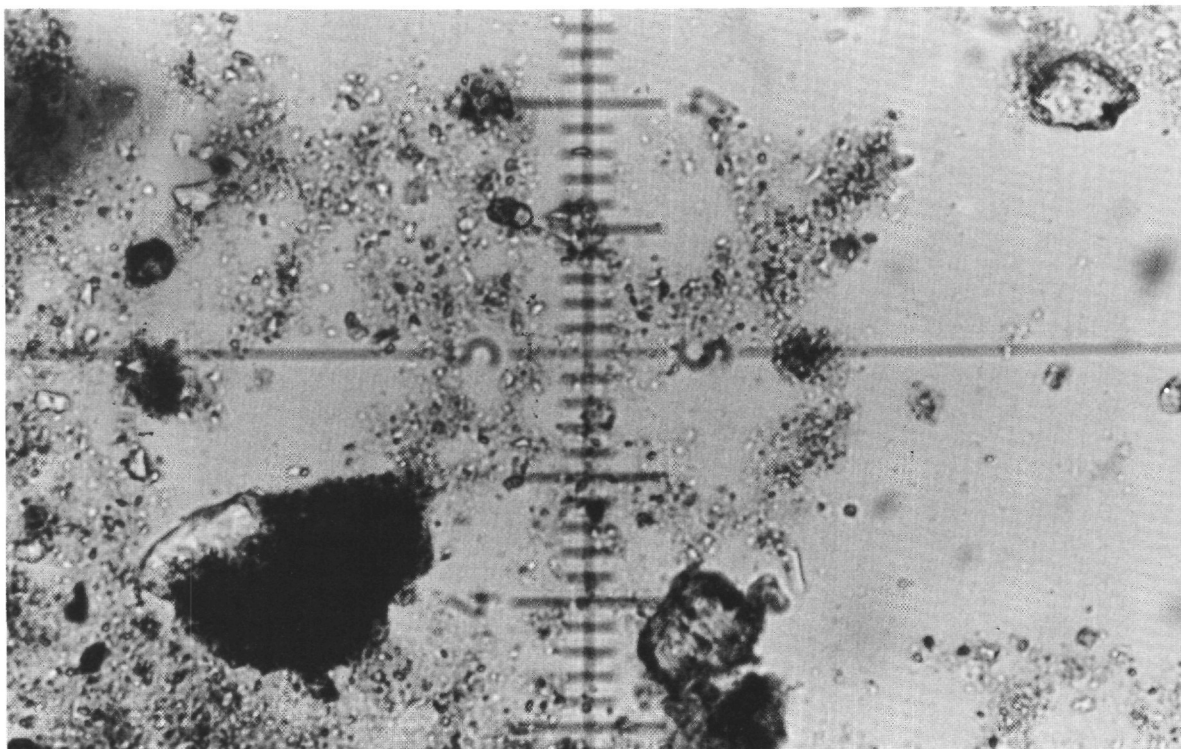


Figure 17. *Basaltic glass fragment with plagioclase phenocryst. Sample 1-1, 78 cm (x10).*

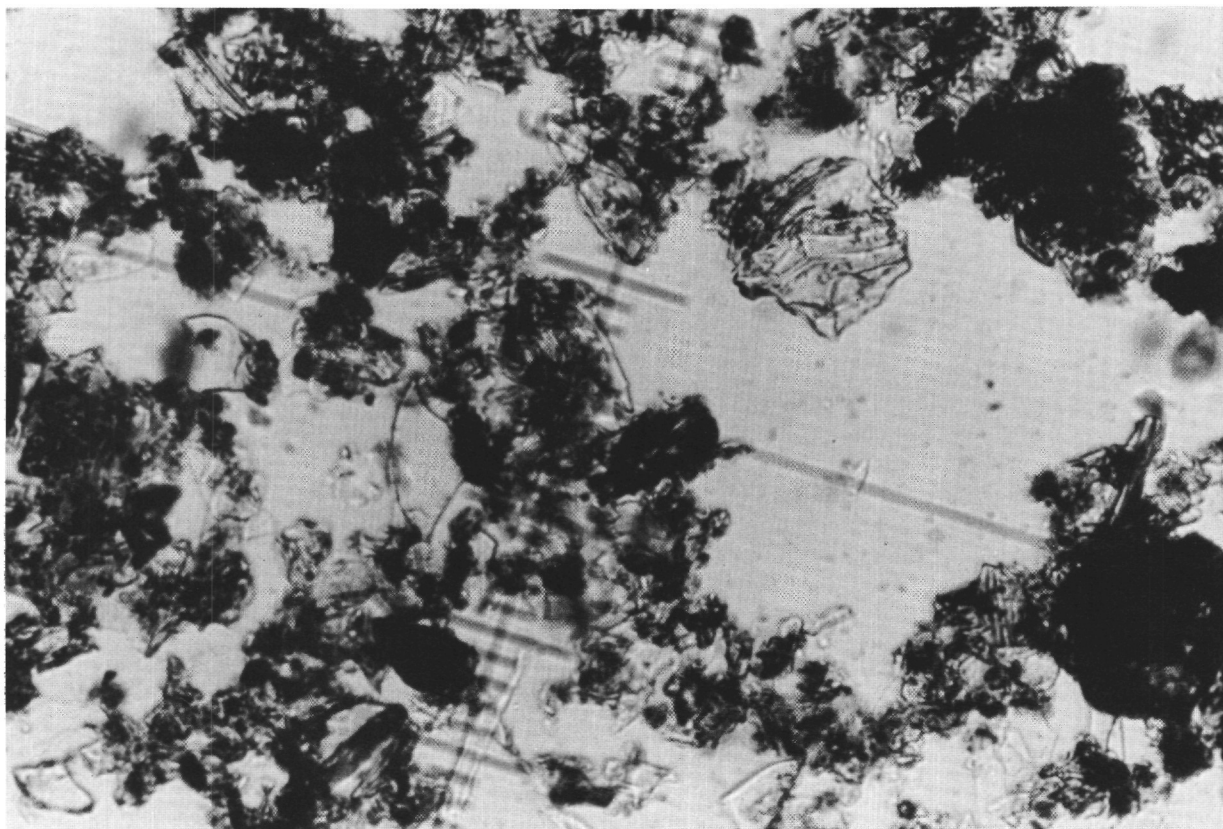


Figure 18. *Basaltic and rhyolitic glass fragments in ash layer.*

relicts, replaced by smectite and calcite, are present in most thin sections. Plagioclase cores range from An₆₂ to An₄₆. Clinopyroxene is present and highly pleochroic, and is probably Ti-rich augite. Alteration products and vesicle fillings include chlorite, zeolite, and smectite.

Conclusions

The relatively thin volcanic section penetrated at Site 408 appears generally homogeneous. The glassy nature of the basalts is favorable for geochemical studies. The most basic lavas are present in the middle part of the section; other lavas show distinct signs of evolution, as with more evolved, iron-rich members in the upper part of the unit (above 330 m) and more Ti-rich basalts in the lower part.

There is no evidence of off-axis volcanism, as at Site 407. The interlayered sediment in Core 37 appears to be the same age as the base of the sedimentary section.

The lavas at Site 408 appear to be similar to those forming the lower lava sequence at Site 407. Both are sparsely phyrlic plagioclase and olivine basalt, with rare but generally altered olivine and a tendency toward relatively sodic (andesine to labradorite) plagioclase and Fe-Ti-rich late clinopyroxenes in variolites.

Chemical data indicate that at least two magma types are present, constituting two distinct units, and that rather wide variations occur within one of them, with important variations in the Fe/Mg ratio.

This shows that even limited penetration provides a variety of rock types. Therefore, contrary to conclusions drawn from geochemistry of samples dredged from various spots along the ridge, indicating simple and regular variations (Schilling, 1973), Leg 49 data indicate a more complicated genetic relationship between basalts erupted from the Reykjanes Ridge.

ALTERATION PETROGRAPHY

Basalt alteration involving the formation primarily of smectite and calcite, but also of other minerals, is well developed at Site 408. The core can be divided, from the point of view of alteration, into two zones, an upper buff-colored, more oxidized zone, and a lower blue-gray, more reduced zone, separated by a sharp contact in Section 1 of Core 37 (342.2 m sub-bottom). Though the more reduced zone appears fresher in hand specimen, the degree of alteration is no less than in the buff zone. It appears that the altering solutions were of different oxidation potential in the two zones, but similarly active.

In hand specimen, the most prominent alteration features are calcite-filled veins, which occur in both zones; the veins are often bordered by rinds of clay minerals, usually the dull green characteristic of smectite, but sometimes the celadon green and blue which usually marks celadonite. The celadonite is especially prominent in the more reduced zone of the core. Almost as prominent as the veins are the vesicles, wholly or partly filled with smectite, but often with centers composed of calcite. In the reduced zone of the core, clusters of pyrite cubes occur along joint surfaces and in vesicles, and in very conspicuous places.

In thin section, more detail can be seen. Smectite replaces olivine almost completely, and the only unaltered crystals survive in glassy chilled margins. Smectite also extensively

replaces interstitial glass or originally fine-grained mesostasis. Smectite lines vesicles, forming successive layers which often differ appreciably in their optical properties. Most spectacular are the inner zones of some samples in which the crystal size of the smectite is very large, and individual crinkled flakes can readily be distinguished, growing quite separately from one another. This is particularly clear in several samples from Core 38.

Calcite always seems to be later than smectite, filling vesicles or veins in which smectite forms the outer rim. Why this should be so is not clear, and must depend on the sources of calcium carbonate, as well as on the physico-chemical conditions of precipitation.

Pyrite occurs in the reduced section of the core, where it is visible as late veins or wisps filling cracks, and as clusters of crystals within vesicles, predating the calcite, and often post-dating the smectite.

Zeolites are not common in these basalts. Most occur in glassy margins, where the higher activity of Al and perhaps of Na, K, and Si in the fluids, resulting from solution of the glass, seems to encourage their formation. It is interesting that veins in the glassy rinds commonly contain zeolites, whereas they are very rare elsewhere in the core. Also associated with alteration of glass is some palagonite, but there is much less fresh glass in this core than at Hole 407. This is partly because the core contains fewer chilled margins, but also because of the greater intensity of alteration here than at Site 407. Although palagonite is the first alteration product of the glass, it rapidly converts to smectite, which eventually replaces most of the glass in any given area. Marked chemical changes must be involved in such a replacement reaction.

Titanomagnetite shows some corrosion to leucoxene, just as it did at Site 407. There is no gradient down the hole. All the samples are corroded to roughly the same degree.

Despite the higher degree of alteration here, plagioclase is still unaffected by replacement by zeolites or albite.

Just as at Site 407, no estimates can be made of alteration temperature from the mineral zones until more work has been done on mineralogy and chemistry in shore-based laboratories.

BASEMENT PALEOMAGNETISM

The 32 meters of basalt sampled for paleomagnetism are normally magnetized; however, a distinct change in magnetic intensity, direction, and stability occurs about two-thirds of the way down the section (Table 3 and Figure 19).

Seventeen specimens were taken from Cores 35 through 38 (323 to 361 m). The average NRM intensity is 1.1×10^{-3} emu cm⁻³ (1000 μ G) for eight specimens (Sections 35-1 through 36-5) within the upper 15 meters. For six specimens (37-2 through 38-3) from depths of 343 meters to 356 meters, the average NRM intensity is 8.9×10^{-3} emu cm⁻³, greater by a factor of eight. NRM intensities are consistently lower in Cores 35 and 36 and much higher from Section 37-2 through Core 38. There is a transitional region of a few meters including the specimens from Core 37, Section 1, which have intensities and direction intermediate between those of the specimens above and below them. A petrographic boundary occurs 3 cm above Section 37-1. It is

TABLE 3
Paleomagnetic Data, Site 408

Sample (Interval in cm)	Depth Sub-Bottom (m)	NRM Intensity (10^{-3} emu cm^{-3})	Initial Inclination ($^{\circ}$)	Stable Inclination ($^{\circ}$)	MDF (Oe)	Comments
408-35-1, 77-79	323.8	1.7	+68.4	+65.4	160	magnetic unit 1
408-35-1, 110-112	324.1	2.8	+70.6	+64.0	230	magnetic unit 1
408-36-1, 100-103	333.5	0.8	+60.4	+55.9	310	magnetic unit 1
408-36-2, 12-14	334.1	0.8	+58.9	+55.4	Thermal	magnetic unit 1
408-36-2, 139-141	335.4	0.9	+58.2	+52.0	310	magnetic unit 1
408-36-3, 46-49	336.0	0.6	+69.8	+63.4	Thermal	magnetic unit 1
408-36-4, 37-40	337.4	1.0	+63.6	+63.4	200	magnetic unit 1
408-36-5, 44-47	339.0	0.3	+52.1	+50.6	250	magnetic unit 1
408-37-1, 13-15	342.2	1.0	+62.7	+60.6	170	transitional
408-37-1, 33-36	342.3	5.7	+67.1	+66.5	Thermal	transitional
408-37-1, 122-124	343.2	4.6	+56.5	+66.3	80	transitional
408-37-2, 125-130	344.8	14.0	+88.9	+87.8	70	magnetic unit 2
408-37-3, 109-116	346.1	11.4	+87.9	+85.8	70	magnetic unit 2
408-38-1, 68-70	352.2	7.0	+79.4	+79.1	140	magnetic unit 2
408-38-1, 131-137	352.8	6.1	+81.0	+85.5	Thermal	magnetic unit 2
408-38-2, 112-118	354.1	6.7	+82.5	+80.3	80	magnetic unit 2
408-38-3, 119-122	355.7	8.5	+81.1	+77.8	75	magnetic unit 2

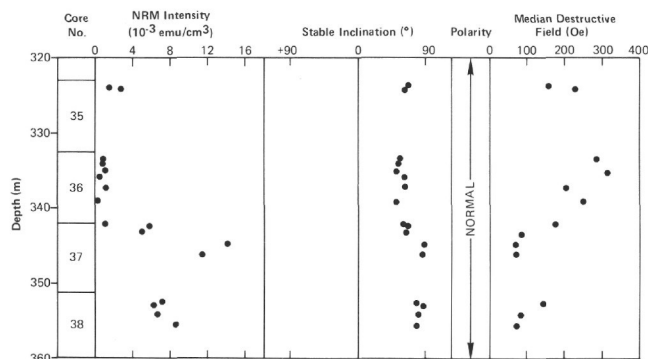


Figure 19. Down-hole plot of paleomagnetism results, Hole 408.

therefore probably that the basalt of the upper portion of the lower magnetic unit (unit 2) was partially remagnetized by heating when unit 1 was extruded on top of it.

Of the 17 specimens (generally taken every one or two meters), 13 were demagnetized in alternating fields (AF) up to 500 to 800 Oe, and 4 were demagnetized thermally up to 500°C. The results of AF demagnetization are shown in Figures 20 and 21. No significant directional changes (with one exception, specimen 36-5, 339 m) occurred upon AF demagnetization. A distinct difference in stable inclination, corresponding to the difference in intensity already discussed, exists between rocks recovered above and below 342 meters (Cores 35 to 36, and 37 to 38). The mean stable inclination from the upper magnetic unit (1) is $59^{\circ} + 2^{\circ}$ and for the lower unit (2) it is $83^{\circ} + 1^{\circ}$ (using the method of Briden and Ward, 1966, to combine inclinations). The inclination at this site predicted by the axial geocentric dipole field is 76° , and that predicted for the present dipole (with axis intersecting the earth's surface at $78.5^{\circ}N$, $70^{\circ}W$) is 82° . The difference between the inclinations of the two magnetic units may arise from secular variations of the

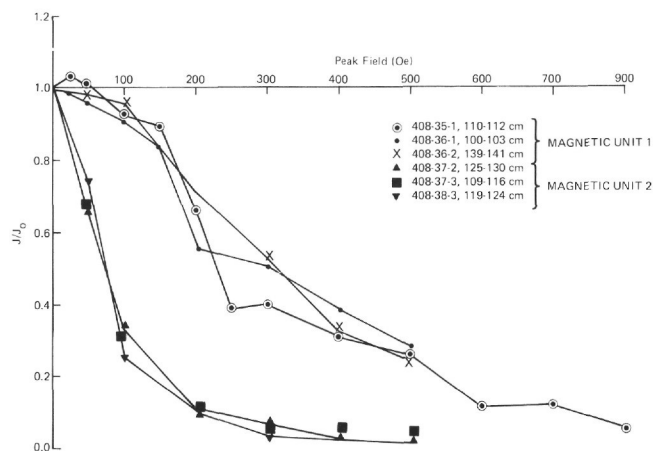


Figure 20. Examples of intensity changes upon AF demagnetization, Hole 408.

geomagnetic field; this would be expected if each unit consisted of flows erupted over a short interval of time, with a time gap between the formation of unit 2 and unit 1.

A marked difference in stability to AF demagnetization also distinguishes the two magnetic units. The median destructive field for unit 1 is about 230 Oe; for the underlying unit 2 it is about 85 Oe. Unit 1 consists of massive brownish basalt, whereas unit 2 is much darker vesicular pillow lavas. This would be consistent with two volcanic episodes, as suggested by the magnetism data.

Thermal demagnetization in 50° increments showed remarkably uniform behavior. Two specimens (36-2 and 36-3) were from unit 1, one (38-1) from unit 2, and a fourth (37-1) from the magnetic transition region just below the contact between brownish and darker basalt. Figures 22 and 23 show the results of stepwise heating. No great difference seems to exist between the specimen from unit 2

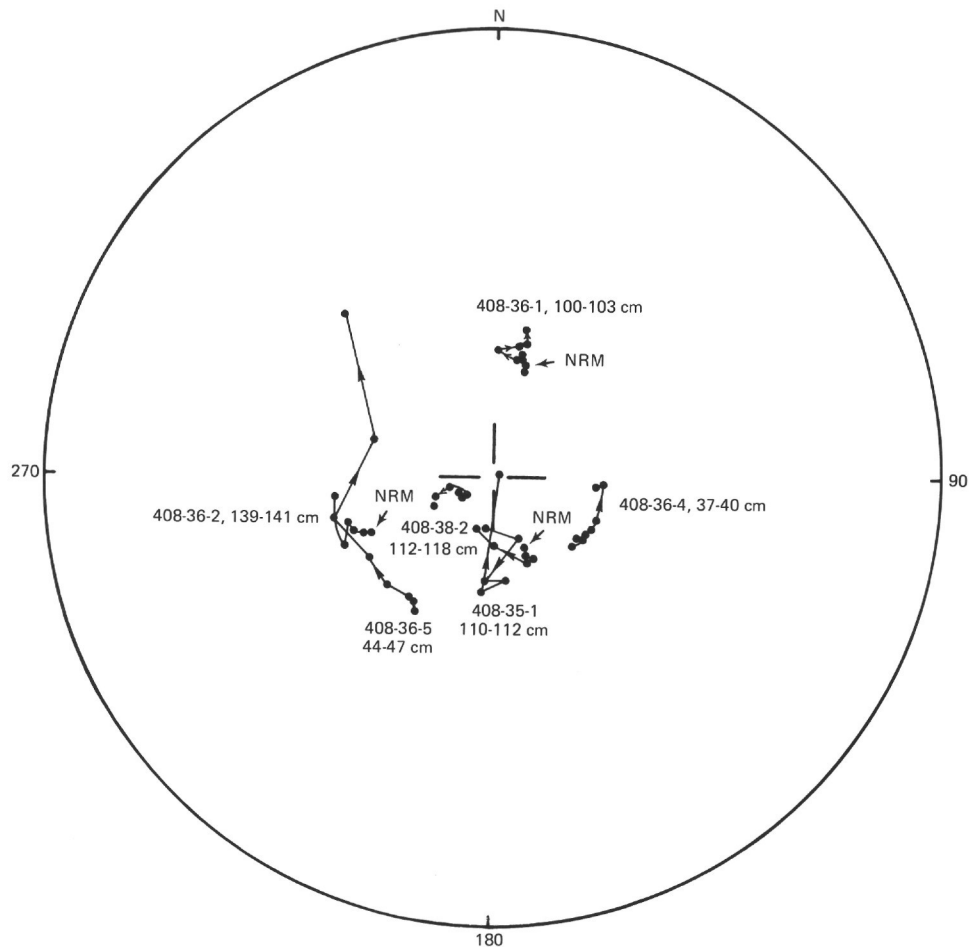


Figure 21. Stereographic (equal-angle) projection showing examples of changes of paleomagnetic direction upon AF demagnetization. Solid circles denote lower hemisphere.

and the pair from unit 1, although the specimen from unit 2 shows slightly more rapid decrease of intensity. The blocking temperature of specimen 36-3 (unit 1) is around 450° and is slightly higher than that of the principal component of magnetization in the other three specimens (about 420°C). This may imply that specimen 36-3 is more oxidized than the others. Decrease of intensity upon heating the specimens from Site 408 is quite regular, in contrast to Site 407, where only one out of four (Section 407-38-2) was similarly regular. Whether the difference between specimens from the two sites results from varied degree of oxidation of titanomagnetite or is more significantly related to difference in titanium content of the ferromagnetic constituents will be examined using thermomagnetic analysis, X-ray diffraction, and X-ray fluorescence in the on-shore laboratory.

No directional change occurred with increasing temperature; all four specimens remained close to their respective NRM directions until their intensities had dropped below about 10 per cent of their NRM value, usually above 400°C (Figure 23). Rotation about 180° of the specimens in the furnace on successive heatings produced large directional changes when the intensities became less

than 10 per cent of the NRM. This suggests that there may from the bulk of the basalt cored at Site 407. However, only 30 meters were cored at Site 408, and the uppermost 20 meters at Site 407 were also normal. The intensities of unit 1 are comparable to those found on other legs that cored over 30 meters of basement. Intensities in unit 2 are considerably higher than has commonly been found, although similar values were recorded between 424 and 434 meters at Site 407. The small amount of directional change upon demagnetization suggests that appreciable secondary remanence, such as viscous remanence and that caused by drilling, did not exist in these specimens; the NRM intensities may therefore be taken as representative of the intensities of these basalts before coring. Since it is unlikely that the earth's magnetic field changes by an order of be a residual field in the cooling chamber which becomes important at intensities as low as $6 \times 10^{-5} \text{ emu cm}^{-3}$.

The polarity at this site, as far as it was cored, agrees with the magnetic anomaly (number 6), and differs in this respect magnitude during one normal epoch, the difference in intensity may arise from many sources, such as different amounts or different grain sizes of the ferromagnetic minerals in the rocks.

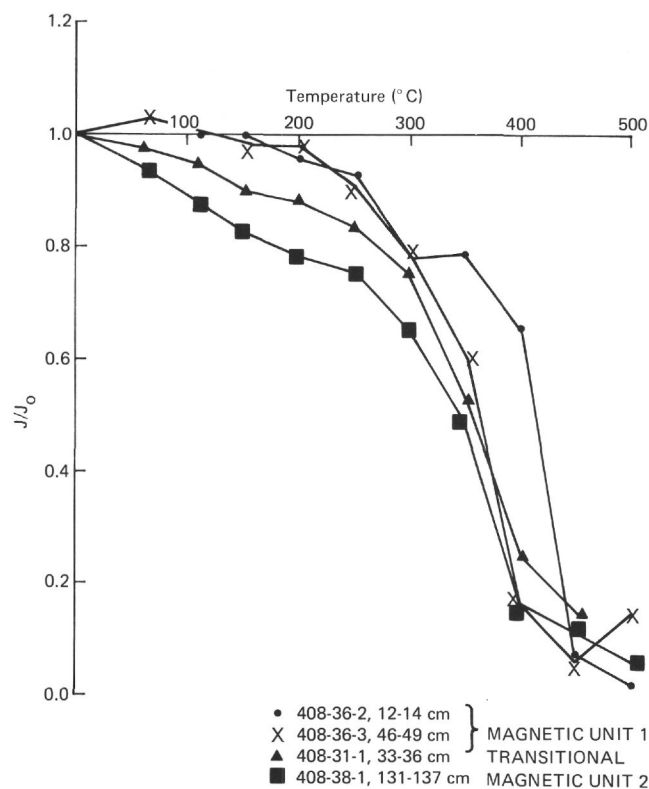


Figure 22. Examples of intensity changes upon thermal demagnetization, Hole 408.

PHYSICAL PROPERTIES OF BASEMENT ROCKS

A limited number of sonic velocity and gamma-ray attenuation measurements were made on the basalt drilled below Core 35.

Although only about a dozen data points (plotted in Figures 24 and 25) are available, both sets suggest negative gradients of velocity and density with depth, at least in these uppermost layers of basement. This is also consistent with the results of Site 407, although the upper basement there has a smaller mean sonic velocity of 4.3 to 4.4 km/s.

HEAT FLOW

Three downhole sediment temperature measurements were made at subbottom depths of 95, 171, and 247 meters, with the same method as at the previous site. Temperature records are similar to that shown for Hole 407, and appears sufficiently good to provide the proper information on the *in-situ* temperature. Temperature of the bottom water was not recorded, and has been estimated from available oceanographic data. Figure 26 is a plot of sediment temperature versus sub-bottom depth. From this figure, the most probable value of temperature gradient is about 5.38°C/100 m.

Fifteen analog thermal conductivity measurements were made on unsplit sections of sediment cores (Table 4). Figure 27 shows the downhole plots of the thermal conductivity. The thermal conductivity of the upper sediment is very slightly greater than that of the lower one. Bulk average of thermal conductivity at this site is 2.34 ± 0.22 mcal/cm s °C.

Heat flow at this site is thus calculated to be 1.26 H.F.U. This value is about the same as that obtained at Site 407 and that of the normal ocean basins.

CORRELATION OF SEISMIC REFLECTION PROFILE WITH DRILLING RESULTS

At Site 408 we were unable to run an on-site sonobuoy, because the ocean currents were not sufficient to stream the airgun away from the ship's hull. Using the approach CSP profile, sediment thickness can be estimated. No significant internal reflectors were apparent; this confirms the drilling results that hardness and/or lithologic contrasts are not evident in the sediment section.

Sediment thickness can be estimated assuming a linear velocity gradient. The thickness is (see Section F, Site 407)

$$H = V_0 (e^{\alpha t} - 1)/a$$

Acoustic basement is at 370 ms (double time); with $V_0 = 1500$ m/s, $H = 304$ meters. The first basalt was felt at 321 meters. This represents only 5 per cent error, and indicates the great utility of this estimation method.

SUMMARY AND CONCLUSIONS

The seismic reflection profile looked very similar to that from Site 407. Transparent sediment a few hundred meters thick lies draped over the basement in a way similar to that at Site 407. We chose a site where a block of this sediment is raised above the surrounding terrain, so that slumping from nearby highs would not obscure the sedimentary record. A complete bathymetric survey was not available for this site, and it is possible that this raised block is elongated toward the north. This site is on magnetic anomaly 6 (about 20 m.y.), chosen to be somewhat older than the oldest exposed crust in Iceland, and thus to provide evidence of the development of Iceland prior to subaerially exposed rocks.

The site was chosen to be on the northwest side of anomaly 6, because of the asymmetry of anomalies relative to crustal blocks of this strike at these latitudes. Fortunately, the conditions of sedimentary high and magnetic setting coincided at this site. We recovered 38 meters of Pleistocene glacial marine sediments and turbidites at the top of the sedimentary section (Figure 28). Turbidites were not expected, because the site is on a hill. The sedimentary block on which the site was drilled may have been uplifted in late Pleistocene time. The basement, however, as seen on the seismic reflection profiles, shows significantly less uplift than the sediment/water interface. The block may instead be connected to high ground away from the line of the profile, most probably to the north.

Coarse (pebble-size or larger) glacial erratics occur to 34 meters sub-bottom (Pleistocene). Similarly, glacial marine sediments are confined to the Pleistocene at Site 407. This contrasts with observations made on Leg 12 that glacial marine sediments can be found well down into the Pliocene, and indicates that part of the upper Pliocene, and possibly part of the Pleistocene, are missing at Holes 407 and 408.

Below the Pleistocene is a thick Pliocene to Miocene unit of almost pure nannofossil ooze that contains about 10 per

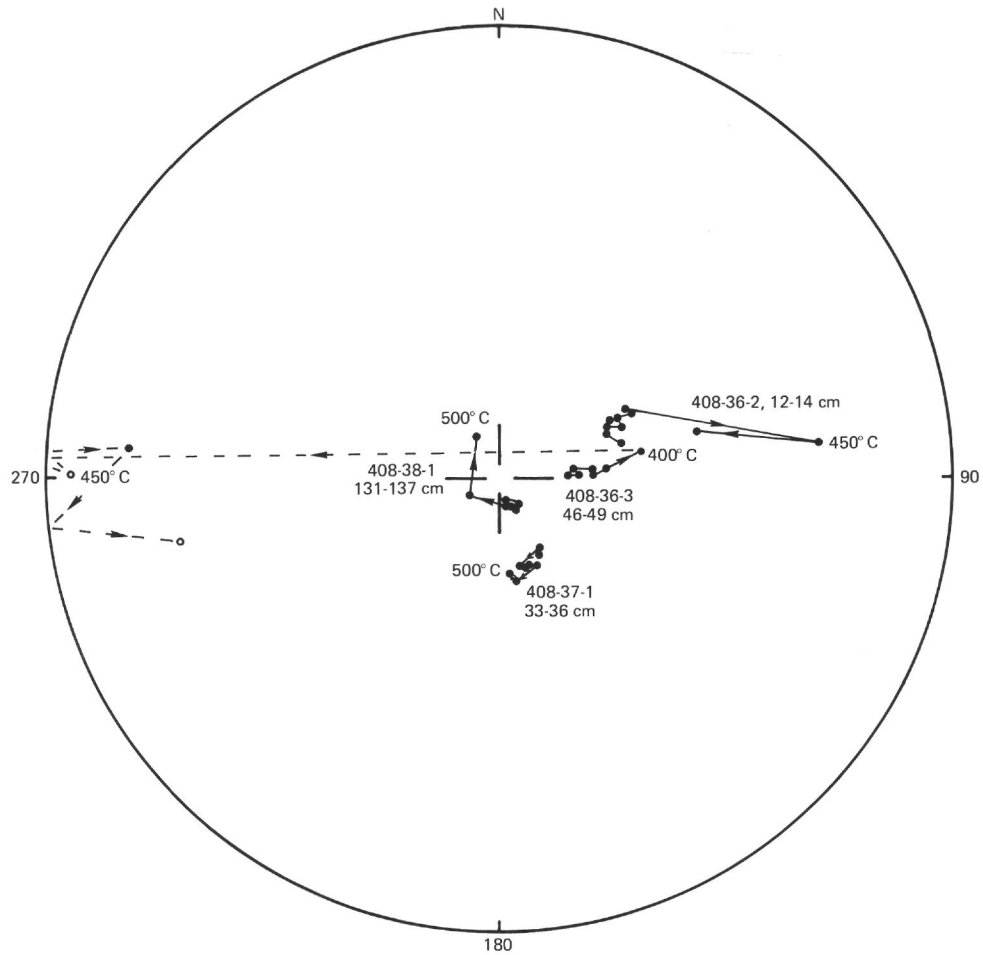


Figure 23. Stereographic (equal-angle) projection showing examples of changes of paleomagnetic direction upon thermal demagnetization. Solid circles denote lower hemisphere.

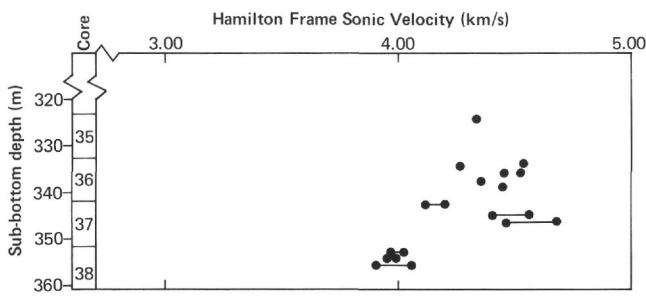


Figure 24. Sonic velocity versus depth, Hole 408.

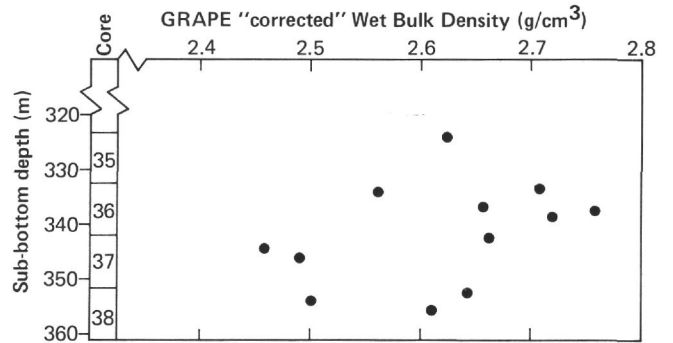


Figure 25. GRAPE "corrected" wet-bulk density versus depth, Hole 408.

cent foraminifers and small amounts of volcanic glass and glauconite. This unit corresponds closely to the unit of similar age at Site 407, where again a thick nannofossil ooze unit was present, and sedimentation rates are similar (about 35 m/m.y. at Site 408). The major hiatus (lower/upper Miocene) at Site 407 does not occur at Site 408, where this nannofossil ooze unit is instead separated from a mid-Miocene siliceous nannofossil ooze by a minor hiatus.

Sediment accumulation rate in the early Miocene-middle Miocene was 15 m/m.y.

A granite pebble $10 \times 6 \times 3$ cm occurs at 209 meters depth. This is an indication of glaciation or an unusual erratic-producing mechanism (tree roots, kelp hold-fasts, aquatic animal gastroliths). It is an arfvedsonite

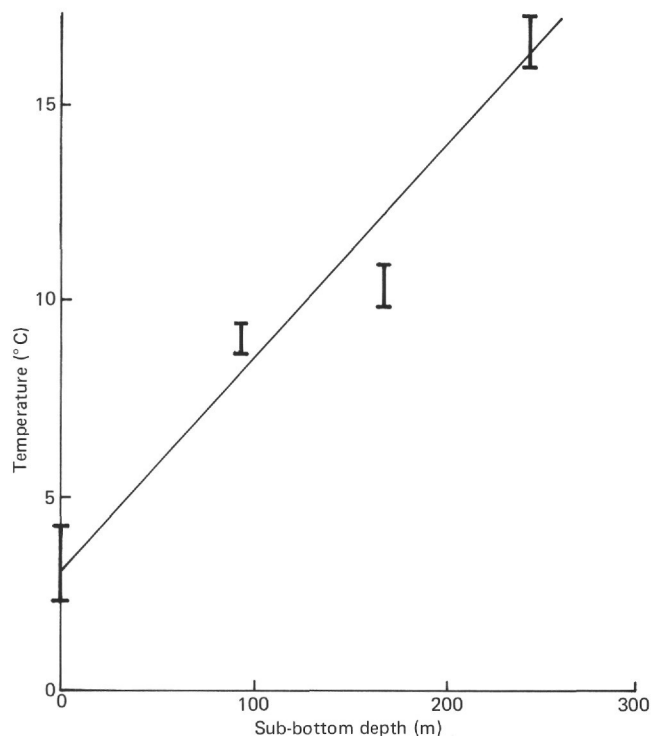


Figure 26. Temperature versus depth sub-bottom, Hole 408.

TABLE 4
Thermal Conductivity of Sediments Site 408

Sample (Interval in cm)	Uncorrected Conductivity	Corrected Conductivity (mcal/cm s °C)
10-4, 50	1.71	1.69
10-4, 90	2.63	2.58
11-4, 78	2.18	2.14
11-5, 30	2.48	2.46
11-5, 78	2.03	2.01
11-5, 127	2.85	2.79
average of Cores 10 and 11:		2.28
18-3, 35	2.82	2.79
18-3, 70	2.62	2.57
18-3, 118	2.70	2.59
19-3, 49.5	2.64	2.61
19-3, 101	2.81	2.78
average of Cores 18 and 19:		2.67
26-5, 50	2.60	2.55
26-5, 90	2.46	2.41
27-1, 55	2.26	2.19
27-1, 90	2.25	2.20
average of Cores 26 and 27:		2.34
average of Cores 18 to 27:		2.52

aegirine-augite sanidine granite, a peralkaline granite with mineralogy suggestive of rapid cooling and texture appropriate for a shallow sub-volcanic environment. Such a granite block may have been ejected by explosive volcanism or transported by one of the carriers listed above.

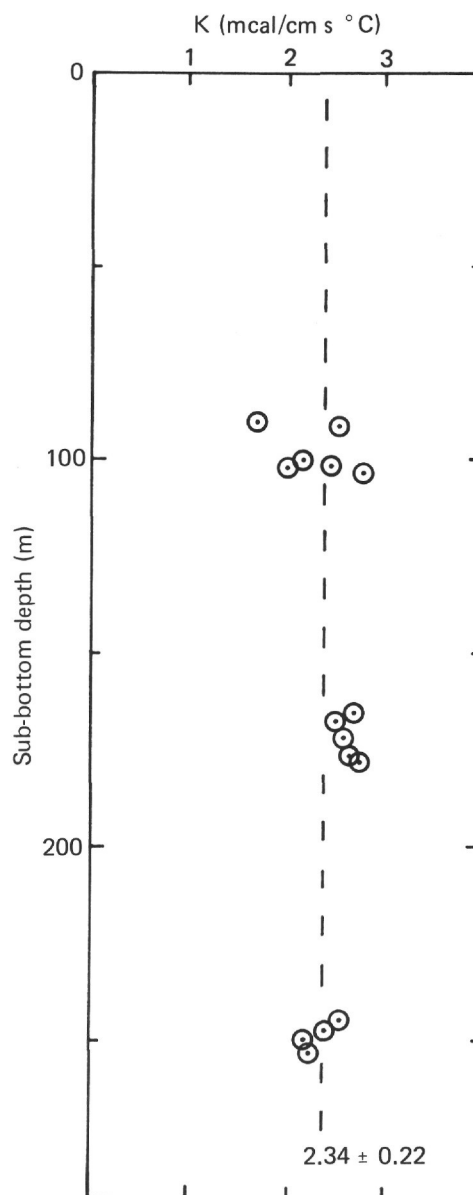


Figure 27. Variations in thermal conductivity with depth sub-bottom, Hole 408.

The basaltic basement was drilled for 37.4 meters, of which 34 per cent was recovered. About nine cooling units are defined by interlayered sediments, chilled margins, drilling rate, and petrography. In the upper part of the lava sequence, flows are generally aphyric or sparsely aphyric, with plagioclase and olivine. Geochemical data indicate compositions intermediate between those for lavas from Sites 407 and 409.

Of the basalts from the three holes on the Reykjanes Ridge, those at Hole 408 are the most altered. The core can be divided into two parts from this point of view, an upper more oxidized part, and a lower more reduced part; both parts show approximately equal proportions of alteration phases. In both parts smectite and calcite are prominent; smectite rims vesicles and bordering veins, and calcite crystallized late to fill the remaining cracks and voids.

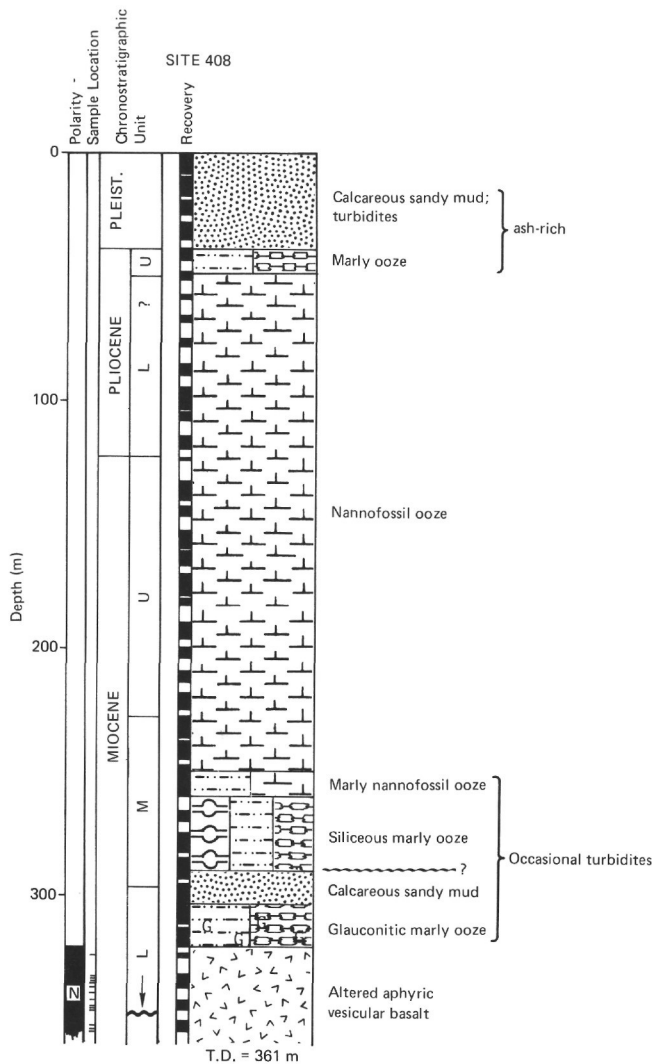


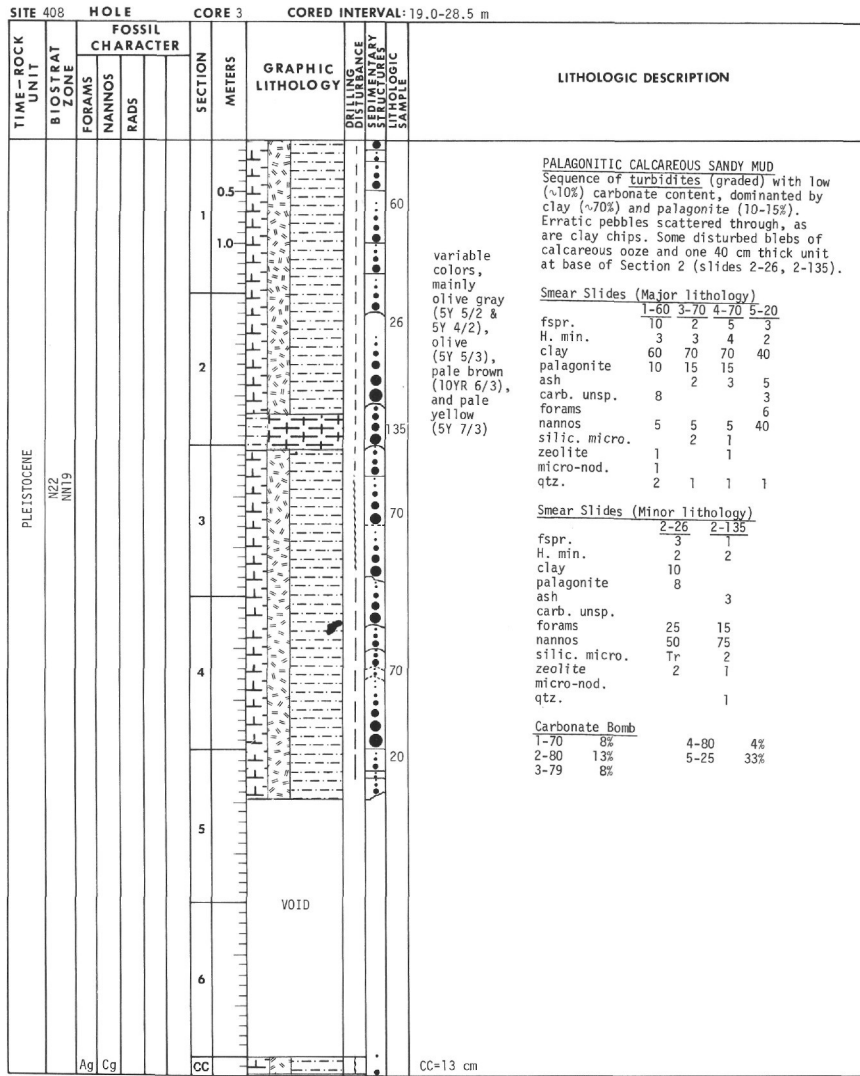
Figure 28. Summary of stratigraphic section for Hole 408.

Pyrite occurs in the reduced section of the core, as cubes crystallizing in veins and vesicles. Zeolites are confined almost entirely to altering glassy rims, which seem to be the only places where activities of such components as Si are high enough for them to precipitate.

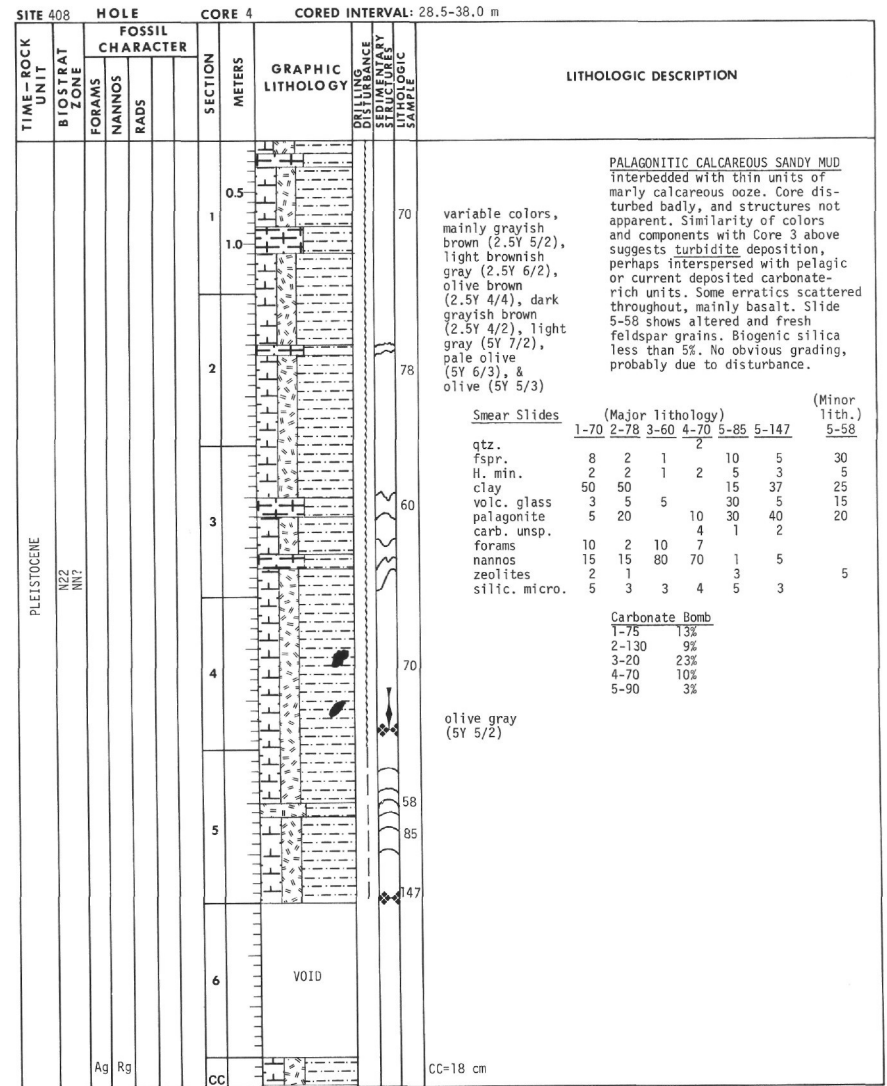
All the basalts in this hole were normally magnetized, as expected from the positive magnetic anomaly (6) on which the hole was placed. However, a distinct change of magnetic inclination, intensity, and stability seems to occur about two-thirds of the way down the section. For the upper group of specimens, the mean inclination was 59°, the mean NRM intensity 1.1×10^{-3} emu cm⁻³ and the median destructive field on AF demagnetization 230 Oe; for the lower group the mean inclination was 83°, the mean NRM intensity 8.9×10^{-3} emu cm⁻³, and the median destructive field 85 Oe. These differences indicate two distinct episodes of volcanism, separated in time by perhaps a few thousand years. The change in magnetic properties coincides, however, with the alteration boundary mentioned above, and the difference in magnetic properties may be related to the different styles of alteration above and below this level.

REFERENCES

Berggren, W.A., 1972. A Cenozoic time-scale — some implications for regional geology and paleobiogeography, *Lethaia*, v. 5, p. 195-215.
 Briden, J.C. and Ward, M.A., 1966. Analysis of magnetic inclinations in borecores, *Pure Applied Geophysics*, v. 63, p. 133.
 Gieskes, J.M., 1975. Interstitial water studies, Leg 35. In Craddock, C., Hollister, C.D., et al., *Initial Reports of the Deep Sea Drilling Project*, v. 35: Washington (U.S. Government Printing Office), p. 407-424.
 Sayles, F.L. and Manheim, F.T., 1975. Interstitial solutions and diagenesis in deeply buried marine sediments: results from the Deep Sea Drilling Project, *Geochim. Cosmochim. Acta*, v. 39, p. 103.
 Schilling, J.G., 1973. Iceland mantle plume: geochemical study of the Reykjanes Ridge, *Nature*, v. 242, p. 565.



Explanatory notes in Chapter 1



SITE 408		HOLE		CORE 8		CORED INTERVAL: 66.5-76.0 m																																																								
TIME-ROCK UNIT	BIOSTRAT ZONE	FOSSIL CHARACTER			SECTION METERS	GRAPHIC LITHOLOGY	LITHOLOGIC DESCRIPTION																																																							
		FORAMS	NANNOS	RADS																																																										
PLIOCENE	N19 N15				0.5		48																																																							
					1.0		intermixed gray (5Y 6/1) and white (7.5YR 8/0) with several blebs of greenish gray (5G 6/1)																																																							
		Ag	Ag		2		105																																																							
					CC		74																																																							
							12																																																							
<p>NANNOFOSSIL OOZE Mostly gray with 5-15% clay, 5-10% forams, few (1-5%) radiolarians, heavy minerals (opaque), volcanic glass, diatoms. Scoria pebble at 1-20.</p> <p>Smear Slides</p> <table border="1"> <thead> <tr> <th></th> <th>1-48</th> <th>1-105</th> <th>2-74</th> <th>CC</th> </tr> </thead> <tbody> <tr> <td>nannos</td> <td>60</td> <td>75</td> <td>75</td> <td>74</td> </tr> <tr> <td>forams</td> <td>10</td> <td>5</td> <td>5</td> <td>5</td> </tr> <tr> <td>diatoms</td> <td>5</td> <td>2</td> <td>1</td> <td>Tr</td> </tr> <tr> <td>sp. spic.</td> <td>2</td> <td>2</td> <td>3</td> <td>3</td> </tr> <tr> <td>silicoflag.</td> <td>Tr</td> <td>--</td> <td>--</td> <td>--</td> </tr> <tr> <td>clay</td> <td>15</td> <td>5</td> <td>7</td> <td>5</td> </tr> <tr> <td>H. min.</td> <td>Tr</td> <td>Tr</td> <td>1</td> <td>1</td> </tr> <tr> <td>volc. glass</td> <td>5</td> <td>3</td> <td>3</td> <td>5</td> </tr> <tr> <td>carb. unsp.</td> <td>3</td> <td>2</td> <td>Tr</td> <td>2</td> </tr> <tr> <td>rads</td> <td>--</td> <td>5</td> <td>5</td> <td>5</td> </tr> </tbody> </table> <p>Carbonate Bomb 1-50 94% 2-55 91%</p>									1-48	1-105	2-74	CC	nannos	60	75	75	74	forams	10	5	5	5	diatoms	5	2	1	Tr	sp. spic.	2	2	3	3	silicoflag.	Tr	--	--	--	clay	15	5	7	5	H. min.	Tr	Tr	1	1	volc. glass	5	3	3	5	carb. unsp.	3	2	Tr	2	rads	--	5	5	5
	1-48	1-105	2-74	CC																																																										
nannos	60	75	75	74																																																										
forams	10	5	5	5																																																										
diatoms	5	2	1	Tr																																																										
sp. spic.	2	2	3	3																																																										
silicoflag.	Tr	--	--	--																																																										
clay	15	5	7	5																																																										
H. min.	Tr	Tr	1	1																																																										
volc. glass	5	3	3	5																																																										
carb. unsp.	3	2	Tr	2																																																										
rads	--	5	5	5																																																										

SITE 408		HOLE		CORE 9		CORED INTERVAL: 76.0-85.5 m																																									
TIME-ROCK UNIT	BIOSTRAT ZONE	FOSSIL CHARACTER			SECTION METERS	GRAPHIC LITHOLOGY	LITHOLOGIC DESCRIPTION																																								
		FORAMS	NANNOS	RADS																																											
PLIOCENE	N19 N15				0.5		37																																								
					1.0		intermixed white (2.5Y 8/0) and gray (10YR 6/1) with scattered streaks and blebs of greenish gray (5G 6/1)																																								
		Ag	Ag		2		96																																								
					CC																																										
<p>SILICA-RICH NANNOFOSSIL OOZE white and gray intermixed with some volcanic glass, forams, radiolarians (mostly spines), sponge spicules, and forams (5-15%) (Minor lith.)</p> <p>Smear Slides</p> <table border="1"> <thead> <tr> <th></th> <th>1-37</th> <th>2-96</th> <th>CC</th> </tr> </thead> <tbody> <tr> <td>nannos</td> <td>81</td> <td>70</td> <td>80</td> </tr> <tr> <td>forams</td> <td>3</td> <td>3</td> <td>15</td> </tr> <tr> <td>diatoms</td> <td>3</td> <td>3</td> <td>--</td> </tr> <tr> <td>rads</td> <td>1</td> <td>10</td> <td>2</td> </tr> <tr> <td>sp. spic.</td> <td>7</td> <td>2</td> <td>--</td> </tr> <tr> <td>silicoflag.</td> <td>Tr</td> <td>2</td> <td>--</td> </tr> <tr> <td>volc. glass</td> <td>5</td> <td>3</td> <td>--</td> </tr> <tr> <td>H. min.</td> <td>Tr</td> <td>2</td> <td>Tr</td> </tr> <tr> <td>palagonite</td> <td>Tr</td> <td>Tr</td> <td>1</td> </tr> </tbody> </table> <p>Carbonate Bomb 1-42 92% 2-42 92%</p>									1-37	2-96	CC	nannos	81	70	80	forams	3	3	15	diatoms	3	3	--	rads	1	10	2	sp. spic.	7	2	--	silicoflag.	Tr	2	--	volc. glass	5	3	--	H. min.	Tr	2	Tr	palagonite	Tr	Tr	1
	1-37	2-96	CC																																												
nannos	81	70	80																																												
forams	3	3	15																																												
diatoms	3	3	--																																												
rads	1	10	2																																												
sp. spic.	7	2	--																																												
silicoflag.	Tr	2	--																																												
volc. glass	5	3	--																																												
H. min.	Tr	2	Tr																																												
palagonite	Tr	Tr	1																																												

Explanatory notes in Chapter 1

SITE 408		HOLE		CORE 10		CORED INTERVAL: 85.5-95.0 m																																																																																																				
TIME-ROCK UNIT	BIOSTRAT ZONE	FOSSIL CHARACTER			SECTION METERS	GRAPHIC LITHOLOGY	LITHOLOGIC DESCRIPTION																																																																																																			
		FORAMS	NANNOS	RADS																																																																																																						
PLIOCENE	N19				0.5		48																																																																																																			
					1.0		owing to intense deformation, intermixing of colors: white (2.5Y 8/0), gray (5Y 6/1), light gray (10YR 7/2), gray (5Y 5/1), with few scattered patches of very dark gray (10YR 3/1), greenish gray (5G 6/1)																																																																																																			
		Ag	Ag		2		102																																																																																																			
					3		105																																																																																																			
					4		102																																																																																																			
					CC		8																																																																																																			
<p>FORAMINIFERA-RICH NANNOFOSSIL OOZE Mixture of white, gray, greenish gray, mostly nannofossils, some samples contain more forams (10-15%) and radiolarians (10%) than others. Some volcanic glass, mostly fresh, up to 20% in one sample (Section 5, 8 cm).</p> <p>Smear Slides (Major lithology)</p> <table border="1"> <thead> <tr> <th></th> <th>1-48</th> <th>2-102</th> <th>3-102</th> <th>5-8</th> </tr> </thead> <tbody> <tr> <td>nannos</td> <td>78</td> <td>75</td> <td>75</td> <td>55</td> </tr> <tr> <td>forams</td> <td>10</td> <td>14</td> <td>10</td> <td>15</td> </tr> <tr> <td>diatoms</td> <td>Tr</td> <td>--</td> <td>5</td> <td>5</td> </tr> <tr> <td>sp. spic.</td> <td>5</td> <td>--</td> <td>8</td> <td>--</td> </tr> <tr> <td>volc. glass</td> <td>3</td> <td>5</td> <td>--</td> <td>20</td> </tr> <tr> <td>rads</td> <td>2</td> <td>--</td> <td>2</td> <td>--</td> </tr> <tr> <td>palagonite</td> <td>2</td> <td>--</td> <td>Tr</td> <td>Tr</td> </tr> <tr> <td>H. min.</td> <td>Tr</td> <td>Tr</td> <td>Tr</td> <td>--</td> </tr> <tr> <td>clay</td> <td>--</td> <td>5</td> <td>--</td> <td>--</td> </tr> <tr> <td>Mica</td> <td>--</td> <td>--</td> <td>--</td> <td>Tr</td> </tr> <tr> <td>Fspr.</td> <td>--</td> <td>--</td> <td>--</td> <td>Tr</td> </tr> </tbody> </table> <p>Smear Slides (Minor lithology)</p> <table border="1"> <thead> <tr> <th></th> <th>1-49</th> <th>2-105</th> </tr> </thead> <tbody> <tr> <td>nannos</td> <td>75</td> <td>75</td> </tr> <tr> <td>forams</td> <td>2</td> <td>5</td> </tr> <tr> <td>diatoms</td> <td>2</td> <td>Tr</td> </tr> <tr> <td>rads</td> <td>10</td> <td>3</td> </tr> <tr> <td>sp. spic.</td> <td>Tr</td> <td>2</td> </tr> <tr> <td>silicoflag.</td> <td>1</td> <td>--</td> </tr> <tr> <td>volc. glass</td> <td>3</td> <td>10</td> </tr> <tr> <td>H. min.</td> <td>1</td> <td>--</td> </tr> <tr> <td>carb. unsp.</td> <td>1</td> <td>Tr</td> </tr> <tr> <td>clay</td> <td>5</td> <td>3</td> </tr> <tr> <td>palagonite</td> <td>Tr</td> <td>1</td> </tr> <tr> <td>fspr.</td> <td>--</td> <td>Tr</td> </tr> </tbody> </table> <p>Carbonate Bomb 1-53 83% 2-51 84% 3-53 91% 4-53 89% 5-23 81%</p>									1-48	2-102	3-102	5-8	nannos	78	75	75	55	forams	10	14	10	15	diatoms	Tr	--	5	5	sp. spic.	5	--	8	--	volc. glass	3	5	--	20	rads	2	--	2	--	palagonite	2	--	Tr	Tr	H. min.	Tr	Tr	Tr	--	clay	--	5	--	--	Mica	--	--	--	Tr	Fspr.	--	--	--	Tr		1-49	2-105	nannos	75	75	forams	2	5	diatoms	2	Tr	rads	10	3	sp. spic.	Tr	2	silicoflag.	1	--	volc. glass	3	10	H. min.	1	--	carb. unsp.	1	Tr	clay	5	3	palagonite	Tr	1	fspr.	--	Tr
	1-48	2-102	3-102	5-8																																																																																																						
nannos	78	75	75	55																																																																																																						
forams	10	14	10	15																																																																																																						
diatoms	Tr	--	5	5																																																																																																						
sp. spic.	5	--	8	--																																																																																																						
volc. glass	3	5	--	20																																																																																																						
rads	2	--	2	--																																																																																																						
palagonite	2	--	Tr	Tr																																																																																																						
H. min.	Tr	Tr	Tr	--																																																																																																						
clay	--	5	--	--																																																																																																						
Mica	--	--	--	Tr																																																																																																						
Fspr.	--	--	--	Tr																																																																																																						
	1-49	2-105																																																																																																								
nannos	75	75																																																																																																								
forams	2	5																																																																																																								
diatoms	2	Tr																																																																																																								
rads	10	3																																																																																																								
sp. spic.	Tr	2																																																																																																								
silicoflag.	1	--																																																																																																								
volc. glass	3	10																																																																																																								
H. min.	1	--																																																																																																								
carb. unsp.	1	Tr																																																																																																								
clay	5	3																																																																																																								
palagonite	Tr	1																																																																																																								
fspr.	--	Tr																																																																																																								

SITE 408		HOLE		CORE 11		CORED INTERVAL: 95.0-104.5 m		
TIME-ROCK UNIT	BIOSTRAT ZONE	FOSSIL CHARACTER			SECTION METERS	GRAPHIC LITHOLOGY	DRILLING FLUID STRUC/FUNERY SAMPLE	LITHOLOGIC DESCRIPTION
		FORAMS	NANNOS	RADS				
PLIOCENE	N19				0.5		72	intermixed white (2.5Y 8/0 to light brownish gray (2.5Y 6/2)
					1.0			FORAMINIFERA-RICH NANNOFOSSIL OOZE Mostly varying shades of gray, forams 10-15%. Very few diatoms, radiolarians, sponge spicules, volcanic glass (1-5%). Some lamination visible near bottom, most above intensely deformed, very few opaque heavy minerals (<1%).
					2			interlayered greenish gray (5GY 6/1), gray (5Y 6/1), white (5Y 8/1)
					3			white (5Y 8/1), gray (5Y 6/1), dark gray (5Y 4/1)
					4			greenish gray (5GY 6/1), gray (5Y 6/1), white (5Y 8/1)
					VOID			
					26		26	olive gray (5Y 4/2), light gray (5Y 7/1)
					66		66	interlayers of light gray (5Y 7/1) and dark gray brown (10YR 4/2) with greenish gray blebs (5G 6/1) at 120-140
					92		92	interlayered gray (5Y 6/1) and light gray (5Y 6/1), white (5Y 8/1) bleb at 95
					43		43	light gray (5Y 7/1) pale olive (10Y 6/2) dusky yellowish green (5GY 5/2) at 41-51 (Sec. 6) CC=dark greenish gray (5GY 4/1)
					CC			

Explanatory notes in Chapter 1

SITE 408		HOLE		CORE 12		CORED INTERVAL: 104.5-114.0 m		
TIME-ROCK UNIT	BIOSTRAT ZONE	FOSSIL CHARACTER			SECTION METERS	GRAPHIC LITHOLOGY	DRILLING FLUID STRUC/FUNERY SAMPLE	LITHOLOGIC DESCRIPTION
		FORAMS	NANNOS	RADS				
PLIOCENE	N19				0.5		74	interlayered white (5Y 8/1) to gray with scattered wisps of greenish gray (5G 6/1), bleb of olive gray (5Y 5/2) at 2-135
					1.0			NANNOFOSSIL OOZE White to gray, intensely deformed, small amounts (<5%) of clay, heavy minerals, diatoms, radiolarians, sponge spicules and foraminifera.
					2			
					3			
					4			
					55		55	
					60		60	
					135		135	
					9		9	
					CC			

Smear Slides

	1-74	2-55	2-60	2-135	3-9	CC-9
nannos	79	8	85	76	73	80
forams	5	5	3	5	7	2
diatoms	1	--	1	3	1	1
rads	5	--	3	5	5	3
sp. spic.	2	2	1	2	--	2
clay	5	--	3	3	5	7
opaque H.	1	1	1	1	1	Tr
silicoflag.	Tr	--	--	--	3	--
fspr.	1	--	--	1	1	Tr
carb. unsp.	1	5	1	1	1	1
volc. glass	--	--	2	2	2	3
palagonite	--	--	Tr	Tr	1	1

Carbonate Bomb

1-53	81%
2-53	80%

SITE 408		HOLE		CORE 13		CORED INTERVAL: 114.0-123.5 m					
TIME-ROCK UNIT	BIOSTRAT ZONE	FOSSIL CHARACTER			SECTION	METERS	GRAPHIC LITHOLOGY	DRILLING DISTURBANCE	SERVICENESS	LITHOLOGIC SAMPLE	LITHOLOGIC DESCRIPTION
		FORAMS	NANNOS	RADS							
PLIOCENE	N18-N19 NN11				1	0.5 1.0				12	interlayered greenish gray (5G 6/1) and gray (5Y 6/1)
					2					109	light gray (5Y 7/1) and very dark gray (5Y 3/1)
		Ag	Ag		3					74	103-110 - ash very dark gray (5Y 2.5/1) light gray (5Y 7/1)
										87	white with rare scattered blebs of very dark gray (5Y 2.5/1)
										12	

Smear Slides (Major lithology)			
	1-42	2-74	3-87
nannos	75	78	83
forams	5	10	10
diatoms	2	2	--
rads	5	1	2
sp. spic.	2	2	3
silicoflag.	1	--	Tr
clay	3	5	--
volc. glass	3	--	Tr
palagonite	1	--	1
H. min.	1	1	Tr
fspr.	1	--	--
zeolite	Tr	--	--
carb. unsp.	1	1	--

Smear Slides (Minor lithology)			
	1-109		
volc. glass	68		
altered glass	20		
palagonite	3		
opaque H.	4		
nannos	5		

Carbonate Bomb	
1-53	84%
2-53	94%
3-53	96%

SITE 408		HOLE		CORE 14		CORED INTERVAL: 123.5-133.0 m					
TIME-ROCK UNIT	BIOSTRAT ZONE	FOSSIL CHARACTER			SECTION	METERS	GRAPHIC LITHOLOGY	DRILLING DISTURBANCE	SERVICENESS	LITHOLOGIC SAMPLE	LITHOLOGIC DESCRIPTION
		FORAMS	NANNOS	RADS							
Late MIOCENE	N17 NN11	Ag	Ag								white (5Y 8/1) CC=15 cm

Explanatory notes in Chapter 1

SITE 408		HOLE		CORE 15		CORED INTERVAL: 133.0-142.5 m					
TIME-ROCK UNIT	BIOSTRAT ZONE	FOSSIL CHARACTER			SECTION	METERS	GRAPHIC LITHOLOGY	DRILLING DISTURBANCE	SERVICENESS	LITHOLOGIC SAMPLE	LITHOLOGIC DESCRIPTION
		FORAMS	NANNOS	RADS							
Late MIOCENE	N17				1	0.5 1.0				63	white (N8)
					2					74	white (5Y 8/1)
					3					93	white (5Y 8/1)
					4					62	gray (5Y 6/1)
					5					55	light gray (5Y 7/1)

Smear Slides					
	1-63	2-93	3-34	3-62	4-55
nannos	70	82	75	65	75
forams	20	10	10	20	10
rads	--	2	5	5	Tr
sp. spic.	5	3	5	5	5
volc. glass	5	2	5	5	10
palagonite	Tr	Tr	Tr	Tr	Tr
zeolite	Tr	--	Tr	--	Tr
glaucinite	Tr	--	--	--	Tr
H. min.	Tr	1	Tr	--	Tr
Mica	--	--	--	Tr	Tr

Carbonate Bomb	
1-53	91%
2-53	95%
3-53	78%
4-53	93%
5-53	95%

SITE 408		HOLE			CORE 18		CORED INTERVAL: 161.5-171.0 m																																																																														
TIME-ROCK UNIT	BIOSTRAT ZONE	FOSSIL CHARACTER		SECTION	METERS	GRAPHIC LITHOLOGY	DRILLING DISTURBANCE	LITHOLOGIC SAMPLE																																																																													
		FORAMS	NANNOS																																																																																		
late MIOCENE	N16-N17	Cg	Ag	CC	0.5		115	LITHOLOGIC SAMPLE																																																																													
					1.0																																																																																
					2																																																																																
					3																																																																																
					85																																																																																
					60																																																																																
					18																																																																																
					<p>LITHOLOGIC DESCRIPTION</p> <p>FORAMINIFERAL NANNOFOSSIL OOZE Light gray with 10-15% foraminifera, few siliceous microfossils (2-10%), trace detrital minerals, some volcanic glass (<5%).</p> <p>Smear Slides</p> <table border="1"> <thead> <tr> <th></th> <th>1-115</th> <th>2-85</th> <th>3-60</th> <th>4-18</th> </tr> </thead> <tbody> <tr> <td>nannos</td> <td>80</td> <td>71</td> <td>63</td> <td>73</td> </tr> <tr> <td>forams</td> <td>10</td> <td>15</td> <td>15</td> <td>15</td> </tr> <tr> <td>rads</td> <td>--</td> <td>2</td> <td>5</td> <td>--</td> </tr> <tr> <td>sp. spic.</td> <td>5</td> <td>5</td> <td>7</td> <td>5</td> </tr> <tr> <td>carb. unsp.</td> <td>2</td> <td>2</td> <td>5</td> <td>3</td> </tr> <tr> <td>ll. min.</td> <td>Tr</td> <td>Tr</td> <td>Tr</td> <td>1</td> </tr> <tr> <td>fsp.</td> <td>--</td> <td>Tr</td> <td>--</td> <td>--</td> </tr> <tr> <td>volc. glass</td> <td>3</td> <td>5</td> <td>5</td> <td>3</td> </tr> <tr> <td>palagonite</td> <td>--</td> <td>Tr</td> <td>Tr</td> <td>Tr</td> </tr> <tr> <td>glauconite</td> <td>Tr</td> <td>Tr</td> <td>--</td> <td>--</td> </tr> <tr> <td>Mica</td> <td>--</td> <td>--</td> <td>Tr</td> <td>Tr</td> </tr> </tbody> </table> <p>Carbonate Bomb</p> <table border="1"> <thead> <tr> <th></th> <th>1-103</th> <th>81%</th> </tr> </thead> <tbody> <tr> <td>2-23</td> <td>93%</td> </tr> <tr> <td>3-13</td> <td>82%</td> </tr> <tr> <td>4-13</td> <td>86%</td> </tr> </tbody> </table> <p>light gray (5Y 7/1) with rare inter-layers of white (5Y 8/1)</p>										1-115	2-85	3-60	4-18	nannos	80	71	63	73	forams	10	15	15	15	rads	--	2	5	--	sp. spic.	5	5	7	5	carb. unsp.	2	2	5	3	ll. min.	Tr	Tr	Tr	1	fsp.	--	Tr	--	--	volc. glass	3	5	5	3	palagonite	--	Tr	Tr	Tr	glauconite	Tr	Tr	--	--	Mica	--	--	Tr	Tr		1-103	81%	2-23	93%	3-13	82%	4-13	86%			
									1-115	2-85	3-60	4-18																																																																									
					nannos				80	71	63	73																																																																									
forams	10	15	15	15																																																																																	
rads	--	2	5	--																																																																																	
sp. spic.	5	5	7	5																																																																																	
carb. unsp.	2	2	5	3																																																																																	
ll. min.	Tr	Tr	Tr	1																																																																																	
fsp.	--	Tr	--	--																																																																																	
volc. glass	3	5	5	3																																																																																	
palagonite	--	Tr	Tr	Tr																																																																																	
glauconite	Tr	Tr	--	--																																																																																	
Mica	--	--	Tr	Tr																																																																																	
	1-103	81%																																																																																			
2-23	93%																																																																																				
3-13	82%																																																																																				
4-13	86%																																																																																				

Explanatory notes in Chapter 1

SITE 408		HOLE			CORE 19		CORED INTERVAL: 171.0-180.5 m																																																																																																												
TIME-ROCK UNIT	BIOSTRAT ZONE	FOSSIL CHARACTER		SECTION	METERS	GRAPHIC LITHOLOGY	DRILLING DISTURBANCE	LITHOLOGIC SAMPLE																																																																																																											
		FORAMS	NANNOS																																																																																																																
late MIOCENE	N16-N17	Cg	Am	CC	0.5		47	LITHOLOGIC SAMPLE																																																																																																											
					1.0																																																																																																														
					2																																																																																																														
					3																																																																																																														
					55																																																																																																														
					60																																																																																																														
					18																																																																																																														
					<p>LITHOLOGIC DESCRIPTION</p> <p>FORAMINIFERAL NANNOFOSSIL OOZE Light gray with grayish green glauconite-rich laminae, 10-15% foraminifera, some (<5%) siliceous microfossils, volcanic glass, clay, and heavy minerals. Scoria pebble at 5-40.</p> <p>Smear Slides</p> <table border="1"> <thead> <tr> <th></th> <th>1-47</th> <th>1-93</th> <th>2-55</th> <th>5-87</th> <th>6-134</th> <th>7-35</th> </tr> </thead> <tbody> <tr> <td>nannos</td> <td>70</td> <td>69</td> <td>88</td> <td>77</td> <td>74</td> <td>55</td> </tr> <tr> <td>forams</td> <td>10</td> <td>15</td> <td>5</td> <td>5</td> <td>10</td> <td>15</td> </tr> <tr> <td>rads</td> <td>--</td> <td>1</td> <td>--</td> <td>--</td> <td>Tr</td> <td>--</td> </tr> <tr> <td>sp. spic.</td> <td>2</td> <td>2</td> <td>1</td> <td>3</td> <td>3</td> <td>5</td> </tr> <tr> <td>carb. unsp.</td> <td>3</td> <td>3</td> <td>2</td> <td>5</td> <td>--</td> <td>--</td> </tr> <tr> <td>H. min.</td> <td>1</td> <td>--</td> <td>1</td> <td>7</td> <td>1</td> <td>Tr</td> </tr> <tr> <td>volc. glass</td> <td>3</td> <td>10</td> <td>2</td> <td>3</td> <td>10</td> <td>25</td> </tr> <tr> <td>palagonite</td> <td>--</td> <td>Tr</td> <td>--</td> <td>--</td> <td>2</td> <td>--</td> </tr> <tr> <td>glauconite</td> <td>4</td> <td>--</td> <td>--</td> <td>--</td> <td>Tr</td> <td>--</td> </tr> <tr> <td>Mica</td> <td>--</td> <td>Tr</td> <td>--</td> <td>--</td> <td>--</td> <td>Tr</td> </tr> <tr> <td>qtz.</td> <td>--</td> <td>--</td> <td>1</td> <td>--</td> <td>--</td> <td>--</td> </tr> </tbody> </table> <p>Carbonate Bomb</p> <table border="1"> <thead> <tr> <th></th> <th>1-23</th> <th>101%</th> </tr> </thead> <tbody> <tr> <td>2-53</td> <td>90%</td> </tr> <tr> <td>3-53</td> <td>98%</td> </tr> <tr> <td>4-53</td> <td>95%</td> </tr> <tr> <td>5-53</td> <td>96%</td> </tr> <tr> <td>6-53</td> <td>92%</td> </tr> <tr> <td>7-13</td> <td>99%</td> </tr> </tbody> </table> <p>light gray (5Y 7/1) to white (5Y 8/1) with thin laminations of grayish green (10GY 5/2)</p>										1-47	1-93	2-55	5-87	6-134	7-35	nannos	70	69	88	77	74	55	forams	10	15	5	5	10	15	rads	--	1	--	--	Tr	--	sp. spic.	2	2	1	3	3	5	carb. unsp.	3	3	2	5	--	--	H. min.	1	--	1	7	1	Tr	volc. glass	3	10	2	3	10	25	palagonite	--	Tr	--	--	2	--	glauconite	4	--	--	--	Tr	--	Mica	--	Tr	--	--	--	Tr	qtz.	--	--	1	--	--	--		1-23	101%	2-53	90%	3-53	98%	4-53	95%	5-53	96%	6-53	92%	7-13	99%			
									1-47	1-93	2-55	5-87	6-134	7-35																																																																																																					
					nannos				70	69	88	77	74	55																																																																																																					
forams	10	15	5	5	10	15																																																																																																													
rads	--	1	--	--	Tr	--																																																																																																													
sp. spic.	2	2	1	3	3	5																																																																																																													
carb. unsp.	3	3	2	5	--	--																																																																																																													
H. min.	1	--	1	7	1	Tr																																																																																																													
volc. glass	3	10	2	3	10	25																																																																																																													
palagonite	--	Tr	--	--	2	--																																																																																																													
glauconite	4	--	--	--	Tr	--																																																																																																													
Mica	--	Tr	--	--	--	Tr																																																																																																													
qtz.	--	--	1	--	--	--																																																																																																													
	1-23	101%																																																																																																																	
2-53	90%																																																																																																																		
3-53	98%																																																																																																																		
4-53	95%																																																																																																																		
5-53	96%																																																																																																																		
6-53	92%																																																																																																																		
7-13	99%																																																																																																																		

SITE 408		HOLE		CORE 20		CORED INTERVAL: 180.5-190.0 m																									
TIME-ROCK UNIT	BIOSTRAT ZONE	FOSSIL CHARACTER		SECTION	METERS	GRAPHIC LITHOLOGY	LITHOLOGIC DESCRIPTION																								
		FORAMS	NANNOS																												
late MIOCENE	N16-N17	Cg	Ag																												
				1	0.5		light gray (5Y 7/1) wisps of gray (2.5YR 6/0) at 14-22 cm and 100-105 cm																								
				2	1.0		white (5Y 8/1)																								
							<p>NANNOFOSSIL OOZE Tight gray to white with grayish green glauconite-rich laminations in Core Catcher. Few (<5%) detrital minerals and volcanic glass. Scoria pebble at 2-85.</p> <p><u>Smear Slides</u></p> <table border="1"> <tr><td>nannos</td><td>1-17</td></tr> <tr><td>forams</td><td>75</td></tr> <tr><td>diatoms</td><td>7</td></tr> <tr><td>rads</td><td>Tr</td></tr> <tr><td>sp. spic.</td><td>6</td></tr> <tr><td>H. min.</td><td>1</td></tr> <tr><td>clay</td><td>3</td></tr> <tr><td>volc. glass</td><td>2</td></tr> <tr><td>palagonite</td><td>1</td></tr> <tr><td>carb. unsp.</td><td>5</td></tr> </table> <p><u>Carbonate Bomb</u></p> <table border="1"> <tr><td>1-53</td><td>92%</td></tr> <tr><td>2-53</td><td>93%</td></tr> </table>	nannos	1-17	forams	75	diatoms	7	rads	Tr	sp. spic.	6	H. min.	1	clay	3	volc. glass	2	palagonite	1	carb. unsp.	5	1-53	92%	2-53	93%
nannos	1-17																														
forams	75																														
diatoms	7																														
rads	Tr																														
sp. spic.	6																														
H. min.	1																														
clay	3																														
volc. glass	2																														
palagonite	1																														
carb. unsp.	5																														
1-53	92%																														
2-53	93%																														
							light gray (5Y 7/1) with gray green (5GY 5/2) laminations																								

SITE 408		HOLE		CORE 21		CORED INTERVAL: 190.0-199.5 m																																																																									
TIME-ROCK UNIT	BIOSTRAT ZONE	FOSSIL CHARACTER		SECTION	METERS	GRAPHIC LITHOLOGY	LITHOLOGIC DESCRIPTION																																																																								
		FORAMS	NANNOS																																																																												
late MIOCENE	N16	Cg	Ag																																																																												
				1	0.5		light gray (5Y 7/1) with wisps of dark gray (5Y 3/1) volcanic ash																																																																								
				2	1.0		grayish yellow green (5GY 7/2)																																																																								
				3	1.0		gray green (10GY 5/2)																																																																								
				4	1.0		mottled grayish yellow green (5GY 7/2) and gray green (10G 4/2)																																																																								
							<p>NANNOFOSSIL OOZE Dominantly light gray with some bio-turbation mottling in Sections 3 and 4. Few foraminifera (5-10%), some (<5%) siliceous microfossils, heavy minerals, volcanic glass, glauconite, clay.</p> <p><u>Smear Slides (Major lithology)</u></p> <table border="1"> <tr><th></th><th>1-110</th><th>3-117</th><th>4-50</th></tr> <tr><td>nannos</td><td>80</td><td>79</td><td>68</td></tr> <tr><td>forams</td><td>10</td><td>5</td><td>5</td></tr> <tr><td>diatoms</td><td>2</td><td>Tr</td><td>4</td></tr> <tr><td>rads</td><td>1</td><td>Tr</td><td>1</td></tr> <tr><td>sp. spic.</td><td>1</td><td>2</td><td>5</td></tr> <tr><td>H. min.</td><td>1</td><td>2</td><td>1</td></tr> <tr><td>clay</td><td>--</td><td>5</td><td>3</td></tr> <tr><td>volc. glass</td><td>3</td><td>5</td><td>3</td></tr> <tr><td>glauconite</td><td>1</td><td>2</td><td>1</td></tr> <tr><td>carb. unsp.</td><td>1</td><td>3</td><td>3</td></tr> <tr><td>palagonite</td><td>--</td><td>Tr</td><td>2</td></tr> <tr><td>zeolite</td><td>--</td><td>--</td><td>2</td></tr> </table> <p><u>Smear Slides (Minor lithology)</u></p> <table border="1"> <tr><td>volc. glass</td><td>CC</td></tr> <tr><td>opaque H. min.</td><td>15</td></tr> <tr><td>nannos</td><td>10</td></tr> <tr><td>forams</td><td>Tr</td></tr> <tr><td>rads</td><td>Tr</td></tr> <tr><td>glauconite</td><td>2</td></tr> </table> <p><u>Carbonate Bomb</u></p> <table border="1"> <tr><td>1-53</td><td>81%</td></tr> <tr><td>2-53</td><td>79%</td></tr> <tr><td>3-53</td><td>84%</td></tr> <tr><td>4-53</td><td>76%</td></tr> </table>		1-110	3-117	4-50	nannos	80	79	68	forams	10	5	5	diatoms	2	Tr	4	rads	1	Tr	1	sp. spic.	1	2	5	H. min.	1	2	1	clay	--	5	3	volc. glass	3	5	3	glauconite	1	2	1	carb. unsp.	1	3	3	palagonite	--	Tr	2	zeolite	--	--	2	volc. glass	CC	opaque H. min.	15	nannos	10	forams	Tr	rads	Tr	glauconite	2	1-53	81%	2-53	79%	3-53	84%	4-53	76%
	1-110	3-117	4-50																																																																												
nannos	80	79	68																																																																												
forams	10	5	5																																																																												
diatoms	2	Tr	4																																																																												
rads	1	Tr	1																																																																												
sp. spic.	1	2	5																																																																												
H. min.	1	2	1																																																																												
clay	--	5	3																																																																												
volc. glass	3	5	3																																																																												
glauconite	1	2	1																																																																												
carb. unsp.	1	3	3																																																																												
palagonite	--	Tr	2																																																																												
zeolite	--	--	2																																																																												
volc. glass	CC																																																																														
opaque H. min.	15																																																																														
nannos	10																																																																														
forams	Tr																																																																														
rads	Tr																																																																														
glauconite	2																																																																														
1-53	81%																																																																														
2-53	79%																																																																														
3-53	84%																																																																														
4-53	76%																																																																														
							grayish yellow green (5GY 7/2)																																																																								
							gray green (10GY 5/2)																																																																								
							mottled grayish yellow green (5GY 7/2) and gray green (10G 4/2)																																																																								
							mottled gray green (10GY 5/2) and tight gray (5Y 7/1)																																																																								

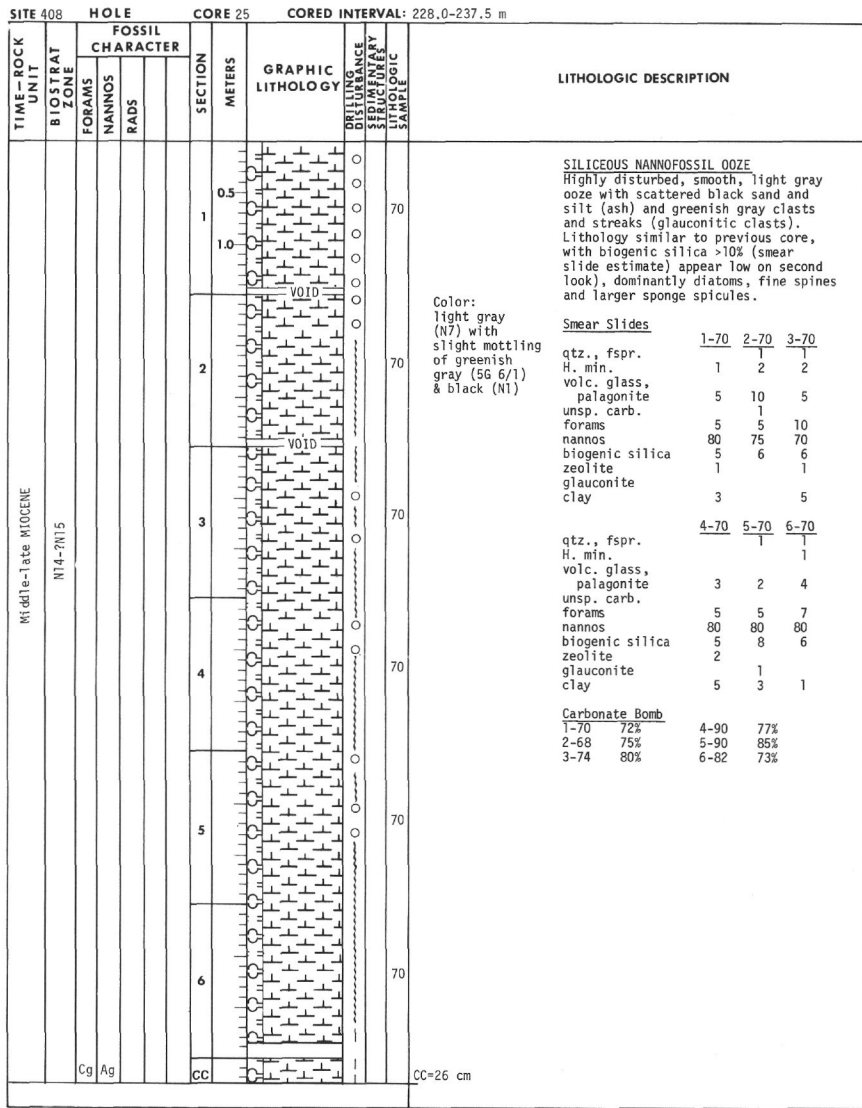
SITE 408		HOLE		CORE 22		CORED INTERVAL: 199.5-209.0 m																																																																																															
TIME-ROCK UNIT	BIOSTRAT ZONE	FOSSIL CHARACTER		SECTION	METERS	GRAPHIC LITHOLOGY	LITHOLOGIC DESCRIPTION																																																																																														
		FORAMS	NANNOS																																																																																																		
late MIOCENE	N16	Cg	Ag																																																																																																		
				1	0.5		VOID																																																																																														
				2	1.0		greenish gray (5G 6/1) and grayish green (10G 4/2)																																																																																														
				3	1.0		VOID																																																																																														
							<p>NANNOFOSSIL OOZE Firm, fine-grained nannofossil ooze with greenish gray (5G 6/1) laminations of glauconite-rich ooze (slide 1-118). Unit mainly light gray to white. Examination of Core Catcher under binocular scope suggests green color possibly due to alteration of volcanic debris (green "reaction rims" forming around glass). Biogenic silica increasing to near 10% in this core, although carbonate bomb results indicate 90-81% CaCO₃. Diatoms throughout the core with abundance comparable to 4-50 of Core 21. Abundances of silica (biogenic) estimated in smear slides are not very reliable, and show a strong bias from one observer to the next. Re-examination (qualitative) suggests a silica-rich unit beginning in Core 21 (slide 4-50) and extending down core to Core 30 (slide 5-36), although the 10% level does not appear to be exceeded in Core 22. Volcanic glass scattered throughout, with minor ash-rich mottles (3-5).</p> <p><u>Smear Slides (Major lithology)</u></p> <table border="1"> <tr><th></th><th>1-10</th><th>1-48</th><th>2-70</th><th>3-9</th></tr> <tr><td>qtz., fspr.</td><td>2</td><td>2</td><td>1</td><td></td></tr> <tr><td>H. min.</td><td>2</td><td>2</td><td>1</td><td></td></tr> <tr><td>volc. glass,</td><td></td><td></td><td></td><td></td></tr> <tr><td> palagonite</td><td>8</td><td>3</td><td>3</td><td>3</td></tr> <tr><td>carb. unsp.</td><td>5</td><td>5</td><td>1</td><td>1</td></tr> <tr><td>forams</td><td>5</td><td>5</td><td>10</td><td>15</td></tr> <tr><td>nannos</td><td>70</td><td>73</td><td>80</td><td>75</td></tr> <tr><td>biogenic silica</td><td>8</td><td>7</td><td>4</td><td>4</td></tr> <tr><td>zeolite</td><td></td><td>2</td><td></td><td>2</td></tr> <tr><td>glauconite</td><td></td><td></td><td></td><td></td></tr> </table> <p><u>Smear Slides</u></p> <table border="1"> <tr><th></th><th>Ash</th><th>Green laminations</th></tr> <tr><td>qtz., fspr.</td><td>3-5</td><td>1-118</td></tr> <tr><td>H. min.</td><td>10</td><td></td></tr> <tr><td>volc. glass,</td><td></td><td></td></tr> <tr><td> palagonite</td><td>77</td><td></td></tr> <tr><td>carb. unsp.</td><td></td><td></td></tr> <tr><td>forams</td><td></td><td>13</td></tr> <tr><td>nannos</td><td></td><td>80</td></tr> <tr><td>biogenic silica</td><td>10</td><td>2</td></tr> <tr><td>zeolite</td><td></td><td></td></tr> <tr><td>glauconite</td><td></td><td>5</td></tr> </table> <p><u>Carbonate Bomb</u></p> <table border="1"> <tr><td>1-53</td><td>90%</td></tr> <tr><td>2-70</td><td>91%</td></tr> <tr><td>3-70</td><td>91%</td></tr> </table>		1-10	1-48	2-70	3-9	qtz., fspr.	2	2	1		H. min.	2	2	1		volc. glass,					palagonite	8	3	3	3	carb. unsp.	5	5	1	1	forams	5	5	10	15	nannos	70	73	80	75	biogenic silica	8	7	4	4	zeolite		2		2	glauconite						Ash	Green laminations	qtz., fspr.	3-5	1-118	H. min.	10		volc. glass,			palagonite	77		carb. unsp.			forams		13	nannos		80	biogenic silica	10	2	zeolite			glauconite		5	1-53	90%	2-70	91%	3-70	91%
	1-10	1-48	2-70	3-9																																																																																																	
qtz., fspr.	2	2	1																																																																																																		
H. min.	2	2	1																																																																																																		
volc. glass,																																																																																																					
palagonite	8	3	3	3																																																																																																	
carb. unsp.	5	5	1	1																																																																																																	
forams	5	5	10	15																																																																																																	
nannos	70	73	80	75																																																																																																	
biogenic silica	8	7	4	4																																																																																																	
zeolite		2		2																																																																																																	
glauconite																																																																																																					
	Ash	Green laminations																																																																																																			
qtz., fspr.	3-5	1-118																																																																																																			
H. min.	10																																																																																																				
volc. glass,																																																																																																					
palagonite	77																																																																																																				
carb. unsp.																																																																																																					
forams		13																																																																																																			
nannos		80																																																																																																			
biogenic silica	10	2																																																																																																			
zeolite																																																																																																					
glauconite		5																																																																																																			
1-53	90%																																																																																																				
2-70	91%																																																																																																				
3-70	91%																																																																																																				
							colors: white (N7), to light gray (5Y 7/1) with laminations of greenish gray (5G 6/1) and grayish green (10G 4/2)																																																																																														

Explanatory notes in Chapter 1

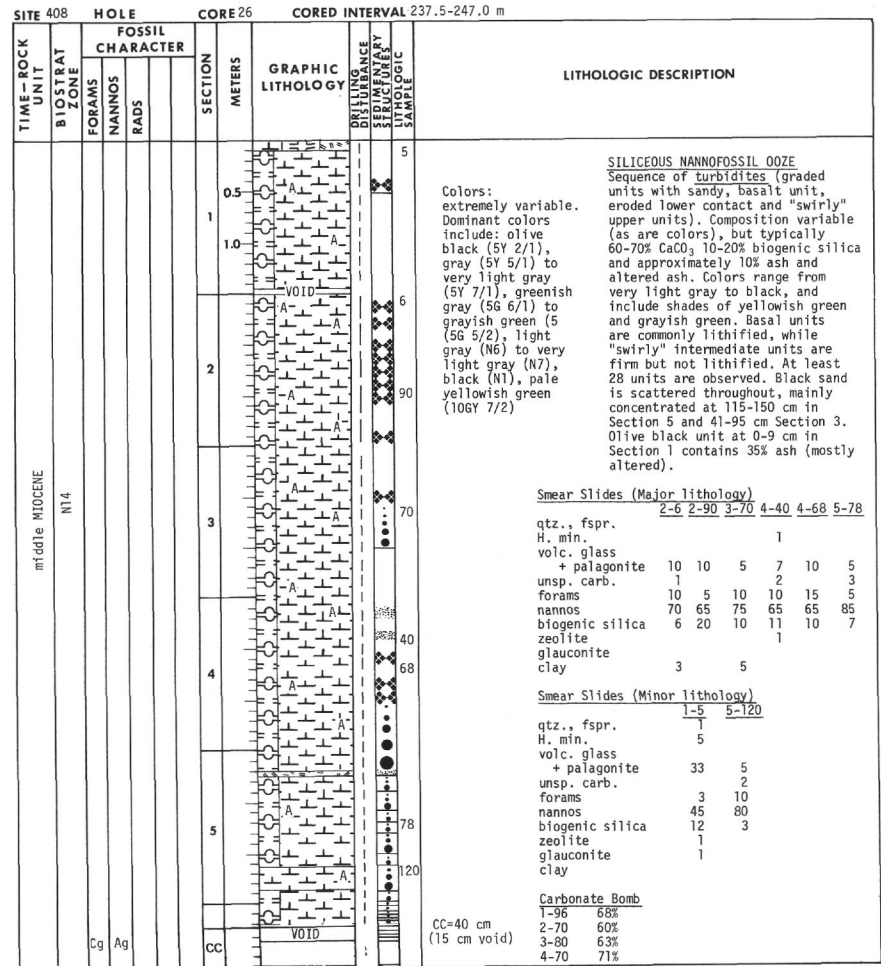
SITE 408		HOLE		CORE 23		CORED INTERVAL: 209.0-218.5 m	
TIME-ROCK UNIT	BIOSTRAT ZONE	FOSSIL CHARACTER			SECTION METERS	GRAPHIC LITHOLOGY	LITHOLOGIC DESCRIPTION
		FORAMS	NANNOS	RADS			
late MIOCENE	N16				0.5		olive brown (2.5Y 4/4) NANNOFOSSIL OOZE with siliceous nanno ooze in most of Section 3. Disturbed nanofossil ooze with glauconite-rich layering (fine laminations and mottling). Typically 3-5% volcanic glass, mainly unaltered, with one ash horizon (3-52) and one ash-rich clay (1-1). Up to 2-3% glauconite in greenish portions. Fine-grained, soupy in many portions. Granite erratic at 4 cm. Taminations: greenish gray (5G 6/1), light gray to white (N7 to N8)
					1.0		Smear Slides (Major lithology) 1-110 2-70 qtz. fspr. H. min. clay volc. glass palagonite glauconite carb. unsp. forams nannos diatoms rads sp. spic. zeolite 1 1 4 3 5 10 85 80 3 1 1 1 2 1
					2.0		light gray (5Y 6/1) Smear Slides (Minor lithology) 1-1 3-41 3-52 3-65 qtz. fspr. H. min. clay volc. glass palagonite glauconite carb. unsp. forams nannos diatoms rads sp. spic. zeolite 10 5 2 2 35 5 5 15 5 90 5 1 3 1 2 5 5 1 5 20 75 70 1 1 8 1 1 1 1 1 9 1 1 2
				3.0		VOID CC=20 cm	Carbonate Bomb 2-90 84% 3-67 62%

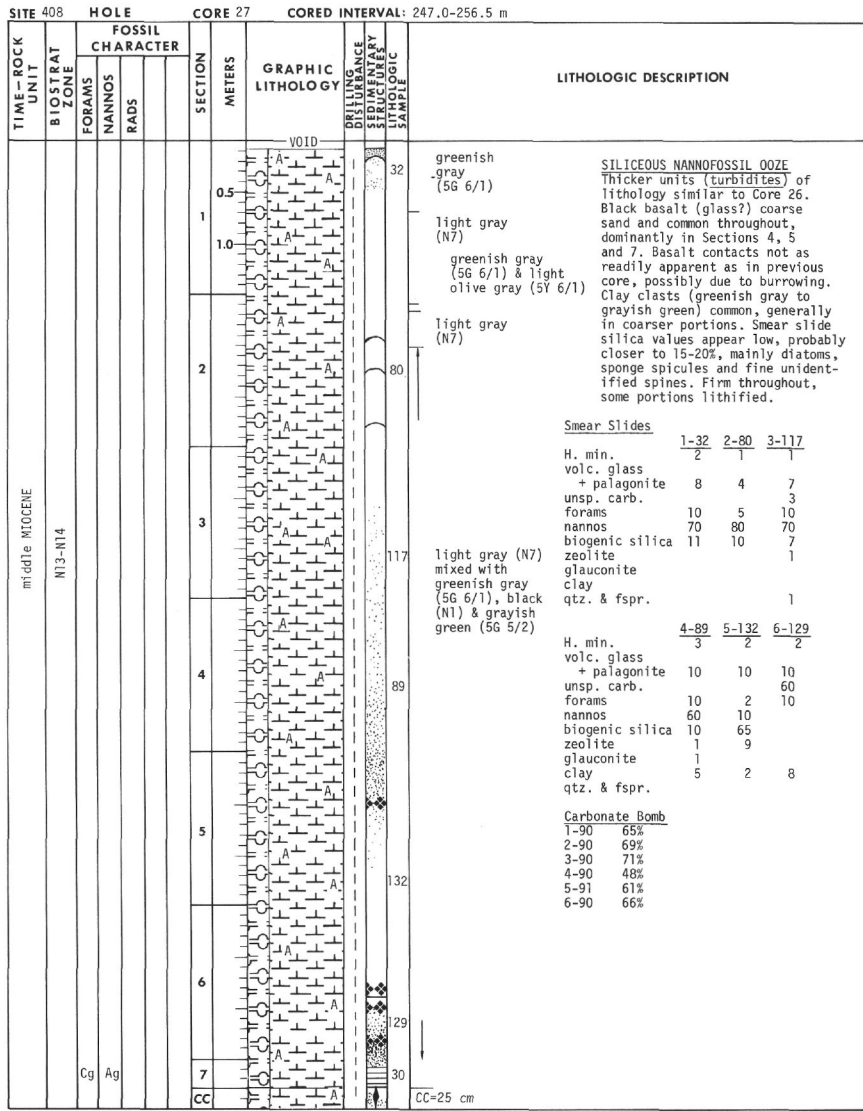
Explanatory notes in Chapter 1

SITE 408		HOLE		CORE 24		CORED INTERVAL: 218.5-228.0 m		
TIME-ROCK UNIT	BIOSTRAT ZONE	FOSSIL CHARACTER			SECTION METERS	GRAPHIC LITHOLOGY	LITHOLOGIC DESCRIPTION	
		FORAMS	NANNOS	RADS				
late MIOCENE	N16				0.5		SILICEOUS NANNOFOSSIL OOZE Disturbed to soupy core of light gray to gray ooze with scattered mottles of black ash plus sand-size ash throughout. Biogenic silica 10% or higher, mainly diatoms, sponge spicules and fine spines (sponge or radiolarian spicules) without central hole. Distinct laminations are absent due to deformation, but sandy texture (black flecks gritty) suggest similar original lithology to Cores 23, 24.	
					1.0		Smear Slides (Major lithology) 1-70 2-108 3-90 5-70 qtz. fspr. H. min. clay palagonite + volc. glass zeolite unsp. carb. forams nannos diatoms rads sp. spic. silicoflag. glauconite 1 2 1 2 5 2 3 5 11 1 1 1 1 4 2 2 7 5 5 8 65 65 65 80 4 4 3 2 1 1 3 1 10 10 3 5	
					2.0		Smear Slides (Minor lithology) 1-130 6-20 qtz. fspr. H. min. clay palagonite + volc. glass zeolite unsp. carb. forams nannos diatoms rads sp. spic. silicoflag. glauconite 1 1 1 1 5 8 5 3 2 8 5 75 75 1 1 2 2	
					3.0		VOID	Carbonate Bomb 1-72 59% 2-93 66% 3-70 70% 5-90 76% 6-45 76%
					4.0		VOID	
					5.0		VOID	
					6.0		VOID CC=32 cm, 6 cm void	

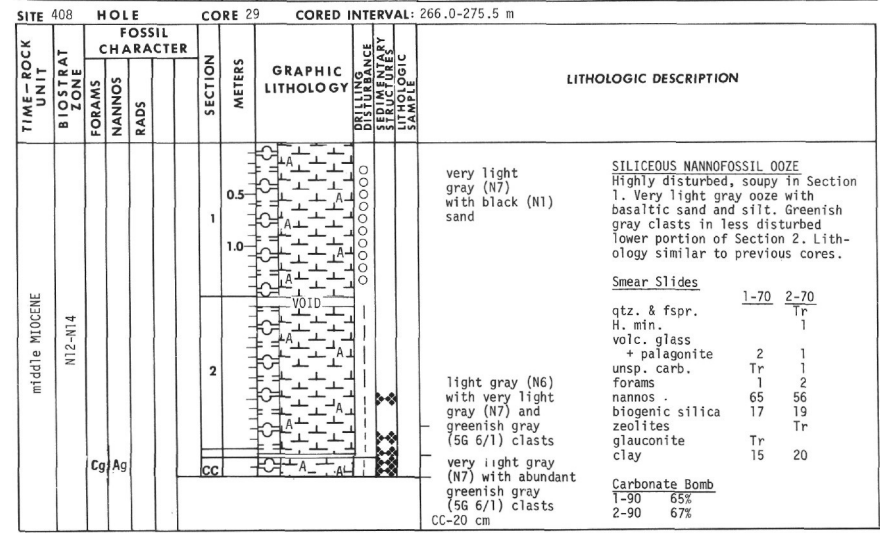
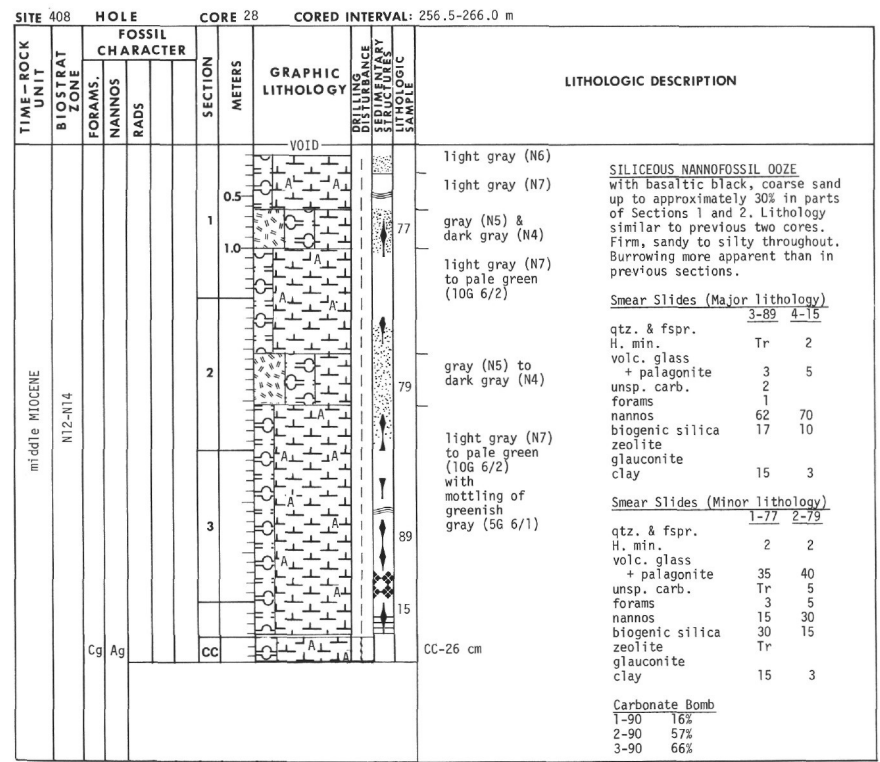


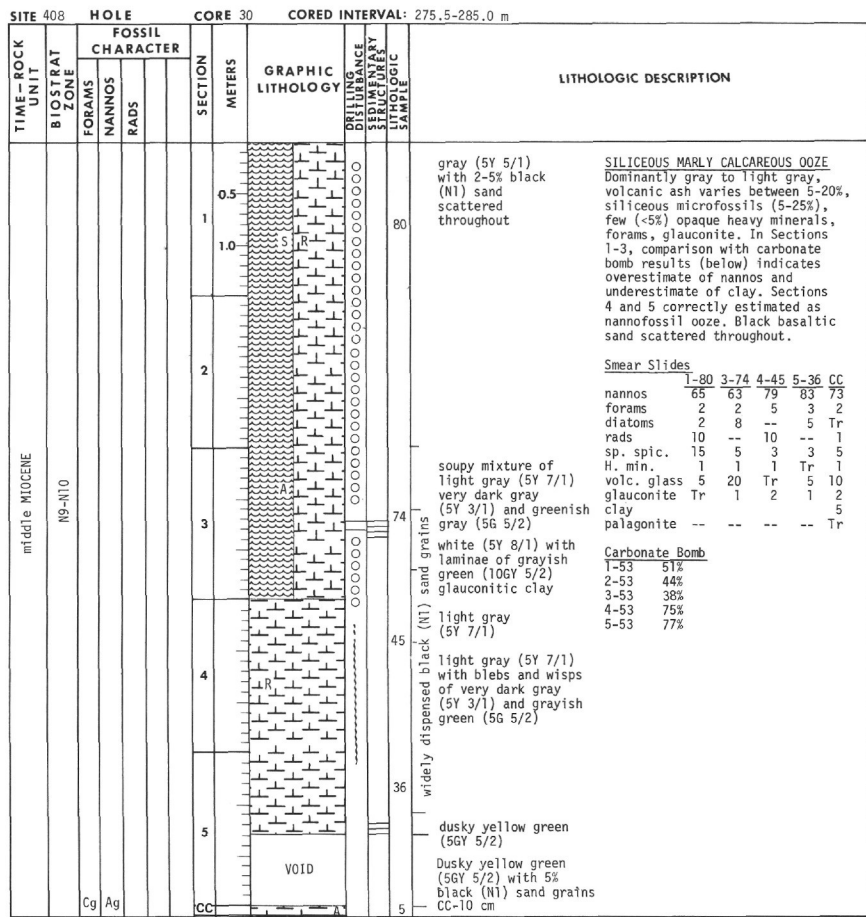
Explanatory notes in Chapter 1



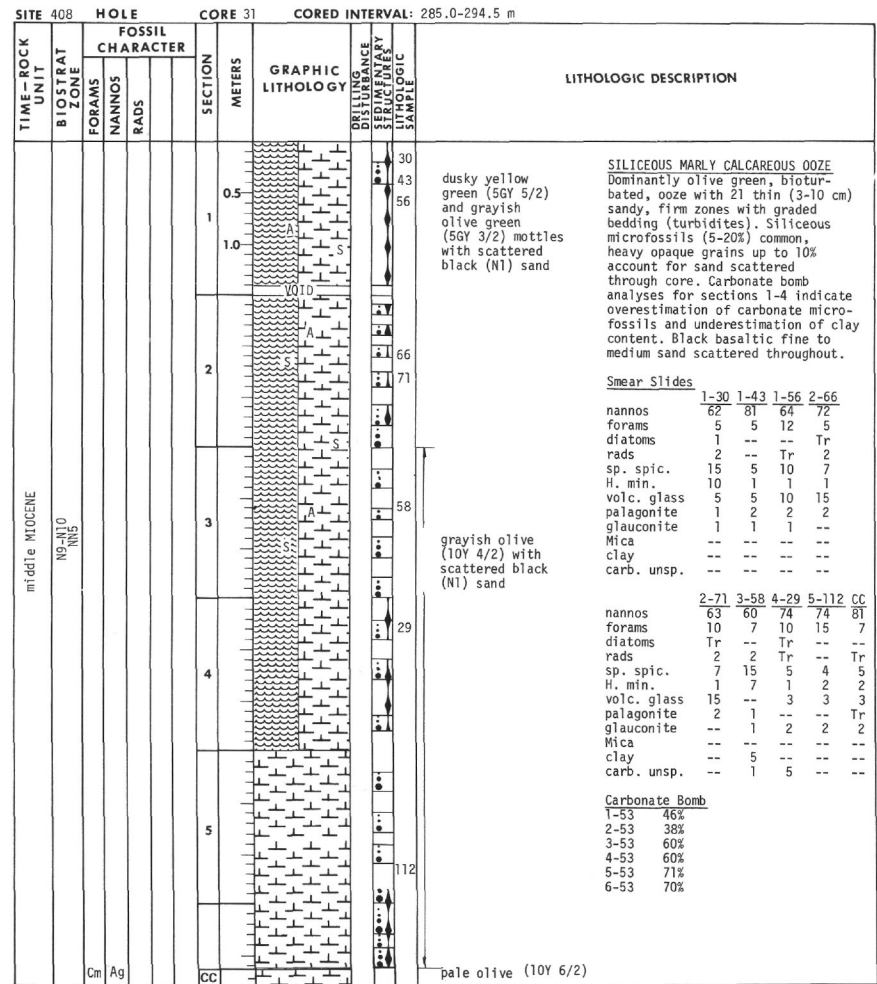


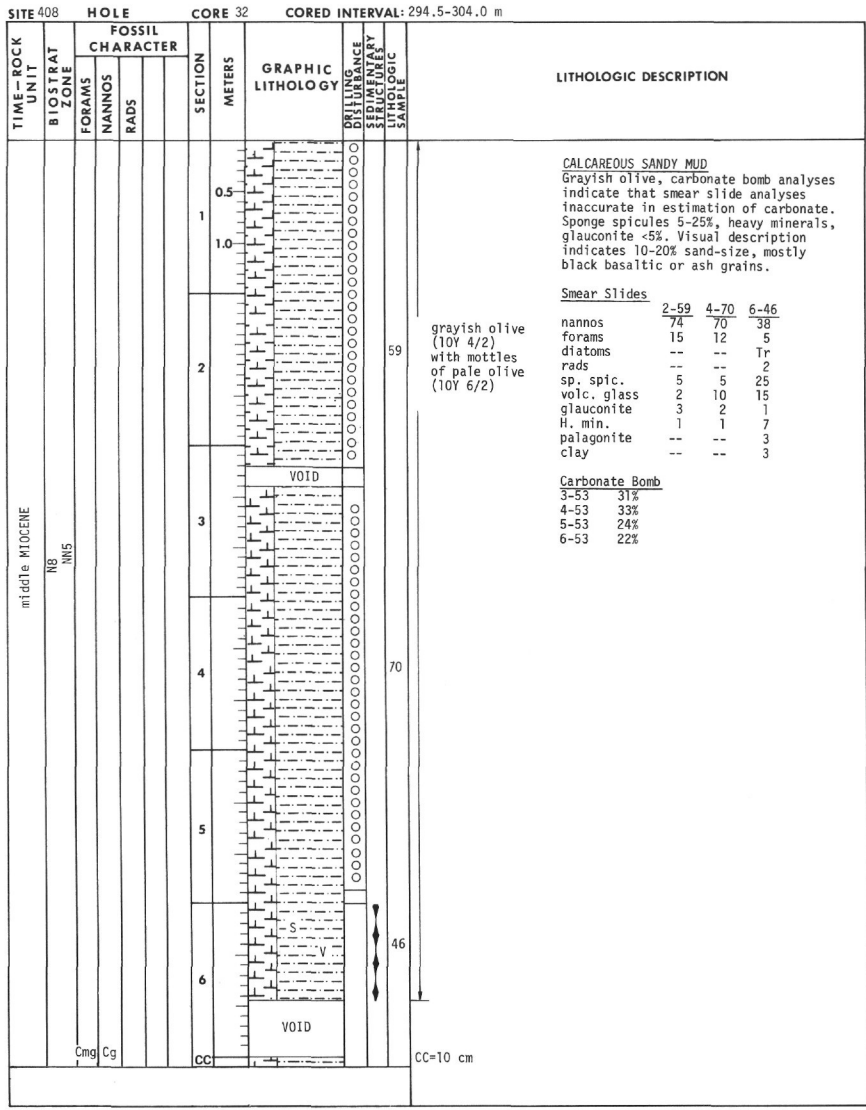
Explanatory notes in Chapter 1



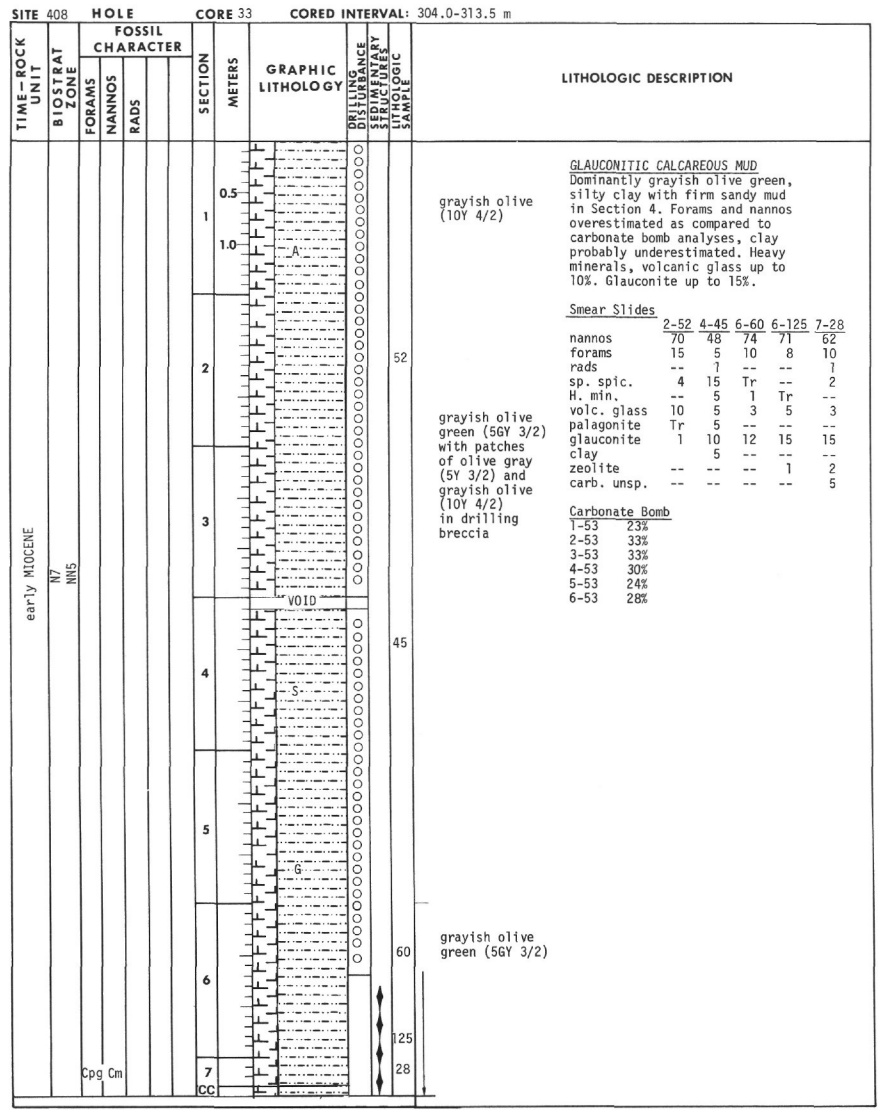


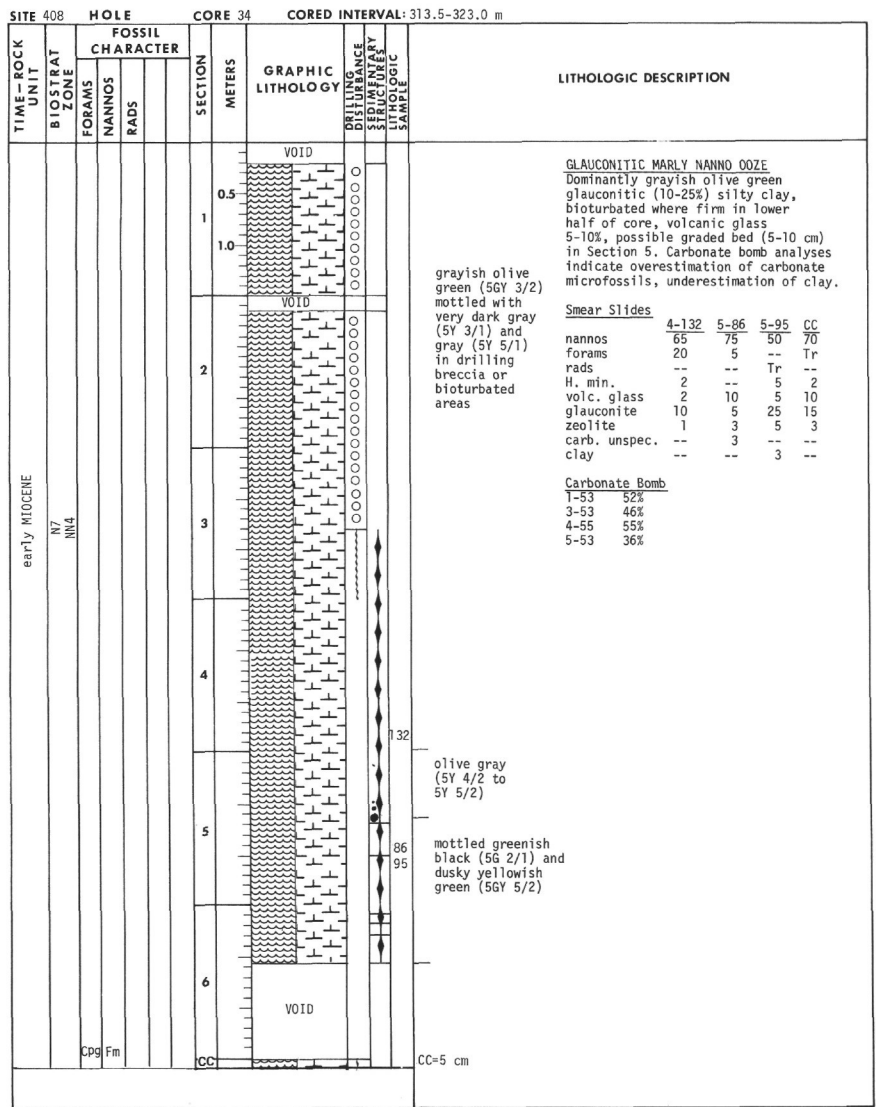
Explanatory notes in Chapter 1



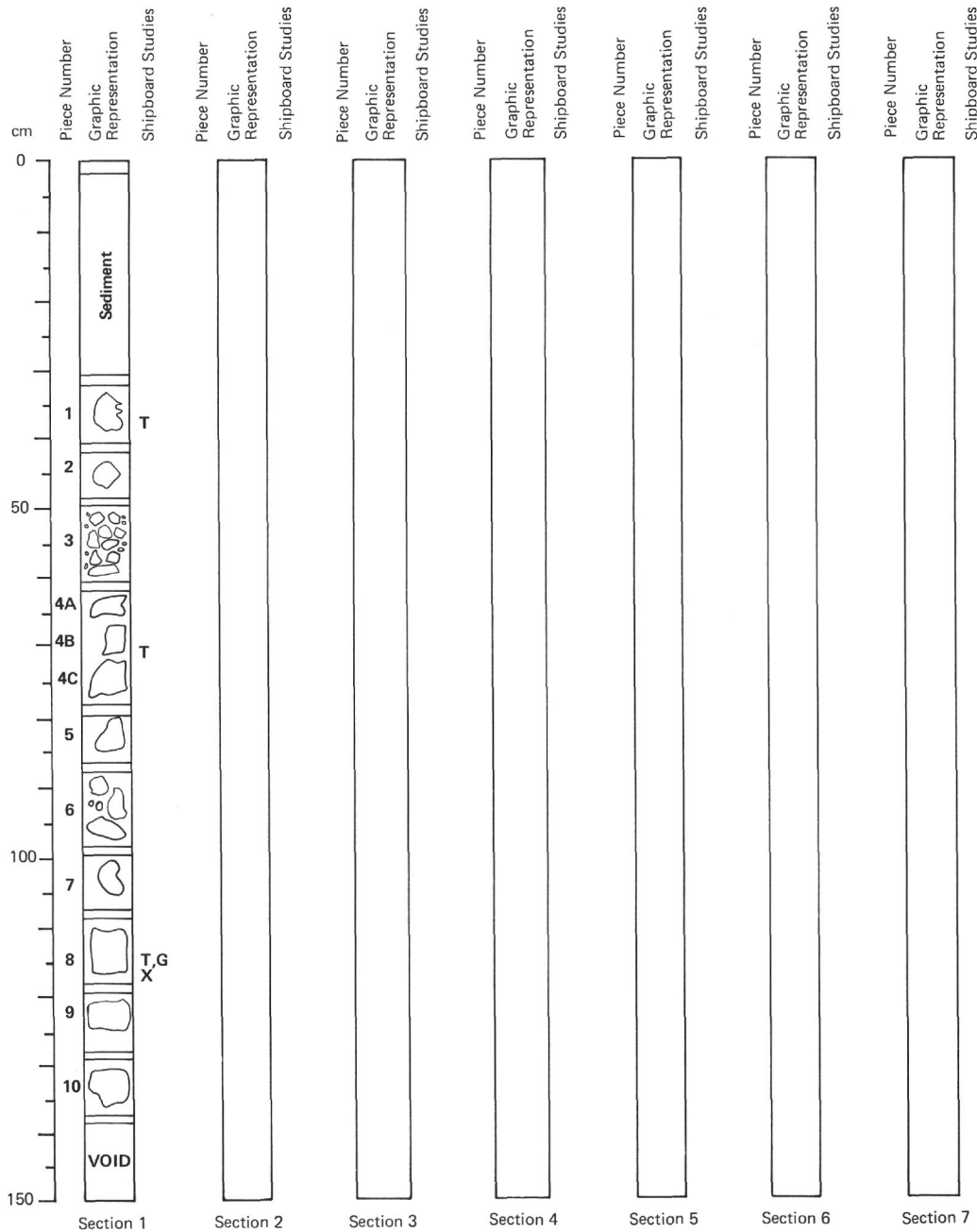


Explanatory notes in Chapter 1





Explanatory notes in Chapter 1



Original basalt recovery was 1 meter. Styrofoam spacers make the length shown here greater than the amount recovered.

Interval 0-20 cm: sand (10YR 6/2) with fragments of basalt, volcanic glass (fresh and palagonitized) and forams.

Interval 20-31 cm: gravel (10YR 6/3) with fragments of basalt (3-20 mm), volcanic glass, forams and clay.

Interval 30-48 cm: fine- to medium-grained tuff with fragments of altered basalt and crystals of plagioclase and clinopyroxene (2.5YR 4/0).

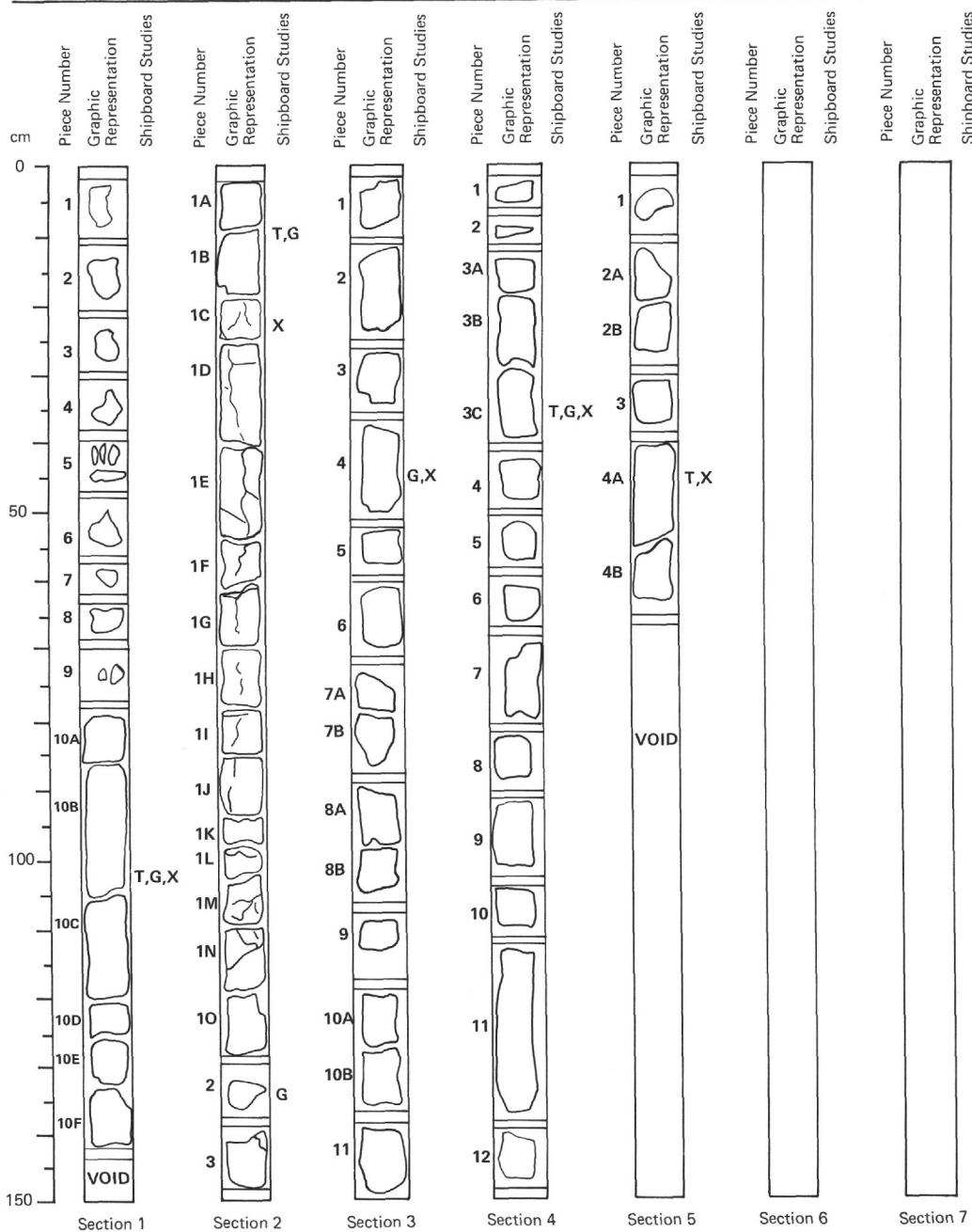
Interval 48-60 cm: basaltic gravel (2.5YR 5/0) fragments range 2 mm - 3 cm.

Interval 60-138 cm: fine-grained vesicular aphyric basalt (10YR 6/1). Vesicles (1-3%) distributed unevenly, some partially filled with calcite, size range 1/2-4 mm. Glass selvage at 63 cm, sediment fragments 80-105 cm.

Basalt: groundmass hyaloophitic to subvariolithic (clinopyroxene spherulites), plagioclase laths have length:width ratio of 25:1. Rare microphenocrysts plagioclase and olivine (pseudomorphed by calcite). Also includes layers of welded hyaloclastic breccia(?).

Shipboard Data

	Vp	NRM	Inc.
Sect. 1, 30 cm:	---	---	Reversed
Sect. 1, 120 cm:	4.32	324	+64°



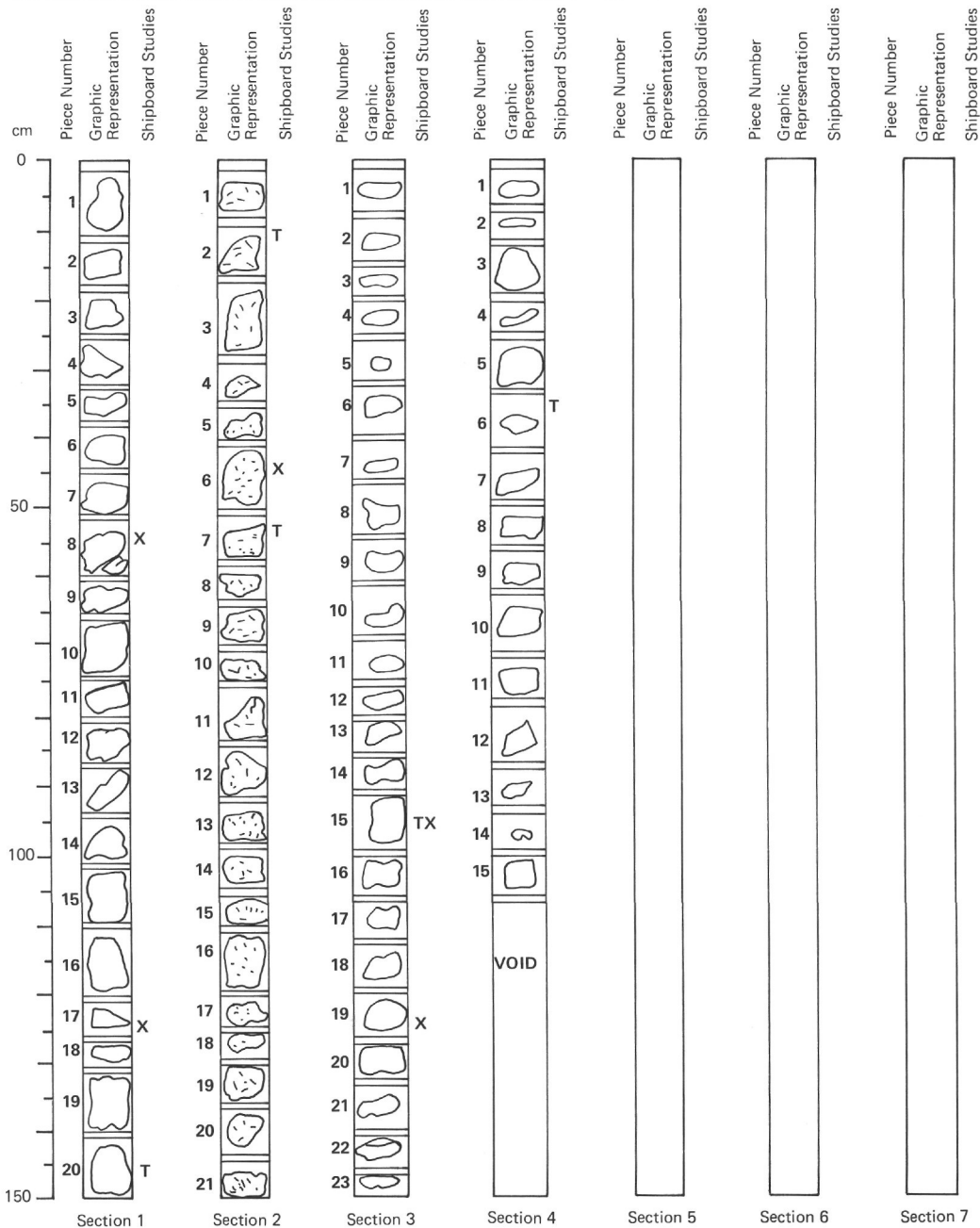
Original basalt recovery was 5.11 meters. Styrofoam spacers make the length shown here greater than the amount recovered.

Medium-grained vesicular aphyric basalt (10YR 6/1) with scattered microphenocrysts of olivine altered to red-brown color. Vesicles (1-5%) range in size 0.3-3.0 mm, some filled with calcite. Vesicle-rich zones at: Section 1, 85-90, 100-105, 125-120; Section 2, 10-23, 90-110; Section 3, 53-59, 100-113; Section 4, 15-20, 45-50, 90-97. Numerous calcite veins concentrated at: Section 1, 15-25, 80-105; Section 2, 10-60, 107-117; Section 3, 10-23, 37-58, 108-135; Section 4, 8-12, 92-103, 140-148; Section 5, 2-20, 40-55.

Petrography: texture sub-ophitic to intergranular, rarely subvolcanic. Microphenocrysts and glomerocrysts of plagioclase groundmass contains smectite, calcite, plagioclase laths, clinopyroxene, opaques, and rare olivine.

Shipboard Data

	Vp	NRM	Inc.
Sect. 1, 100 cm:	4.54	269	+56°
Sect. 2, 10 cm:	4.27	—	Normal
Sect. 2, 135 cm:	—	225	+52°
Sect. 3, 60 cm:	44.46	349	+63°
Sect. 4, 40 cm:	4.36	123	+63°
Sect. 5, 50 cm:	4.43	107	+51°



Original basalt recovery was 3.7 meters. Styrofoam spacers make the length shown here greater than the amount recovered.

Aphyric subvariolic vesicular basalt with varying degree of hydrothermal alteration (2.5YR 5/1). Finer-grained nonvesicular zone at Section 2, 35-38. No visible contacts between units. Vesicles lined or occasionally filled with smectite, calcite, zeolites(?) and/or pyrite in that order of abundance. Smectite-pyrite vein at Section 1, 55-60 cm.

Petrography: texture variolitic to sub-ophitic, plagioclase ranges An₆₅₋₄₅. Glass and olivine replaced by smectite and carbonate. Vesicles contain smectite, carbonate and rare zeolites. Clinopyroxene shows faint brown pleochroism.

Shipboard Data

	Vp	NRM	Inc.
Sect. 1, 65 cm:	—	3351	+79°
Sect. 1, 135 cm:	4.00	—	Normal
Sect. 2, 100 cm:	3.99	505	+80°
Sect. 3, 120 cm:	3.91	932	+78°

